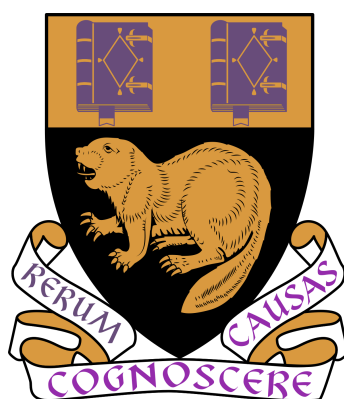


Parisian times, Bessel processes and
Poisson-Dirichlet random variables



Junyi Zhang

The Department of Statistics

London School of Economics and Political Science

A thesis submitted for the degree of

Doctor of Philosophy

April 2021

This thesis is dedicated to my parents
Qing Zhang and Shuhua Yin

Declaration

I certify that the thesis I have presented for examination for the PhD degree of the London School of Economics and Political Science is solely my own work other than where I have clearly indicated that it is the work of others (in which case the extent of any work carried out jointly by me and any other person is clearly identified in it). The copyright of this thesis rests with the author. Quotation from it is permitted, provided that full acknowledgement is made. This thesis may not be reproduced without my prior written consent. I warrant that this authorization does not, to the best of my belief, infringe the rights of any third party.

Statement of co-authored work

1. A version of Chapter 2 has been adapted into a manuscript entitled “First hitting time of Brownian motion with drift on simple graph” jointly authored with Professor Angelos Dassios, and is published in *Methodology and Computing in Applied Probability*, see Dassios and Zhang (2021b).
2. A version of Chapter 3 has been adapted into a manuscript entitled “Parisian time of reflected Brownian motion with drift on ray and its application in banking” jointly authored with Professor Angelos Dassios, and is published in *Risks*, see Dassios and Zhang (2020).
3. A version of Chapter 5 has been adapted into a manuscript entitled “Exact simulation of two-parameter Poisson-Dirichlet random variables” jointly authored with Professor Angelos Dassios, and is published in *Electronic Journal of Probability*, see Dassios and Zhang (2021a).

Acknowledgements

First of all, I would like to express my sincere gratitude to my PhD supervisor, Professor Angelos Dassios. I can still remember the day when Prof. Dassios told me that I was admitted by LSE, and the day we first met at the sixth floor of Columbia House. Since then, his fantastic ideas have led me throughout my PhD study. During the four years of PhD journey, I have learned so much from Prof. Dassios. His passion and genius in academic have impressed me so deeply. There were many times when I was stuck in the middle of the proof, and received a piece of paper from Prof. Dassios, which solved the whole problem elegantly.

I also want to thank my advisor, Professor Beatrice Acciaio, who gave me a great deal of encouragement in research. I learned a lot from her lectures during the first and second years of study, not only the academic aspects but also the teaching style and the patience to students. Prof. Acciaio was very kind to me and helped me in many issues.

Furthermore, I would like to thank Dr. James Abdey, Prof. Johannes Ruf and Prof. Mihail Zervos for providing me the teaching opportunity in ST102 Elementary Statistical Theory, ME117 Further Statistics for Economics and Econometrics and ME302 Introduction to Financial Mathematics. It was great honour to teach the talent students at LSE. The teaching experience gave me an opportunity to enhance my knowledge in these subjects, and to improve my interpersonal communication skills.

Moreover, I would like to express my appreciation to all the faculties and staffs in our department. In particular, I want to thank Ms. Penny Montague, Mr. Steve Ellis, Ms. Yanli Ji, Ms. Sarah McManus and Ms. Imelda Andolfo for their help in all the administrative issues. The Department of Statistics is always giving us the greatest freedom to concentrate on our own interest and achieve our goal, this environment is created by the successful management team.

Besides, I would like to thank the members of our office: Cheng Chen, Camilo Cardenas-Hurtado, Junchao Jia, Yirui Liu, Yan Lu, Despoina

Makariou, Cheng Qian, Jing Han Tee, Tianlin Xu, Jialin Yi, Christine Yuen and Yajing Zhu. Together we made Columbia House 5.02 a friendly and comfortable place to work. Moreover, we share our happiness and sadness, care about others and offer help whenever we can. With all of you, the office becomes a place that we can call it 'home'. The days and nights we spent together is a treasure that I will keep in my mind for a lifetime.

My PhD study is fully funded by the LSE PhD studentship, I am extremely grateful to the School and studentship panel for giving me this fantastic opportunity. The studentship is very generous and enables me to focus on my research.

Last but not the least, thanks my parents Qing Zhang and Shuhua Yin for their always love and support.

Abstract

In this thesis, we study the first hitting time and Parisian time of Brownian motion and squared Bessel process, as well as the exact simulation algorithm of the two-parameter Poisson-Dirichlet distribution. Let the underlying process be a reflected Brownian motion with drift moving on a finite collection of rays. Using a recursive method, we derive the Laplace transform of the first hitting time of the underlying process. This generalises the well-known result about the first hitting time of a Walsh Brownian motion on spider. We also invert the Laplace transform explicitly using two different methods, and obtain the density and distribution functions of the first hitting time. Then we consider the Parisian time of the underlying process, which is defined as the first exceeding time of the excursion time length. Using the same recursive method, we derive the Laplace transform of the Parisian time. The exact simulation algorithm for the Parisian time is also proposed. Next, we extend the result to the Parisian time of a squared Bessel process with a linear excursion boundary. Based on a variation of the Azéma martingale, we obtain the distributional properties of the Parisian time, and design the algorithm for sampling from the Parisian time. Finally, as an extension of the simulation of the Parisian time, we propose two exact simulation algorithms for sampling from the two-parameter Poisson-Dirichlet distribution.

Contents

1	Introduction	9
2	First hitting time of reflected Brownian motion with drift on rays	16
2.1	A construction of the planar process and the first hitting time	18
2.2	Laplace transform of τ	20
2.3	Density of the first hitting time	24
2.4	Numerical Implementation	32
3	Parisian time of reflected Brownian motion with drift on rays	38
3.1	Construction of the underlying process and the Parisian time	39
3.2	Laplace transform of τ	41
3.3	Exact simulation algorithm of the Parisian time	45
3.4	Discussion	50
4	Parisian time of a squared Bessel process with a linear excursion boundary and the pricing of moving Parisian options	53
4.1	Introduction	53
4.2	Preliminaries	55
4.3	An extension of the Azéma martingale	56
4.4	A martingale projection onto the filtration \mathcal{F}_U	58
4.5	Distributional properties of the Parisian time	63
4.5.1	Laplace transform for the stopping time	63
4.5.2	Density of the Parisian time	64
4.6	Exact simulation	65

4.6.1	Exact simulation algorithm	65
4.6.2	Numerical illustration	67
4.7	Application: Pricing moving Parisian options	68
5	Exact simulation of two-parameter Poisson-Dirichlet random variables	73
5.1	Introduction	73
5.2	Decompositions of $1/V_k$ under $\mathbb{P}_{\alpha,\theta}$	75
5.3	Exact simulation algorithms	83
5.4	Numerical results	88
5.4.1	Sample average	91
5.4.2	Covariance	91
5.4.3	Complexity	91
5.4.4	CPU time	92
6	Epilogue	96
A	Proofs of the main results in Chapter 2	98
B	Exact simulation of truncated subordinator	102
C	Proofs of the main results in Chapter 4	105
D	Joint density of the random vector $(R_1, \dots, R_{n-1} \mid \Delta_1^{-\alpha} = w)$	111
E	Simulation of G^*	113
	Bibliography	115

Chapter 1

Introduction

Research about the first hitting time and Parisian time of stochastic processes has a long history and attracts a lot of interests. Their applications range from financial mathematics to risk management. The main objective of this thesis is to generalise the existing results concerning the first hitting time and Parisian time of Brownian motion, and to emphasise their connection to the Lévy subordinator. The first two chapters are about the first hitting time and the Parisian time of a reflected Brownian motion with drift on rays. The third chapter considers the Parisian time of a squared Bessel process with a linear excursion boundary. The fourth chapter presents the exact simulation algorithms for two-parameter Poisson-Dirichlet distribution.

The study of the first hitting time of a Brownian motion with an one-sided linear boundary goes back to Doob (1949). Other types of boundary have also been considered. The second-order boundary was studied by Salminen (1988) using the infinitesimal generator method. The square-root boundary was considered by Breiman (1967) via the Doob's transform approach. Wang and Pötzelberger (1997) obtained the crossing probability for Brownian motion with a piecewise linear boundary using the Brownian bridge. Scheike (1992) derived an exact formula for the broken linear boundary. Peskir (2002) provided a general result for the continuous boundary using the Chapman-Kolmogorov formula, and gave the probability density function of the first hitting time in terms of a Volterra integral system.

For the first hitting time of Brownian motion with a two-sided boundary, the Laplace transform and density are well-known; see Borodin and Salminen (1996) Section II.1.3. Barba Escribá (1987) obtained the moment generating function of the time at which Brownian motion exits a region bounded by two nonconvergent straight lines. Che and Dassios (2013) used a martingale method to derive the crossing probability with a two-sided boundary involving random jumps. Sacerdote et al.

(2014) constructed a Volterra integral system for the probability density function of the first hitting time of Brownian motion with a general two-sided boundary.

Another case that we are interested in is the first hitting time of Walsh Brownian motion on spider. In the epilogue of Walsh (1978), Walsh introduced a planar process which is now known as the Walsh Brownian motion. The idea in Walsh (1978) is to take each excursion of a reflected Brownian motion $|W(t)|$ and, instead of giving it a random sign (we obtain a skew Brownian motion and in particular, a standard Brownian motion by doing so), to assign it a random variable Θ with a given distribution in $[0, 2\pi)$, and to do this independently for each excursion. That is, if the excursion occurs during the time interval (u, v) , we replace $|W(t)|$ by the pair $(|W(t)|, \Theta)$ for $u \leq t < v$, Θ being a random variable with values in $[0, 2\pi)$. This provides a planar process $(|W(t)|, \Theta(t))$, where $\Theta(t)$ is constant during each excursion away from 0, has the same distribution as Θ , and is independent for different excursions. Then the process $(|W(t)|, \Theta(t))$, when away from the origin, is a Brownian motion along a ray, and is kicked away from 0 immediately by the law Θ . In much of the existing literature, the angular measure Θ has a finite support, and in this case, we call the state space of the planar process a spider.

The Walsh Brownian motion was further studied by Barlow et al. (1989). The Walsh Brownian motion and Walsh diffusion on a spider were studied in Tsirelson (1997), Watanabe (1999) and Evans and Sowers (2003). Itô's formula for Walsh Brownian motion with arbitrary angular measure was proved in Hajri and Touhami (2014), and the stochastic calculus was developed in Freidlin and Sheu (2000), Freidlin and Wentzell (1993) and Picard (2005). Walsh semimartingales and Walsh diffusions with arbitrary angular measure were introduced in Ichiba et al. (2018), and further studied in Karatzas and Yan (2019) with control problems. The convergence and stationary distributions for Walsh diffusions are considered in Ichiba and Sarantsev (2019). The Laplace transform of the first hitting time of the Walsh Brownian motion on a spider has been derived by Papanicolaou et al. (2012) and Yor (1997). A literature review can be found in Yan (2018).

In this thesis, we will consider a generic planar process, the reflected Brownian motion with drift on rays. More specifically, we generalise the Walsh Brownian motion $(|W(t)|, \Theta(t))$ to $(|X(t)|, \Theta(t))$, where $|X(t)|$ is a reflected Brownian motion with drift whose coefficients depends on $\Theta(t)$. It is clear that the standard Brownian motion and Walsh Brownian motion on spider can be viewed as the special cases of the reflected Brownian motion with drift on rays. Then the first hitting problems of the one-sided, two-sided and Walsh types can also be viewed as the special cases of the first hitting time of the latter process. In view of this, we will derive the Laplace

transform of the first hitting time of the reflected Brownian motion with drift on rays, and use the existing literature to verify our results.

We are also interested in the probability density function of the first hitting time. In the one-sided and two-sided cases, the probability density function can be seen in Borodin and Salminen (1996). However, these formulas are in a series whose truncated function converges to the original function fast only when the variable t is small. This causes some computational problems as it is hard to calculate the probability when the first hitting time takes a large value. For example, from Borodin and Salminen (1996) we know

$$\mathbb{P}(\tau \in dt) = \sum_{k=-\infty}^{\infty} (-1)^k \frac{(2k+1)b}{\sqrt{2\pi t^3}} e^{-\frac{(2k+1)^2 b^2}{2t}} dt, \quad b > 0,$$

where $\tau := \inf\{t \geq 0 \mid |W_t| = b\}$. To calculate the value of this function, we need to truncate the summation at some level n , i.e., to use the truncated function

$$\sum_{k=-n}^n (-1)^k \frac{(2k+1)b}{\sqrt{2\pi t^3}} e^{-\frac{(2k+1)^2 b^2}{2t}}.$$

But we will show that the truncated function provides a good approximation for the original function only when t is small, and we will derive an expression for the density function that is useful when t is large.

On the other hand, no explicit formula is known for the density of the first hitting time of a Walsh Brownian motion on spider. In this thesis, we propose two different methods to invert the Laplace transform and derive the density function. These methods will result in two explicit expressions that are useful for large t and small t respectively.

Apart from the first hitting time, we also look at the Parisian time of the reflected Brownian motion with drift on rays. Parisian time is part of excursion theory, and is defined as the first time that the excursion time length of the underlying process reaches a threshold. The study of excursion time length of Brownian motion goes back to Chung (1976). Other aspects of Brownian excursion have also been considered. Durrett et al. (1977) developed the relationships between the Brownian excursions, meanders and bridges using the limit processes of conditional functionals of Brownian motion. Imhof (1984) derived the joint density concerning the maximum of Brownian motion and 3-dimensional Bessel process. Kennedy (1976a) derived the distribution of the maximum of excursion via the limiting processes and relates it to the standard Brownian motion. Gettoor and Sharpe (1979) obtained

a limiting result on the distribution of the amount of time a Brownian excursion spends in a small interval around the origin. A literature review can be found in Zhang (2014).

More recently, Chesney et al. (1997) studied the Parisian time of Brownian motion. Let W_t be a standard Brownian motion, we define its last zero time to be

$$g(t) := \sup\{s \leq t \mid W(s) = 0\},$$

and the excursion time length to be

$$U(t) := t - g(t).$$

Then $U(t)$ represents the time length W_t has stayed away from zero, and the Parisian time is defined as the first hitting time of $U(t)$, i.e.,

$$\tau := \inf\{t \geq 0 \mid U(t) = d\},$$

where d is a constant. The Laplace transform of the Parisian time τ was obtained by Chesney et al. (1997). In this thesis, we will generalise the concept of Parisian time to the reflected Brownian motion with drift on rays. We calculate the Laplace transform of the Parisian time and design an exact simulation algorithm to sample from it.

Chesney et al. (1997) also used their results to price the Parisian type options. They are path-dependent options whose payoff depends not only on the final value of the underlying asset, but also on the path trajectory of the underlying above or below a predetermined barrier for a length of time. The two-sided Parisian option was considered in Dassios and Wu (2010), its pricing depends on the Parisian time of a drifted Brownian motion with a two-sided excursion time threshold. For more details about Parisian options, see Schröder (2003), Anderluh and van der Weide (2009) and Labart and Lelong (2009). It turns out that the results in Chesney et al. (1997) and Dassios and Wu (2010) can be viewed as the special cases of the Parisian time of a reflected Brownian motion with drift on rays. Moreover, we will discuss the application of the Parisian time in the real-time gross settlement system.

Another topic within the excursion theory is the Parisian time of a squared Bessel process with a linear excursion boundary. In most of the existing literatures, the attention has been given to the Parisian time of a reflected Brownian motion. But a reflected Brownian motion $|W_t|$ has the same excursion time length as $|W_t|^2$ because

they share the same zeros, and the latter process can be viewed as the special case of a squared Bessel process. To see this, consider the squared Bessel process Z_t with the stochastic differential equation

$$dZ_t = 2(1 - \alpha)dt + 2\sqrt{Z_t}dW_t, \quad Z_0 = 0, \quad 0 < \alpha < 1.$$

When $\alpha = 1/2$, the right hand side reduces to the SDE of $|W_t|^2$. This relationship inspires us to study the Parisian time of a larger class of processes, the squared Bessel process.

In addition, we generalise the constant excursion boundary to a linear excursion boundary. Recall that we define the Parisian time to be $\tau := \inf\{t \geq 0 \mid U(t) = d\}$, where d is a constant. But it is also possible to generalise the threshold d to a function of time. In particular, we are interested in the Parisian time defined as

$$\tau := \inf\{t \geq 0 \mid U(t) = a + bt\},$$

where $a > 0$ and $0 < b < 1$. This is motivated by the pricing problem of a new type of Parisian option, the moving Parisian option. The owner of such options is betting the price of the underlying asset is above or below a barrier for an increasingly long term. We will propose two methods to price the moving Parisian options. To our knowledge, the only existing literature about the moving Parisian option is Guer (2020).

In order to study the distribution of this Parisian time, we will construct a martingale based on the excursion time length U_t . When the underlying process is a Brownian motion W_t , $U_t := t - \sup\{s \leq t \mid W(s) = 0\}$ represents the excursion length of W_t , and the martingale based on U_t is called a Azéma martingale. The most well-known Azéma martingale is

$$\text{sgn}(W_t) \frac{\pi}{2} \sqrt{U_t},$$

see Çetin (2012). There are also other types of Azéma martingale, see Dassios and Lim (2019). When the underlying process is a squared Bessel process, we call the martingale based on U_t an extension of the Azéma martingale. We will use the extension to study the distributional properties of the Parisian time of the squared Bessel process.

Finally, we study the exact simulation algorithm of the two-parameter Poisson-Dirichlet distribution (PD distribution). The PD distribution is a probability distribution on the set of decreasing positive sequences with sum 1. It can be defined in a ‘stick-breaking’ manner as follows. For $0 \leq \alpha < 1$ and $\theta > -\alpha$, suppose

that $\tilde{Y}_i, i = 1, 2, \dots$ is a sequence of independent random variables such that \tilde{Y}_i has Beta($1 - \alpha, \theta + i\alpha$) distribution. Let

$$\tilde{V}_1 = \tilde{Y}_1, \quad \tilde{V}_i = (1 - \tilde{Y}_1) \dots (1 - \tilde{Y}_{i-1})\tilde{Y}_i \quad (i \geq 2)$$

and let $V_1 \geq V_2 \geq \dots$ be the ranked values of the \tilde{V}_i . Then the PD distribution with parameters (α, θ) is defined to be the distribution of $V_i, i = 1, 2, \dots$.

The PD distribution arises in many fields, for example, as the asymptotic distribution of the ranked relative cycle lengths in a random permutation, see Shepp and Lloyd (1966) and Schmidt and Vershik (1977); as the limiting proportions of genes in some populations genetics models, see Hoppe (1987) and Watterson (1976); as the distribution of the ranked sizes of atoms in the Dirichlet process prior in Bayesian statistics, see Ferguson (1973) and Blackwell and MacQueen (1973). It also appears in the research fields such as number theory Billingsley (1972), Vershik (1986) and combinatorics Aldous (1985), Hansen (1994). More recently, the PD distribution is used to approximate the capital distribution curves in equity markets, see Sosnovskiy (2015).

From Pitman and Yor (1997), we know the PD distribution is related to the truncated Lévy subordinator. On the other hand, we will show that the Parisian time of a reflected Brownian motion can also be interpreted as a truncated Lévy subordinator at an exponential time. Hence, we find a connection between the PD distribution and the previous research. Using a Laplace transform approach, we propose a decomposition for the components of the PD distribution. The decomposition leads us to an exact simulation algorithm. Moreover, when the parameters of the distribution meet certain conditions, we provide a modified algorithm which is much faster than the general case.

This thesis is organised as follows:

Chapter 2 studies the first hitting time of reflected Brownian motion with drift on rays. Using a recursive method, we derive the Laplace transforms of the first hitting time. Moreover, we propose two methods to invert the Laplace transform explicitly, and obtain the density and distribution functions of the first hitting time.

Chapter 3 considers the Parisian time of reflected Brownian motion with drift on rays. Using the same recursive method, we obtain the Laplace transform of the Parisian time. Then we interpret the Laplace transform as a truncated Lévy subordinator at an exponential random time, and propose an exact simulation algorithm to sample from the Parisian time.

Chapter 4 concentrates on the Parisian time of a squared Bessel process with a linear excursion boundary. We provide an extension of the Azéma martingale, and interpret it as the projection of a martingale with respect to the full filtration. Then we derive a recursive formula for the density of the Parisian time, and develop an exact simulation algorithm for sampling from the Parisian time. Moreover, we use the previous results to price the moving Parisian options. Numerical results are also provided.

Chapter 5 focuses on the two-parameter Poisson-Dirichlet distribution. We derive two decompositions for the components of the distribution, and propose the exact simulation algorithms for sampling from these components. Numerical examples are provided to illustrate the accuracy and effectiveness of our algorithms.

Chapter 6 concludes the thesis and sets out some topics for future research.

Chapter 2

First hitting time of reflected Brownian motion with drift on rays

Suppose we have a system of rays emanating from a common origin and a particle $X(t)$ moving on this system. On each ray, the particle behaves as a reflected Brownian motion with drift; and once at the origin, it instantaneously chooses a ray for its next voyage randomly according to a given distribution. On each ray, there is an upper boundary (see Fig. 2.1). We are interested in the first time that the boundary is hit by $X(t)$.

In order to derive the Laplace transform of the first hitting time, we will construct a perturbed process which makes a small jump at the origin. This enables us to use a recursive method to calculate the Laplace transform. Next, we reduce the process to a Walsh Brownian motion on spider by taking zero drift and unit dispersion.

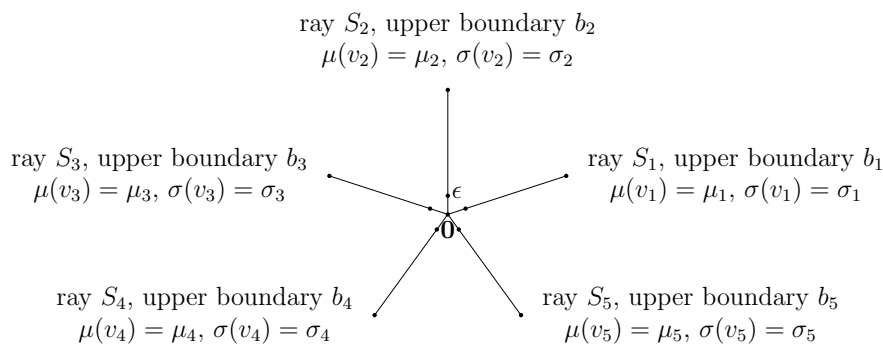


Figure 2.1 A reflected Brownian motion with drift on a collection of 5 rays.

By doing so, we also get a simpler expression for the Laplace transform of the first hitting time. We invert the Laplace transform using two different methods, and study the density and distribution functions of the first hitting time.

This chapter is motivated by the real-time gross settlement system (RTGS, and known as CHAPS in the UK, see McDonough 1997 and Padoa-Schioppa 2005). The participating banks in the RTGS system are concerned about liquidity risk and wish to prevent the excessive liquidity exposure between two banks. There is evidence suggesting that in CHAPS, banks usually set bilateral or multilateral limits on the exposed position with others (see Becher et al. 2008a and Becher et al. 2008b), this mechanism was studied by Che and Dassios (2013) using a Markov model. For a single bank, namely bank A , let a reflected Brownian motion be the net balance between bank A and bank i , and let u_i be the bilateral limit set up by bank A for bank i , Che and Dassios (2013) calculated the probability that the limit is exceeded in a finite time.

We generalize this model by considering an individual bank A and n counterparties. Assume that bank A uses an internal queue to manage its outgoing payments, and once the current payment is settled, it has probability P_i to make another payment to bank i , where $i \in \{1, \dots, n\}$. Let a reflected Brownian motion with drift be the net balance between bank A and bank i . To avoid the excessive exposure to liquidity risk, a limit b_i has been set for the net balance between bank A and bank i (this limit might be set by either the participating banks or the central bank, see Padoa-Schioppa 2005), and they are interested in the first time that such a limit is exceeded. In practice, an individual bank could set multiple limits or even remove the limit on different types of counterparties. This problem can be reduced to the calculation of the first hitting time of a reflected Brownian motion with drift on rays. For more details about the RTGS system, see Che (2011) and Soramäki et al. (2007). Applications of the current chapter also include the communication in a network, see Deng and Li (2009).

The rest of this chapter is organised as follows. We construct the reflected Brownian motion with drift on rays $X(t)$ in Section 2.1, then calculate the Laplace transform of the first hitting time τ and present some special cases of the result in Section 2.2. Next, we consider a special case where $X(t)$ is a Walsh Brownian motion on spider, and provide two methods to invert the Laplace transform explicitly in Section 2.3. Numerical implementations are presented in Section 2.4.

2.1 A construction of the planar process and the first hitting time

In this section we construct the reflected Brownian motion with drift on a finite collection of rays, and define the first hitting time we are interested in. Let n be a finite positive integer, we denote by S a system containing n rays emanating from the common origin, i.e., $S := \{S_1, \dots, S_n\}$, and fix a distribution $P := \{P_i\}_{i=1, \dots, n}$, so that $\sum_{i=1}^n P_i = 1$. Once at the origin, the underlying process will choose a ray for its next voyage randomly according to P . We also define the functions $\mu(S_i) := \mu_i$ and $\sigma(S_i) := \sigma_i$ for $i = 1, \dots, n$, where $\mu_i \in \mathbb{R}$ and $\sigma_i \in \mathbb{R}^+$ are constants (see Fig 2.1).

Consider a planar process $X(t)$ on the system of rays S . We represent the position of $X(t)$ by $(|X(t)|, \Theta(t))$, where $|X(t)|$ denotes the distance between $X(t)$ and the origin, and $\Theta(t) \in \{S_1, \dots, S_n\}$ indicates the current ray of the process. We want $|X(t)|$ to behave as a reflected Brownian motion with drift. From Peskir (2006), we know that the latter process can be expressed in terms of the Skorokhod reflection of a “driving process”, which is a Brownian motion with the same drift and volatility that we expect for $|X(t)|$. To this end, let $U(t) := \mu(\Theta(t))t + \sigma(\Theta(t))W_t$ be the driving process, and $|X(t)|$ be the Skorokhod reflection of $U(t)$, i.e.,

$$|X(t)| = U(t) + \max_{0 \leq s \leq t} (-U(s))^+, \quad t \geq 0.$$

Then $|X(t)|$ has the same distribution as a reflected Brownian motion with drift $\mu(\Theta(t))$ and dispersion $\sigma(\Theta(t))$, a proof of this can be seen in Jeanblanc et al. (2009) Section 4.1, Peskir (2006) and Graversen and Shiryaev (2000).

We expect $\Theta(t)$ to be constant during each excursion of $X(t)$ away from the origin and has the same distribution as P when $X(t)$ returns to the origin. To this end, we initialise $\Theta(t)$ with $\mathbb{P}(\Theta(0) = S_i) = P_i$, $i = 1, \dots, n$, and let $\Theta(t)$ remain constant whenever $|X(t)| \neq 0$. Once $|X(t)| = 0$, $\Theta(t)$ is randomised according to P , i.e.,

$$\mathbb{P}(\Theta(t) = S_i \mid |X(t^-)| = 0) = P_i, \quad i = 1, \dots, n, \quad \forall t > 0.$$

This means the coefficients of $U(t)$ remain constant whenever $|X(t)| \neq 0$, then the Skorokhod reflection of $U(t)$ has the same distribution as a reflected Brownian motion with drift μ_i and dispersion σ_i on each ray S_i .

Therefore, we summarise the behaviour of $X(t)$ as follows. The initial state of $X(t)$ is distributed as $\mathbb{P}(X(0) = (0, S_i)) = P_i$, $i = 1, \dots, n$. Then it behaves as a Brownian

motion with drift μ_i and dispersion σ_i on ray S_i before the next time it returns to the origin, i.e., $\inf\{t > 0 | X(t) = 0\}$. Once at the origin, it instantaneously chooses a new ray according to P , independently of the past behaviour, that is

$$\mathbb{P}(X(t) = (0, S_i) \mid |X(t^-)| = 0) = P_i, \quad i = 1, \dots, n.$$

There are some special cases of $X(t)$. When $\mu_i = 0$ and $\sigma_i = 1$ for $i = 1, \dots, n$, $X(t)$ becomes a Walsh Brownian motion on spider. When $n = 2$, $P_1 = \alpha = 1 - P_2$, $\mu_1 = \mu_2 = 0$ and $\sigma_1 = \sigma_2 = 1$, $X(t)$ recovers the skew Brownian motion. We also obtain a Brownian motion with drift μ and dispersion σ by setting $n = 2$, $P_1 = P_2 = \frac{1}{2}$, $\mu_1 = \mu$, $\mu_2 = -\mu$ and $\sigma_1 = \sigma_2 = \sigma$; and a reflected Brownian motion by setting $n = 1$, $P_1 = 1$, $\mu = 0$ and $\sigma = 1$.

Next, we define the first hitting time of $X(t)$. On each ray i , there is an upper boundary $b_i > 0$, our target is to find the first time that the boundary is hit by $X(t)$. Thus, we are interested in the first hitting time τ defined as

$$\begin{aligned} \tau_i &:= \inf\{t \geq 0 \mid |X(t)| \geq d_i, \Theta(t) = S_i\}, \quad \text{for } i = 1, \dots, n, \\ \tau &:= \min_{i=1, \dots, n} \tau_i. \end{aligned} \tag{2.1}$$

We need to calculate the excursion time length of $X(t)$ before hitting the boundary, but the problem is there is no first excursion from zero; before any $t > 0$, the process has made an infinite number of small excursions away from the origin. To approximate the dynamic of a Brownian motion, Dassios and Wu (2010) introduced the ‘‘perturbed Brownian motion’’, we will extend this idea here.

For every $0 < \epsilon < \min_{i=1, \dots, n} b_i$, we define a perturbed process $X^\epsilon(t) = (|X^\epsilon(t)|, \Theta^\epsilon(t))$ on the system of rays S . On each ray S_i , $X^\epsilon(t)$ behaves as a reflected Brownian motion with drift μ_i , dispersion σ_i and starting from ϵ , as long as it does not return to the origin. Once at the origin, $X^\epsilon(t)$ not only chooses a new ray according to P , but also jumps to ϵ on the new ray. In other words, $X^\epsilon(t)$ has a perturbation of size ϵ at the origin which can be described as

$$\mathbb{P}(X^\epsilon(t) = (\epsilon, S_i) \mid |X^\epsilon(t^-)| = 0) = P_i, \quad i \in \{1, \dots, n\}.$$

Hence, we describe the behaviour of $X^\epsilon(t)$ as follows. The initial state of $X^\epsilon(t)$ is distributed as $\mathbb{P}(X^\epsilon(0) = (\epsilon, S_i)) = P_i$, $i = 1, \dots, n$. Then it behaves as a Brownian motion with drift μ_i , dispersion σ_i and starting from ϵ on ray S_i , as long as it does

not return to the origin. Once at the origin, it instantaneously chooses a new ray according to P and jumps to ϵ on the new ray.

We define the first hitting time of $X^\epsilon(t)$ similarly as before. We are interested in the first hitting time τ^ϵ defined as

$$\begin{aligned}\tau_i^\epsilon &:= \inf\{t \geq 0 \mid |X^\epsilon(t)| \geq b_i, \Theta^\epsilon(t) = S_i\}, \text{ for } i = 1, \dots, n, \\ \tau^\epsilon &:= \min_{i=1, \dots, n} \tau_i^\epsilon.\end{aligned}$$

As $\epsilon \rightarrow 0$, the perturbation at origin vanishes, and $X^\epsilon(t) \rightarrow X(t)$ in a pathwise sense, then $\tau^\epsilon \rightarrow \tau$ in distribution. Hence we will first derive the Laplace transform of τ^ϵ , then take the limit $\lim_{\epsilon \rightarrow 0} \mathbb{E}(e^{-\beta\tau^\epsilon})$ to calculate the Laplace transform of the first hitting time τ .

2.2 Laplace transform of τ

In this section, we derive the Laplace transform of the first hitting time. We first prepare some preliminary formulas in the following lemma.

Lemma 2.2.1. *Let $W_t^i := \epsilon + \mu_i t + \sigma_i W_t$ be a Brownian motion with drift μ_i , dispersion σ_i and starting from ϵ , define the first exit time*

$$H = H_{0, b_i} := \inf\{t \geq 0 \mid W_t^i \notin (0, b_i)\},$$

then H has the Laplace transforms

$$U_i(\epsilon) := \mathbb{E}\left(e^{-\beta H} \mathbf{1}_{\{W_H^i = b_i\}}\right) = e^{\frac{\mu_i}{\sigma_i^2}(b_i - \epsilon)} \frac{\sinh\left(\epsilon \frac{\sqrt{\mu_i^2 + 2\sigma_i^2 \beta}}{\sigma_i}\right)}{\sinh\left(b_i \frac{\sqrt{\mu_i^2 + 2\sigma_i^2 \beta}}{\sigma_i}\right)}, \quad (2.2)$$

$$L_i(\epsilon) := \mathbb{E}\left(e^{-\beta H} \mathbf{1}_{\{W_H^i = 0\}}\right) = e^{-\frac{\mu_i}{\sigma_i^2} \epsilon} \frac{\sinh\left((b_i - \epsilon) \frac{\sqrt{\mu_i^2 + 2\sigma_i^2 \beta}}{\sigma_i}\right)}{\sinh\left(b_i \frac{\sqrt{\mu_i^2 + 2\sigma_i^2 \beta}}{\sigma_i}\right)}. \quad (2.3)$$

Moreover, they have the limits

$$\lim_{\epsilon \rightarrow 0} U_i(\epsilon) = 0 \quad \text{and} \quad \lim_{\epsilon \rightarrow 0} L_i(\epsilon) = 1,$$

and their derivatives have the limits

$$\lim_{\epsilon \rightarrow 0} \left(\frac{d}{d\epsilon} U_i(\epsilon) \right) = e^{\frac{\mu_i}{\sigma_i^2} b_i} \frac{\frac{\sqrt{\mu_i^2 + 2\sigma_i^2 \beta}}{\sigma_i^2}}{\sinh \left(b_i \frac{\sqrt{\mu_i^2 + 2\sigma_i^2 \beta}}{\sigma_i^2} \right)}, \quad (2.4)$$

$$\lim_{\epsilon \rightarrow 0} \left(\frac{d}{d\epsilon} L_i(\epsilon) \right) = -\frac{\mu_i}{\sigma_i^2} - \frac{\sqrt{\mu_i^2 + 2\sigma_i^2 \beta}}{\sigma_i^2} \frac{\cosh \left(b_i \frac{\sqrt{\mu_i^2 + 2\sigma_i^2 \beta}}{\sigma_i^2} \right)}{\sinh \left(b_i \frac{\sqrt{\mu_i^2 + 2\sigma_i^2 \beta}}{\sigma_i^2} \right)}. \quad (2.5)$$

Proof. See Borodin and Salminen (2002) Part II.2.3. \square

Remark 1. For simplicity, we will refer to (2.2) and (2.3) as U_i and L_i . From Section 2.1, we know $X^\epsilon(t)$ starts from ϵ on ray i and behaves as a Brownian motion with drift as long as it does not hit the origin. In their Laplace transforms respectively, U_i represents the excursion length of $X^\epsilon(t)$ on ray i if it arrives at b_i before hitting 0, and L_i represents the excursion length if it arrives at 0 before hitting b_i .

Next, we present the main result of this section.

Theorem 2.2.2. Let $X(t)$ be a reflected Brownian motion with drift on a finite collection of rays, where $\mu_i \in \mathbb{R}$, $\sigma_i \in \mathbb{R}^+$, $P_i \in (0, 1]$ and $b_i > 0$ are the drift, dispersion, entering probability and boundary of ray i , $i = 1, \dots, n$. For $\beta \geq 0$, the Laplace transform of the first hitting time τ is

$$\mathbb{E}(e^{-\beta\tau}) = \frac{\sum_{i=1}^n P_i e^{\frac{\mu_i}{\sigma_i^2} b_i} \frac{D_i}{\sinh(b_i D_i)}}{\sum_{i=1}^n P_i \frac{\mu_i}{\sigma_i^2} + \sum_{i=1}^n P_i D_i \frac{\cosh(b_i D_i)}{\sinh(b_i D_i)}}, \quad (2.6)$$

where we denote by $D_i := \frac{\sqrt{\mu_i^2 + 2\sigma_i^2 \beta}}{\sigma_i^2}$.

Proof. Define the sequence of random times

$$\zeta_0 = 0, \quad \zeta_{m+1} = \inf\{t > \zeta_m \mid |X^\epsilon(t)| = 0\}, \quad \text{for } m \in \mathbb{N}_0$$

recursively, and the mutually exclusive events

$$C_m := \{\zeta_m \leq \tau^\epsilon < \zeta_{m+1}\}, \quad \text{for } m \in \mathbb{N}_0,$$

where C_m denotes the event that $X^\epsilon(t)$ hits the boundary during the $(m+1)$ -th excursion. We set $\{X^\epsilon(0) = (\epsilon, v_i)\}$ for an arbitrary but fixed i , and calculate the Laplace transforms $\mathbb{E}(e^{-\beta\tau^\epsilon} \mathbf{1}_{\{C_m\}} \mid X^\epsilon(0) = (\epsilon, v_i))$ for $m \in \mathbb{N}_0$.

For $m = 0$, we interpret C_0 as follows. Starting from ϵ on ray i , $X^\epsilon(t)$ arrives at b_i before hitting the origin, hence the boundary is hit during the first excursion. Using Remark 1, we have

$$\mathbb{E} \left(e^{-\beta\tau^\epsilon} \mathbf{1}_{\{C_0\}} \mid X^\epsilon(0) = (\epsilon, v_i) \right) = U_i.$$

Next, we consider the event C_1 . In this case, $X^\epsilon(t)$ arrives at 0 before hitting b_i during the first excursion, and the Laplace transform of the first excursion is L_i . After the first excursion, $X^\epsilon(t)$ returns to the origin and jumps to (ϵ, v_k) with probability P_k , then arrives at b_k before returning to the origin. But the behaviour of $X^\epsilon(t)$ during the second excursion is similar to what we described for C_0 , with the index i replaced by k . Thus, we have

$$\begin{aligned} \mathbb{E} \left(e^{-\beta\tau^\epsilon} \mathbf{1}_{\{C_1\}} \mid X^\epsilon(0) = (\epsilon, v_i) \right) &= L_i \left(\sum_{k=1}^n P_k \mathbb{E} \left(e^{-\beta\tau^\epsilon} \mathbf{1}_{\{C_0\}} \mid X^\epsilon(0) = (\epsilon, v_k) \right) \right) \\ &= L_i \left(\sum_{k=1}^n P_k U_k \right). \end{aligned}$$

In the same way, we consider the event C_2 . In this case, $X^\epsilon(t)$ arrives at 0 before hitting b_i during the first excursion, and the Laplace transform of the first excursion is L_i . After the first excursion, $X^\epsilon(t)$ returns to the origin and jumps to (ϵ, v_k) with probability P_k . Restarting from (ϵ, v_k) , $X^\epsilon(t)$ will hit the boundary exactly during the second excursion (hence the third in total). But the behaviour of $X^\epsilon(t)$ during the second and third excursions is similar to what we described for C_1 , with the index i replaced by k . Hence,

$$\begin{aligned} \mathbb{E} \left(e^{-\beta\tau^\epsilon} \mathbf{1}_{\{C_2\}} \mid X^\epsilon(0) = (\epsilon, v_i) \right) &= L_i \left(\sum_{k=1}^n P_k \mathbb{E} \left(e^{-\beta\tau^\epsilon} \mathbf{1}_{\{C_1\}} \mid X^\epsilon(0) = (\epsilon, v_k) \right) \right) \\ &= L_i \left(\sum_{k=1}^n P_k L_k \left(\sum_{j=1}^n P_j U_j \right) \right) = L_i \left(\sum_{k=1}^n P_k L_k \right) \left(\sum_{j=1}^n P_j U_j \right). \end{aligned}$$

The same explanation applies to C_m for any positive integer m , i.e., $X^\epsilon(t)$ arrives at 0 before hitting b_i during the first excursion, after that it restarts from (ϵ, v_k) and hits the boundary exactly during the m -th excursion. Hence we deduce that

$$\mathbb{E} \left(e^{-\beta\tau^\epsilon} \mathbf{1}_{\{C_m\}} \mid X^\epsilon(0) = (\epsilon, v_i) \right) = L_i \left(\sum_{k=1}^n P_k \mathbb{E} \left(e^{-\beta\tau^\epsilon} \mathbf{1}_{\{C_{m-1}\}} \mid X^\epsilon(0) = (\epsilon, v_k) \right) \right).$$

This implies a recursive structure between the Laplace transforms of τ^ϵ conditioned on C_m and C_{m-1} , we solve for

$$\mathbb{E} \left(e^{-\beta\tau^\epsilon} \mathbf{1}_{\{C_m\}} \mid X^\epsilon(0) = (\epsilon, v_i) \right) = L_i \left(\sum_{k=1}^n P_k L_k \right)^{m-1} \left(\sum_{j=1}^n P_j U_j \right),$$

where $m = 1, 2, \dots$. Since the boundary hitting may occur during any excursion of $X^\epsilon(t)$, we need to sum the result over $m \in \mathbb{N}_0$, this gives

$$\begin{aligned} \mathbb{E} \left(e^{-\beta\tau^\epsilon} \mid X^\epsilon(0) = (\epsilon, v_i) \right) &= \sum_{m=0}^{\infty} \mathbb{E} \left(e^{-\beta\tau^\epsilon} \mathbf{1}_{\{C_m\}} \mid X^\epsilon(0) = (\epsilon, v_i) \right) \\ &= U_i + \sum_{m=1}^{\infty} \left(L_i \left(\sum_{k=1}^n P_k L_k \right)^{m-1} \left(\sum_{j=1}^n P_j U_j \right) \right) = U_i + \frac{L_i \left(\sum_{j=1}^n P_j U_j \right)}{1 - \sum_{k=1}^n P_k L_k}, \end{aligned} \quad (2.7)$$

the last equation holds because for each $k = 1, \dots, n$ and $\beta \geq 0$, $0 < L_k < 1$, thus

$$0 < \sum_{k=1}^n P_k L_k < \sum_{k=1}^n P_k = 1.$$

Equation (2.7) boils down the Laplace transform of τ^ϵ to the initial state of $X^\epsilon(t)$. Since $\mathbb{P}(X^\epsilon(0) = (\epsilon, v_i)) = P_i$, we have

$$\begin{aligned} \mathbb{E} \left(e^{-\beta\tau^\epsilon} \right) &= \sum_{i=1}^n P_i \mathbb{E} \left(e^{-\beta\tau^\epsilon} \mid X^\epsilon(0) = (\epsilon, v_i) \right) \\ &= \sum_{i=1}^n P_i \left(U_i + \frac{L_i \left(\sum_{j=1}^n P_j U_j \right)}{1 - \sum_{k=1}^n P_k L_k} \right) = \frac{\sum_{i=1}^n P_i U_i(\epsilon)}{1 - \sum_{k=1}^n P_k L_k(\epsilon)}. \end{aligned} \quad (2.8)$$

As $\epsilon \rightarrow 0$, both numerator and denominator of (2.8) tend to 0, then we can calculate the limit $\lim_{\epsilon \rightarrow 0} \mathbb{E} \left(e^{-\beta\tau^\epsilon} \right)$ using (2.4) and (2.5), and this gives $\mathbb{E} \left(e^{-\beta\tau} \right)$. \square

As in Section 2.1, $X(t)$ can be reduced to some special cases by choosing the parameters accordingly, then we can compare Theorem 2.2.2 with the results in the existing literature.

Remark 2. When $n = 1$, $P_1 = 1$, $\mu_1 = 0$, $\sigma_1 = 1$ and $b_1 > 0$, equation (2.6) gives the Laplace transform of the first hitting time of a reflected Brownian motion (see Borodin and Salminen 2002 Section II.3.2),

$$\mathbb{E} \left(e^{-\beta\tau} \right) = \frac{1}{\cosh(b_1 \sqrt{2\beta})}. \quad (2.9)$$

When $n = 2$, $\mu_1 = \mu = -\mu_2$, $\sigma_1 = \sigma_2 = 1$, $P_1 = P_2 = \frac{1}{2}$ and $b_1 > 0$, $b_2 > 0$, equation (2.6) becomes the Laplace transform of the first exit time of a drifted Brownian motion from the stripe $(-b_2, b_1)$ (see Borodin and Salminen 2002 Section II.2.3),

$$\mathbb{E}(e^{-\beta\tau}) = \frac{e^{\mu b_1} \sinh(b_2 \sqrt{\mu^2 + 2\beta}) + e^{-\mu b_2} \sinh(b_1 \sqrt{\mu^2 + 2\beta})}{\sinh((b_1 + b_2) \sqrt{\mu^2 + 2\beta})}.$$

Moreover, when n is a finite positive integer and $\mu_i = 0$, $\sigma_i = 1$, for $j = 1, \dots, n$, $X(t)$ becomes a Walsh Brownian motion. Let the upper boundaries be $b_1 > 0, \dots, b_n > 0$, then the first hitting time τ has the Laplace transform

$$\mathbb{E}(e^{-\beta\tau}) = \frac{\sum_{k=1}^n P_k \frac{1}{\sinh(b_k \sqrt{2\beta})}}{\sum_{k=1}^n P_k \frac{\cosh(b_k \sqrt{2\beta})}{\sinh(b_k \sqrt{2\beta})}}, \quad (2.10)$$

this is the Laplace transform of the first hitting time of a Walsh Brownian motion on spider, see Fitzsimmons and Kuter (2015). In particular, when $P_1 = \dots = P_n = \frac{1}{n}$, we revert the main result of Papanicolaou et al. (2012) and Yor (1997) Section 17.2.3.

2.3 Density of the first hitting time

In this section, we concentrate on a special case where $\mu_i = 0$ and $\sigma_i = 1$, for $j = 1, \dots, n$, then the underlying process reduces to a Walsh Brownian motion on spider, and the first hitting time τ has the Laplace transform (2.10). We provide two methods to invert the Laplace transform (2.10). For simplicity, we denote by $g(x, t)$ and $\Psi(x, t)$ the density and distribution functions of an inverse Gaussian random variable with parameter x :

$$g(x, t) := \frac{x}{\sqrt{2\pi t^3}} e^{-\frac{x^2}{2t}} \quad \text{and} \quad \Psi(x, t) := 2 - 2\Phi\left(\frac{x}{\sqrt{t}}\right),$$

where $\Phi(\cdot)$ is the standard normal distribution function.

We first present an auxiliary result concerning the poles of the Laplace transform (2.10). In general, the poles of a Laplace transform refer to the zeros of its denominator, and they are useful in the inverse Laplace transform problem (see, for example, Arfken and Weber 2001 Section 20.10). For the current section, we are interested in the solutions to the equation $\sum_{k=1}^n P_k \frac{\cosh(b_k \sqrt{2\beta})}{\sinh(b_k \sqrt{2\beta})} = 0$ with respect to β .

It is also shown in the proof of Lemma 2.3.1 that there is no pole from the numerator part $\sum_{k=1}^n P_k \frac{1}{\sinh(b_k \sqrt{2\beta})}$ of the Laplace transform.

Lemma 2.3.1. *Denote by $-\beta^*$ the poles of the Laplace transform (2.10), then $-\beta^*$ are negative real numbers. Moreover, when $n > 1$ and the upper boundaries $\{b_i\}_{i=1,\dots,n}$ are rational numbers, we can find out the poles by solving the equation*

$$\sum_{i=1}^n P_i \left(\sum_{k \text{ even}} (-1)^{\frac{k}{2}} \binom{C_i}{k} y^k \prod_{j=\{1,\dots,n\}\setminus\{i\}} \left(\sum_{k \text{ odd}} (-1)^{\frac{k-1}{2}} \binom{C_j}{k} y^k \right) \right) = 0$$

with respect to y , and look for $\beta^* > 0$ which satisfies

$$y = \tan \left(\frac{1}{\prod_{j=1}^n d_j} \sqrt{2\beta^*} \right),$$

where we have set $b_i = \frac{c_i}{d_i}$, for $i = 1, \dots, n$, such that c_i and d_i are positive integers, and $C_i := c_i \prod_{j=\{1,\dots,n\}\setminus\{i\}} d_j$.

Since all the poles of the Laplace transform (2.10) are negative real numbers, we sort them in descending order as $-\beta_1^* > -\beta_2^* > \dots$, and denote the set of all poles by $\{-\beta_i^*\}_{i \in \mathbb{N}}$. We also make the convention that the expression $\sum_{-\beta^*} f(-\beta^*)$ represents the summation with respect to all the poles.

Note that we do not use the expression $\sum_{i=1}^{\infty} f(-\beta_i^*)$ because sometimes it is more convenient to write it as $\sum_{k=-\infty}^{\infty} f(a_k)$, where a_k is a constant concerning the poles; see Example 2.3.5 and Example 2.3.6 below.

Next, we provide an explicit method to invert the Laplace transform (2.10).

Theorem 2.3.2. *Assume that the upper boundaries $\{b_i\}_{i=1,\dots,n}$ are rational numbers, then the density of the first hitting time τ is*

$$f(t) = \sum_{-\beta^*} e^{-\beta^* t} \frac{\sum_{k=1}^n P_k \frac{\sqrt{2\beta^*}}{\sin(b_k \sqrt{2\beta^*})}}{\sum_{k=1}^n P_k b_k + \sum_{k=1}^n P_k b_k \frac{\cos^2(b_k \sqrt{2\beta^*})}{\sin^2(b_k \sqrt{2\beta^*})}}, \quad (2.11)$$

and the distribution of τ is

$$F(t) = \sum_{-\beta^*} \frac{1}{-\beta^*} (e^{-\beta^* t} - 1) \frac{\sum_{k=1}^n P_k \frac{\sqrt{2\beta^*}}{\sin(b_k \sqrt{2\beta^*})}}{\sum_{k=1}^n P_k b_k + \sum_{k=1}^n P_k b_k \frac{\cos^2(b_k \sqrt{2\beta^*})}{\sin^2(b_k \sqrt{2\beta^*})}}. \quad (2.12)$$

We now consider the usefulness of this theorem. Recall that all the poles $-\beta^*$ are negative real numbers and have been sorted in descending order. On the other hand, we notice that the term

$$e^{-\beta^* t} \frac{\sum_{k=1}^n P_k \frac{\sqrt{2\beta^*}}{\sin(b_k \sqrt{2\beta^*})}}{\sum_{k=1}^n P_k b_k + \sum_{k=1}^n P_k b_k \frac{\cos^2(b_k \sqrt{2\beta^*})}{\sin^2(b_k \sqrt{2\beta^*})}}$$

converges to zero fast when t is large. Hence, to evaluate the value of the function (2.11), we can truncate the summation $\sum_{-\beta^*}$ at the largest n poles. In other words, we define a truncated function

$$\bar{f}_n(t) := \sum_{\{-\beta_1^*, \dots, -\beta_n^*\}} e^{-\beta^* t} \frac{\sum_{k=1}^n P_k \frac{\sqrt{2\beta^*}}{\sin(b_k \sqrt{2\beta^*})}}{\sum_{k=1}^n P_k b_k + \sum_{k=1}^n P_k b_k \frac{\cos^2(b_k \sqrt{2\beta^*})}{\sin^2(b_k \sqrt{2\beta^*})}}.$$

The truncated function provides a good approximation for $f(t)$ when t is large, because the truncation error

$$f(t) - \bar{f}_n(t) = \sum_{\{-\beta_{n+1}^*, -\beta_{n+2}^*, \dots\}} e^{-\beta^* t} \frac{\sum_{k=1}^n P_k \frac{\sqrt{2\beta^*}}{\sin(b_k \sqrt{2\beta^*})}}{\sum_{k=1}^n P_k b_k + \sum_{k=1}^n P_k b_k \frac{\cos^2(b_k \sqrt{2\beta^*})}{\sin^2(b_k \sqrt{2\beta^*})}}$$

converges to zero fast when t is large.

However, this method is not useful for small t because the truncation error does not converge to zero when t is small. Hence, to control the size of the truncation error, we need to significantly increase the value of n , i.e., to include much more poles in the truncated function $\bar{f}_n(t)$, such that the truncation error contains less terms and becomes smaller. This is not efficient because t can be arbitrarily close to zero, and that would make the value of n extremely large.

We are not establishing the exact bound for the truncation error here, and this is a potential topic for a further study. An immediate example can be constructed based on the density of the first hitting time of a reflected Brownian motion (see Example 2.3.3), which is exactly the Jacobi Theta function. And there are many literatures about the convergence speed of the Jacobi Theta function, see for example Bellman (1961). More generally (Example 2.3.4, 2.3.5 and 2.3.6 where the density is not a special function), it might be useful to apply the Tauberian theorem for the Laplace transform (2.10) to derive the asymptotic behaviour of the density function at zero and infinity, see Bingham et al. (1989).

Inspired by the general Theta function transformation (see Bellman 1961 Section 19), we now provide an alternative expressions for the density function of τ that is

useful when t is small.

Remark 3. When $\{b_i\}_{i=1,\dots,n}$ are rational numbers, there exist positive integers c_i and d_i , such that $b_i = \frac{c_i}{d_i}$, for $i = 1, \dots, n$. Denote by $x := e^{-\sqrt{2\beta} \frac{1}{d_1 \dots d_n}}$, then Laplace transform (2.10) can be written as a quotient of two polynomials $M(x)/N(x)$, the series expansion with respect to x gives

$$\frac{M(x)}{N(x)} = \sum_{k=1}^{\infty} a_k x^k = \sum_{k=1}^{\infty} a_k e^{-\sqrt{2\beta} \frac{k}{d_1 \dots d_n}}. \quad (2.13)$$

Since $e^{-\sqrt{2\beta} \frac{k}{d_1 \dots d_n}}$ is the Laplace transform of an inverse Gaussian random variable with parameter $\frac{k}{d_1 \dots d_n}$, we can invert (2.13) term by term to derive the density of τ :

$$f(t) := \sum_{k=1}^{\infty} a_k \frac{\frac{k}{d_1 \dots d_n}}{\sqrt{2\pi t^3}} e^{-\frac{\left(\frac{k}{d_1 \dots d_n}\right)^2}{2t}} = \sum_{k=1}^{\infty} a_k g\left(\frac{k}{d_1 \dots d_n}, t\right),$$

We define the truncated function

$$\bar{f}_n(t) = \sum_{k=1}^n a_k \frac{\frac{k}{d_1 \dots d_n}}{\sqrt{2\pi t^3}} e^{-\frac{\left(\frac{k}{d_1 \dots d_n}\right)^2}{2t}},$$

and the truncation error

$$f(t) - \bar{f}_n(t) = \sum_{k=n+1}^{\infty} a_k \frac{\frac{k}{d_1 \dots d_n}}{\sqrt{2\pi t^3}} e^{-\frac{\left(\frac{k}{d_1 \dots d_n}\right)^2}{2t}}.$$

Using a similar argument as before, we find out that the truncated function $\bar{f}_n(t)$ provides a good approximation for $f(t)$ when t is small, because the truncation error converges to zero fast when t is small. But this method is not useful when t is large.

We also integrate the density over $(0, t)$ for the distribution of τ :

$$F(t) = \sum_{k=1}^{\infty} a_k \left(2 - 2\Phi\left(\frac{\frac{k}{d_1 \dots d_n}}{\sqrt{t}}\right)\right) = \sum_{k=1}^{\infty} a_k \Psi\left(\frac{k}{d_1 \dots d_n}, t\right).$$

We provide some examples to illustrate the use of Theorem 2.3.2 and Remark 3.

Example 2.3.3 (reflected Brownian motion). Consider the Laplace transform (2.9). To find the poles of the Laplace transform, we need to solve the equation $\coth(b_1 \sqrt{2\beta}) = 0$. Set $\beta = -\beta^*$, we have $\coth(b_1 \sqrt{-2\beta^*}) = \cos(b_1 \sqrt{2\beta^*}) = 0$, and $b_1 \sqrt{2\beta^*} = \frac{2k-1}{2}\pi$,

$k \in \mathbb{Z}^+$. Therefore, the Laplace transform (2.9) has the poles

$$-\beta^* = -\frac{(2k-1)^2}{8b_1^2}\pi^2, \quad k \in \mathbb{Z}^+.$$

Using Theorem 2.3.2, we calculate the density function of τ to be

$$f(t) = \sum_{k=1}^{\infty} (-1)^{k-1} \pi \frac{(2k-1)}{2b_1^2} e^{-\frac{(2k-1)^2}{8b_1^2}\pi^2 t},$$

which is useful when t is large. We also integrate the density over $(0, t)$ to derive the distribution function

$$F(t) = \sum_{k=1}^{\infty} (-1)^{k-1} \frac{4}{(2k-1)\pi} \left(1 - e^{-\frac{(2k-1)^2}{8b_1^2}\pi^2 t} \right).$$

On the other hand, denote by $x := e^{-\sqrt{2\beta}}$, the negative binomial expansion implies

$$\mathbb{E}(e^{-\beta\tau}) = \frac{2}{x^{b_1} + x^{-b_1}} = \frac{2x^{b_1}}{x^{2b_1} + 1} = 2 \sum_{k=1}^{\infty} (-1)^{k-1} x^{(2k-1)b_1}.$$

For every $k \in \mathbb{Z}^+$, $x^{(2k-1)b_1} = e^{-(2k-1)b_1\sqrt{2\beta}}$ is the Laplace transform of an inverse Gaussian random variable with parameter $(2k-1)b_1$, then Remark 3 gives

$$f(t) = 2 \sum_{k=1}^{\infty} (-1)^{k-1} g((2k-1)b_1, t),$$

which is useful when t is small. The distribution function is given by

$$F(t) = 2 \sum_{k=1}^{\infty} (-1)^{k-1} \Psi((2k-1)b_1, t).$$

Example 2.3.4 (standard Brownian motion). Let $n = 2$, $b_1 = 1$, $b_2 = 2$ and $P_1 = P_2 = \frac{1}{2}$ in Laplace transform (2.10), then

$$\mathbb{E}(e^{-\beta\tau}) = \frac{\frac{1}{\sinh(\sqrt{2\beta})} + \frac{1}{\sinh(2\sqrt{2\beta})}}{\frac{\cosh(\sqrt{2\beta})}{\sinh(\sqrt{2\beta})} + \frac{\cosh(2\sqrt{2\beta})}{\sinh(2\sqrt{2\beta})}}.$$

Using Lemma 2.3.1, we can derive the poles of the Laplace transform by solving

$y^2 - 3 = 0$ and $y = \tan(\sqrt{2\beta^*})$. Thus, the poles are

$$-\beta^* = -\frac{1}{2}\pi^2\left(k + \frac{1}{3}\right)^2, \quad k \in \mathbb{Z}.$$

Using Theorem 2.3.2, we calculate the density function of τ to be

$$\begin{aligned} f(t) &= \frac{\pi}{2\sqrt{3}} \sum_{k=-\infty}^{\infty} e^{-\frac{1}{2}\pi^2\left(k-\frac{2}{3}\right)^2 t} \left(k - \frac{2}{3}\right) \left((-1)^{k+1} + 1\right) \\ &= \frac{\pi}{2\sqrt{3}} \sum_{k=1}^{\infty} e^{-\frac{1}{2}\pi^2\left(k-\frac{2}{3}\right)^2 t} \left(k - \frac{2}{3}\right) \left((-1)^{k+1} + 1\right) \\ &\quad + \frac{\pi}{2\sqrt{3}} \sum_{k=1}^{\infty} e^{-\frac{1}{2}\pi^2\left(k-\frac{1}{3}\right)^2 t} \left(k - \frac{1}{3}\right) \left((-1)^{k+1} - 1\right), \end{aligned} \quad (2.14)$$

which is useful when t is large. We also integrate the density over $(0, t)$ to derive the distribution function

$$\begin{aligned} F(t) &= \frac{1}{\sqrt{3}\pi} \sum_{k=1}^{\infty} \frac{1}{\left(k - \frac{2}{3}\right)} \left(1 - e^{-\frac{1}{2}\pi^2\left(k-\frac{2}{3}\right)^2 t}\right) \left((-1)^{k+1} + 1\right) \\ &\quad + \frac{1}{\sqrt{3}\pi} \sum_{k=1}^{\infty} \frac{1}{\left(k - \frac{1}{3}\right)} \left(1 - e^{-\frac{1}{2}\pi^2\left(k-\frac{1}{3}\right)^2 t}\right) \left((-1)^{k+1} - 1\right). \end{aligned} \quad (2.15)$$

On the other hand, denote by $x := e^{-\sqrt{2\beta}}$, the negative binomial expansion implies

$$\mathbb{E}(e^{-\beta\tau}) = \frac{(x - x^{-1}) + (x^2 - x^{-2})}{x^3 - x^{-3}} = \frac{x(x+1)}{x^3 + 1} = \sum_{k=1}^{\infty} (-1)^{k-1} (x^{3k-1} + x^{3k-2}).$$

For every $k \in \mathbb{Z}^+$, we invert x^{3k-1} and x^{3k-2} using the inverse Gaussian density, then

$$f(t) = \sum_{k=1}^{\infty} (-1)^{k-1} g(3k-2, t) + \sum_{k=1}^{\infty} (-1)^{k-1} g(3k-1, t), \quad (2.16)$$

which is useful when t is small. The distribution function is given by

$$F(t) = \sum_{k=1}^{\infty} (-1)^{k-1} \Psi(3k-2, t) + \sum_{k=1}^{\infty} (-1)^{k-1} \Psi(3k-1, t). \quad (2.17)$$

Example 2.3.5 (skew Brownian motion). Let $n = 2$, $b_1 = 1$, $b_2 = 2$ and $P_1 =$

$1 - P_2 = \frac{1}{3}$ in Laplace transform (2.10), it becomes

$$\mathbb{E}(e^{-\beta\tau}) = \frac{\frac{1}{3} \frac{1}{\sinh(\sqrt{2}\beta)} + \frac{2}{3} \frac{1}{\sinh(2\sqrt{2}\beta)}}{\frac{1}{3} \frac{\cosh(\sqrt{2}\beta)}{\sinh(\sqrt{2}\beta)} + \frac{2}{3} \frac{\cosh(2\sqrt{2}\beta)}{\sinh(2\sqrt{2}\beta)}}.$$

Using Lemma 2.3.1, we can derive the poles of the Laplace transform by solving $y^2 - 2 = 0$ and $y = \tan(\sqrt{2}\beta^*)$. Thus, the poles are

$$-\beta^* = -\frac{1}{2}(k\pi + \theta)^2, \quad k \in \mathbb{Z}, \quad \text{where } \theta = \arctan(\sqrt{2}).$$

Using Theorem 2.3.2, we calculate the density function of τ to be

$$f(t) = \frac{1}{2\sqrt{6}} \sum_{k=-\infty}^{\infty} e^{-\frac{1}{2}(\theta+k\pi)^2 t} (\theta + k\pi) \left((-1)^k + \sqrt{3} \right), \quad (2.18)$$

which is useful when t is large. We also integrate the density over $(0, t)$ to derive the distribution function

$$F(t) = \frac{1}{\sqrt{6}} \sum_{k=-\infty}^{\infty} \frac{1}{(\theta + k\pi)} \left(1 - e^{-\frac{1}{2}(\theta+k\pi)^2 t} \right) \left((-1)^k + \sqrt{3} \right). \quad (2.19)$$

On the other hand, denote by $x := e^{-\sqrt{2}\beta}$, the series expansion implies

$$\mathbb{E}(e^{-\beta\tau}) = \frac{2x + 2x^3 + 4x^2}{3 + 3x^4 + 2x^2} = \frac{2}{3}x + \frac{4}{3}x^2 + \frac{2}{9}x^3 - \frac{8}{9}x^4 - \frac{22}{27}x^5 - \frac{20}{27}x^6 + O(x^7).$$

We invert it term by term to derive the density function

$$f(t) = \frac{2}{3}g(1, t) + \frac{4}{3}g(2, t) + \frac{2}{9}g(3, t) - \frac{8}{9}g(4, t) - \frac{22}{27}g(5, t) - \frac{20}{27}g(6, t) + O(g(7, t)), \quad (2.20)$$

which is useful when t is small. The distribution function is given by

$$F(t) = \frac{2}{3}\Psi(1, t) + \frac{4}{3}\Psi(2, t) + \frac{2}{9}\Psi(3, t) - \frac{8}{9}\Psi(4, t) - \frac{22}{27}\Psi(5, t) - \frac{20}{27}\Psi(6, t) + O(\Psi(7, t)). \quad (2.21)$$

Example 2.3.6 (Walsh Brownian motion). Let $b_1 = 1$, $b_2 = 2$, $b_3 = 3$ and $P_i = \frac{1}{3}$

for $i = 1, 2, 3$ in (2.10), then the Laplace transform of τ becomes

$$\mathbb{E}(e^{-\beta\tau}) = \frac{\frac{1}{3} \frac{1}{\sinh(\sqrt{2}\beta)} + \frac{1}{3} \frac{1}{\sinh(2\sqrt{2}\beta)} + \frac{1}{3} \frac{1}{\sinh(3\sqrt{2}\beta)}}{\frac{1}{3} \frac{\cosh(\sqrt{2}\beta)}{\sinh(\sqrt{2}\beta)} + \frac{1}{3} \frac{\cosh(2\sqrt{2}\beta)}{\sinh(2\sqrt{2}\beta)} + \frac{1}{3} \frac{\cosh(3\sqrt{2}\beta)}{\sinh(3\sqrt{2}\beta)}}.$$

Using Lemma 2.3.1, we can derive the poles of the Laplace transform by solving $y^4 - 12y^2 + 11 = 0$ and $y = \tan(\sqrt{2}\beta^*)$. Thus, we know $\pm 1 = \tan(\sqrt{2}\beta^*)$ and $\pm\sqrt{11} = \tan(\sqrt{2}\beta^*)$, and the poles are

$$-\beta^* = -\frac{1}{2} \left(\frac{1}{4}\pi + k\pi \right)^2 \quad \text{and} \quad -\beta^* = -\frac{1}{2} (\theta + k\pi)^2, \quad k \in \mathbb{Z}, \quad \text{where } \theta = \arctan(\sqrt{11}).$$

Using Theorem 2.3.2, we calculate the density function of τ to be

$$\begin{aligned} f(t) &= \frac{1}{10} \sum_{k=-\infty}^{\infty} e^{-\frac{1}{2}(\frac{1}{4}\pi + k\pi)^2 t} \left(2\sqrt{2}(-1)^k + 1 \right) \left(\frac{1}{4}\pi + k\pi \right) \\ &\quad + \frac{1}{15} \sum_{k=-\infty}^{\infty} e^{-\frac{1}{2}(\theta + k\pi)^2 t} \left((-1)^k \frac{\sqrt{12}}{\sqrt{11}} + \frac{6}{\sqrt{11}} + (-1)^{k+1} \frac{3\sqrt{3}}{\sqrt{11}} \right) (\theta + k\pi), \end{aligned} \tag{2.22}$$

which is useful when t is large. We also integrate the density over $(0, t)$ to derive the distribution function

$$\begin{aligned} F(t) &= \frac{1}{5} \sum_{k=-\infty}^{\infty} \frac{1}{(\frac{1}{4}\pi + k\pi)} \left(1 - e^{-\frac{1}{2}(\frac{1}{4}\pi + k\pi)^2 t} \right) \left(2\sqrt{2}(-1)^k + 1 \right) \\ &\quad + \frac{2}{15} \sum_{k=-\infty}^{\infty} \frac{1}{(\theta + k\pi)} \left(1 - e^{-\frac{1}{2}(\theta + k\pi)^2 t} \right) \left((-1)^k \frac{\sqrt{12}}{\sqrt{11}} + \frac{6}{\sqrt{11}} + (-1)^{k+1} \frac{3\sqrt{3}}{\sqrt{11}} \right). \end{aligned} \tag{2.23}$$

On the other hand, denote by $x := e^{-\sqrt{2}\beta}$, the series expansion implies

$$\begin{aligned} \mathbb{E}(e^{-\beta\tau}) &= \frac{2(x^{11} + x^{10} + x^9 - x^8 - 2x^7 - 2x^5 - x^4 + x^3 + x^2 + x)}{3x^{12} - x^{10} - x^8 - 2x^6 - x^4 - x^2 + 3} \\ &= \frac{2}{3}x + \frac{2}{3}x^2 + \frac{8}{9}x^3 - \frac{4}{9}x^4 - \frac{22}{27}x^5 + \frac{2}{27}x^6 + O(x^7). \end{aligned}$$

We invert it term by term to derive the density function

$$f(t) = \frac{2}{3}g(1,t) + \frac{2}{3}g(2,t) + \frac{8}{9}g(3,t) - \frac{4}{9}g(4,t) - \frac{22}{27}g(5,t) + \frac{2}{27}g(6,t) + O(g(7,t)), \quad (2.24)$$

which is useful when t is small. The distribution function is given by

$$F(t) = \frac{2}{3}\Psi(1,t) + \frac{2}{3}\Psi(2,t) + \frac{8}{9}\Psi(3,t) - \frac{4}{9}\Psi(4,t) - \frac{22}{27}\Psi(5,t) + \frac{2}{27}\Psi(6,t) + O(\Psi(7,t)). \quad (2.25)$$

2.4 Numerical Implementation

In this section, we present the numerical illustration for Example 2.3.4, 2.3.5 and 2.3.6. We will plot the density and distribution functions in each example, and study the accuracy of these functions.

For Example 2.3.4, we first consider the density function when t is large. As we discussed before, (2.14) is useful for large t . We define the truncated function

$$\begin{aligned} \bar{f}_n(t) := & \frac{\pi}{2\sqrt{3}} \sum_{k=1}^n e^{-\frac{1}{2}\pi^2(k-\frac{2}{3})^2 t} \left(k - \frac{2}{3}\right) \left((-1)^{k+1} + 1\right) \\ & + \frac{\pi}{2\sqrt{3}} \sum_{k=1}^n e^{-\frac{1}{2}\pi^2(k-\frac{1}{3})^2 t} \left(k - \frac{1}{3}\right) \left((-1)^{k+1} - 1\right), \end{aligned} \quad (2.26)$$

and plot $\bar{f}_2(t)$, $\bar{f}_4(t)$ and $\bar{f}_6(t)$ in Fig. 2.2a. To demonstrate the accuracy of the truncated functions, we also invert the Laplace transform $\mathbb{E}(e^{-\beta\tau})$ numerically using the Gaver-Stehfest method (see Cohen 2007), and view the resulting curve $\tilde{f}(t)$ as the benchmark in Fig. 2.2a.

Notice that we use the Gaver-Stehfest method to invert the Laplace transform because the method does not involve any complex number, hence it is easy to implement. Also, the computation speed of Gaver-Stehfest method is faster than other common numerical inverse Laplace transform methods, for example the Euler method.

We see from Fig. 2.2a that, when t is small, $\bar{f}_2(t)$, $\bar{f}_4(t)$ and $\bar{f}_6(t)$ are not accurate because they are far from the benchmark. As t increases, $\bar{f}_6(t)$ converges to $\tilde{f}(t)$ earlier than $\bar{f}_4(t)$ and $\bar{f}_2(t)$. When t is large enough, all the curves converge to $\tilde{f}(t)$.

The difference between $\bar{f}_n(t)$ and $\tilde{f}(t)$ is recorded in Table 2.1a. We denote by $d_n := |\tilde{f}(t) - \bar{f}_n(t)|$ the truncation error of $\bar{f}_n(t)$, for $n = 2, 4, 6$. We also set the

error tolerance level to be 0.0001. Then, if $d_n < 0.0001$, we say $\bar{f}_n(t)$ is sufficiently accurate; otherwise, it is not sufficiently accurate. From Table 2.1a, we know $d_6 < 0.0001$ for $t \geq 0.054$, so $\bar{f}_6(t)$ is a sufficiently accurate approximation for the density function of τ when $t \geq 0.054$.

For the distribution function (2.15), we define the truncated function

$$\begin{aligned} \bar{F}_n(t) := & \frac{1}{\sqrt{3\pi}} \sum_{k=1}^n \frac{1}{(k - \frac{2}{3})} \left(1 - e^{-\frac{1}{2}\pi^2(k - \frac{2}{3})^2 t}\right) \left((-1)^{k+1} + 1\right) \\ & + \frac{1}{\sqrt{3\pi}} \sum_{k=1}^n \frac{1}{(k - \frac{1}{3})} \left(1 - e^{-\frac{1}{2}\pi^2(k - \frac{1}{3})^2 t}\right) \left((-1)^{k+1} - 1\right), \end{aligned} \quad (2.27)$$

and plot $\bar{F}_2(t)$, $\bar{F}_4(t)$ and $\bar{F}_6(t)$ in Fig. 2.2b. We also invert the Laplace transform $\frac{\mathbb{E}(e^{-\beta\tau})}{\beta}$ numerically, and use the resulting curve $\tilde{F}(t)$ as the benchmark in Fig. 2.2b.

Next, we consider the density function when t is small. As we discussed before, (2.16) is useful for small t . We define the truncated function

$$\bar{f}_n(t) = \sum_{k=1}^n (-1)^{k-1} g(3k - 2, t) + \sum_{k=1}^n (-1)^{k-1} g(3k - 1, t), \quad (2.28)$$

and plot $\bar{f}_2(t)$, $\bar{f}_4(t)$ and $\bar{f}_6(t)$ in Fig. 2.2c. We also use the same benchmark as before, i.e., $\tilde{f}(t)$ obtained by inverting the Laplace transform $\mathbb{E}(e^{-\beta\tau})$ numerically.

We see from Fig. 2.2c that, when t is small, $\bar{f}_2(t)$, $\bar{f}_4(t)$ and $\bar{f}_6(t)$ are accurate. As t increases, $\bar{f}_2(t)$ diverges from the benchmark earlier than $\bar{f}_4(t)$ and $\bar{f}_6(t)$. When t is large enough, all the curves diverge from the benchmark.

The difference between $\bar{f}_n(t)$ and $\tilde{f}(t)$ is recorded in Table 2.1b. We denote by $e_n := |\tilde{f}(t) - \bar{f}_n(t)|$ the truncation error of $\bar{f}_n(t)$, for $n = 2, 4, 6$. From Table 2.1b we know, with the error tolerance level 0.0001, $\bar{f}_6(t)$ is sufficiently accurate when $t \leq 26.945$.

For the distribution function (2.17), we define the truncated function

$$\bar{F}_n(t) = \sum_{k=1}^n (-1)^{k-1} \Psi(3k - 2, t) + \sum_{k=1}^n (-1)^{k-1} \Psi(3k - 1, t), \quad (2.29)$$

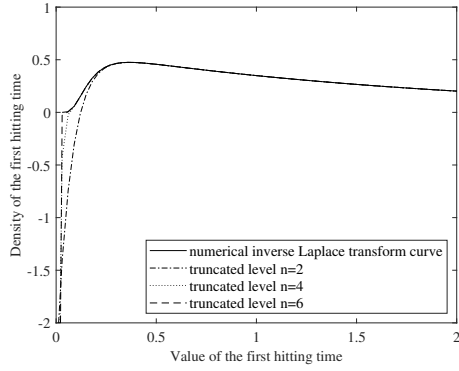
and plot $\bar{F}_2(t)$, $\bar{F}_4(t)$ and $\bar{F}_6(t)$ in Fig. 2.2d. We also invert the Laplace transform $\frac{\mathbb{E}(e^{-\beta\tau})}{\beta}$ numerically, and use the resulting curve $\tilde{F}(t)$ as the benchmark in Fig. 2.2d.

In conclusion, with the truncation level $n = 6$ and the error tolerance level 0.0001, the truncated density function (2.26) is sufficiently accurate for $t \geq 0.054$; while the

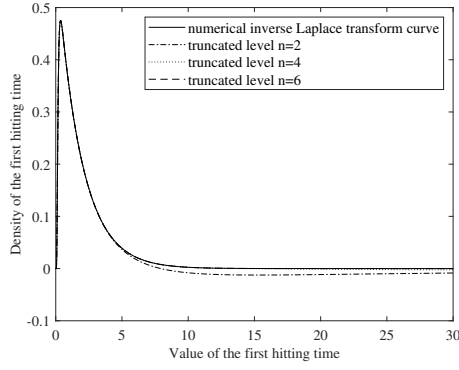
truncated density function (2.28) is sufficiently accurate for $t \leq 26.945$.

A similar analysis is conducted for Example 2.3.5, with the results recorded in the Fig. 2.3 and Table 2.2. In conclusion, with the truncation level $n = 6$ and the error tolerance level 0.0001, the truncated function of (2.18) is sufficiently accurate for $t \geq 0.055$; while the truncated function of (2.20) is sufficiently accurate for $t \leq 3.181$.

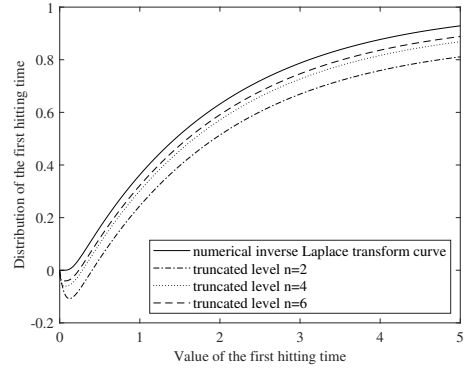
For Example 2.3.6, the numerical results are recorded in Fig. 2.4 and Table 2.3. In conclusion, with the truncation level $n = 6$ and the error tolerance level 0.0001, the truncated function of (2.22) is sufficiently accurate for $t \geq 0.261$; while the truncated function of (2.24) is sufficiently accurate for $t \leq 2.995$.



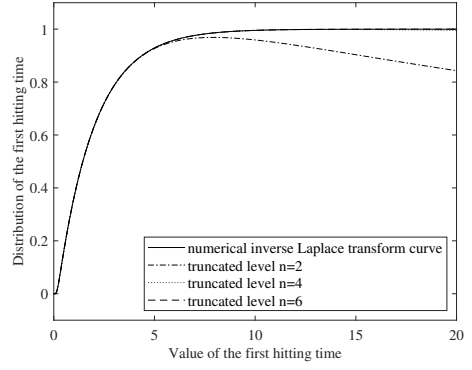
(a) Truncated functions (2.26).



(c) Truncated functions (2.28).



(b) Truncated functions (2.27).



(d) Truncated functions (2.29).

Figure 2.2 Density and distribution functions in Example 2.3.4.

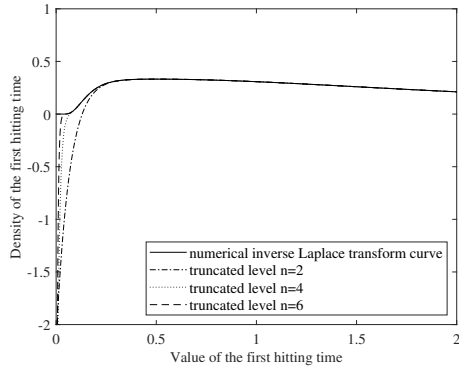
Table 2.1 Truncation error of (2.26) and (2.28) for $n = 2, 4, 6$.

(a) Truncation error of (2.26).

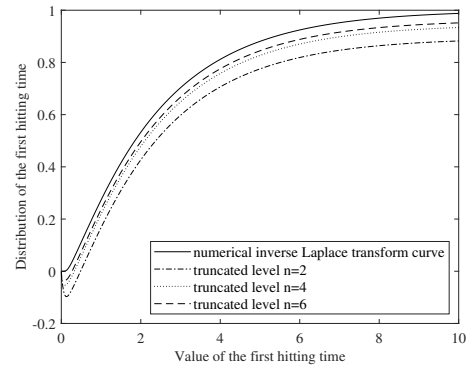
t	d_2	d_4	d_6
0.001	2.3776	4.4812	6.0890
...
0.053	0.8770	0.0577	0.0001
0.054	0.8578	0.0508	0.0000
...
0.134	0.1148	0.0001	0.0000
0.135	0.1118	0.0000	0.0000
...
0.551	0.0001	0.0000	0.0000
0.552	0.0000	0.0000	0.0000

(b) Truncation error of (2.28).

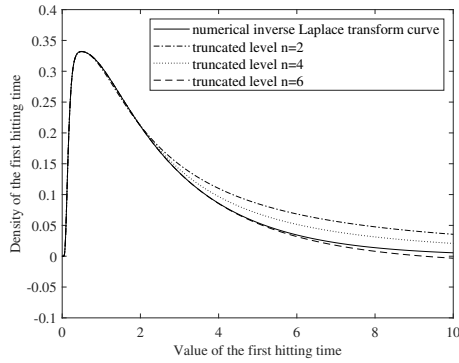
t	e_2	e_4	e_6
2.732	0.0000	0.0000	0.0000
2.733	0.0001	0.0000	0.0000
...
11.688	0.0119	0.0000	0.0000
11.689	0.0119	0.0001	0.0000
...
26.945	0.0094	0.0021	0.0000
26.946	0.0094	0.0021	0.0001



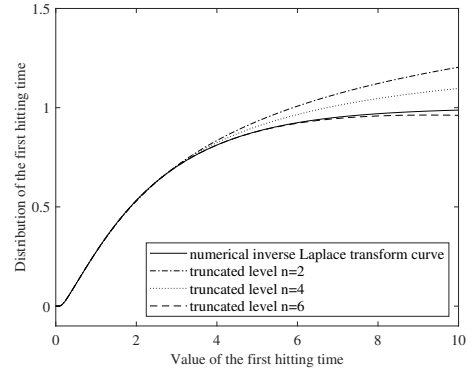
(a) Density function (2.18) truncated at $n = 2, 4, 6$.



(b) Distribution function (2.19) truncated at $n = 2, 4, 6$.



(c) Density function (2.20) truncated at $n = 2, 4, 6$.



(d) Distribution function (2.21) truncated at $n = 2, 4, 6$.

Figure 2.3 Density and distribution functions in Example 2.3.5.

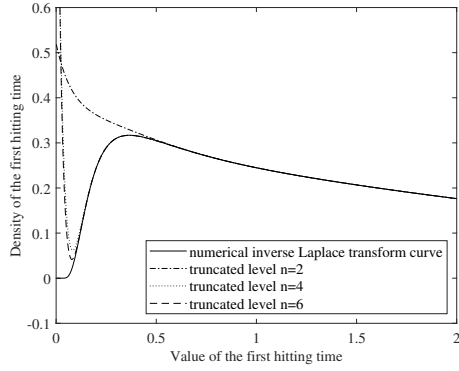
Table 2.2 Truncation error of (2.18) and (2.20) for $n = 2, 4, 6$.

(a) Truncation error of (2.18).

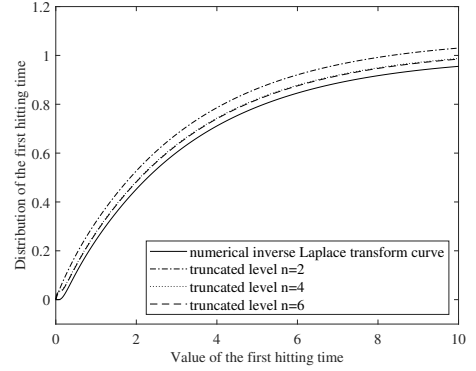
t	d_2	d_4	d_6
0.001	2.1157	3.9877	5.4186
...
0.054	0.7607	0.0477	0.0001
0.055	0.7444	0.0436	0.0000
...
0.134	0.1107	0.0001	0.0000
0.135	0.1080	0.0000	0.0000
...
0.536	0.0001	0.0000	0.0000
0.537	0.0000	0.0000	0.0000

(b) Truncation error of (2.20).

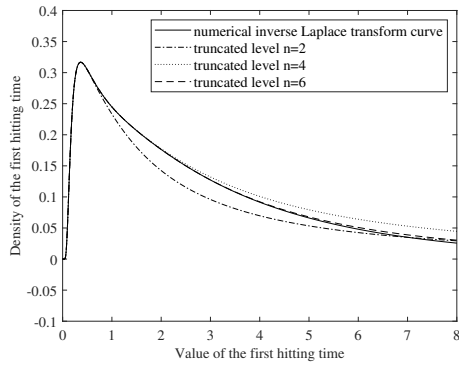
t	e_2	e_4	e_6
0.301	0.0000	0.0000	0.0000
0.302	0.0001	0.0000	0.0000
...
1.431	0.0035	0.0000	0.0000
1.432	0.0035	0.0001	0.0000
...
3.181	0.0154	0.0066	0.0000
3.182	0.0155	0.0066	0.0001



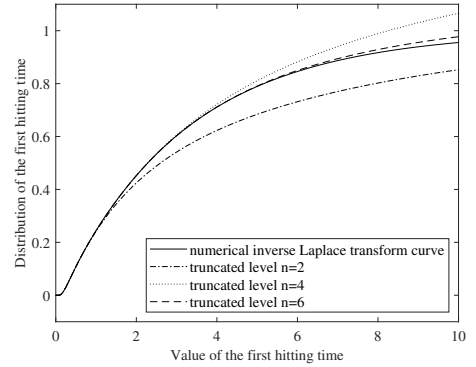
(a) Density function (2.22) truncated at $n = 2, 4, 6$.



(b) Distribution function (2.23) truncated at $n = 2, 4, 6$.



(c) Density function (2.24) truncated at $n = 2, 4, 6$.



(d) Distribution function (2.25) truncated at $n = 2, 4, 6$.

Figure 2.4 Density and distribution functions in Example 2.3.6.

Table 2.3 Truncation error of (2.22) and (2.24) for $n = 2, 4, 6$.

(a) Truncation error of (2.22).

t	d_2	d_4	d_6
0.001	0.5183	1.2908	1.3865
...
0.260	0.0537	0.0002	0.0001
0.261	0.0530	0.0002	0.0000
...
0.275	0.0437	0.0001	0.0000
0.276	0.0431	0.0000	0.0000
...
0.897	0.0001	0.0000	0.0000
0.898	0.0000	0.0000	0.0000

(b) Truncation error of (2.24).

t	e_2	e_4	e_6
0.029	0.0000	0.0000	0.0000
0.030	0.0001	0.0000	0.0000
...
1.336	0.0225	0.0000	0.0000
1.337	0.0225	0.0001	0.0000
...
2.995	0.0314	0.0048	0.0000
2.996	0.0314	0.0048	0.0001

Chapter 3

Parisian time of reflected Brownian motion with drift on rays

Suppose we have a system of rays emanating from a common origin and a particle $X(t)$ moving on this system. On each ray, the particle behaves as a reflected Brownian motion with drift; and once at the origin, it instantaneously chooses a ray for its next voyage randomly according to a given distribution. We are interested in the time length the particle spends on each ray, and the first time that the excursion time length on a ray exceeds a predefined threshold (see Fig 3.1). We call this first exceeding time of threshold a Parisian time, as it generalises the same concept in literature.

This chapter is also motivated by the RTGS system (see Chapter 2). In this chapter, we are interested in another source of liquidity risk, the time-lag between the exe-

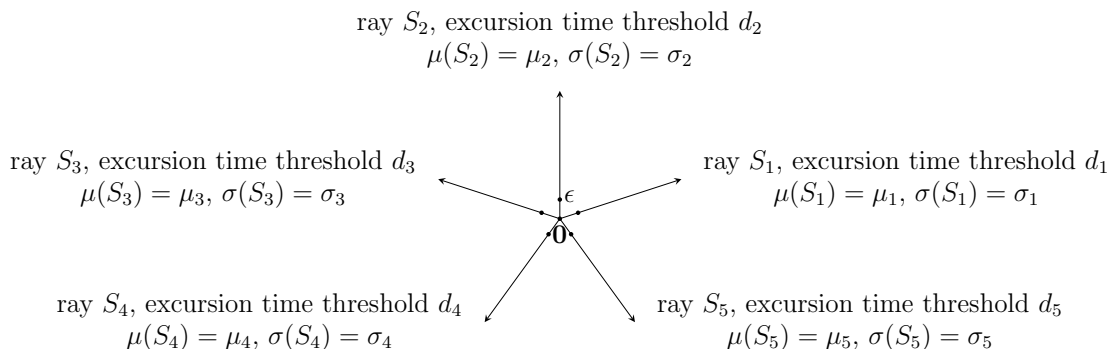


Figure 3.1 A reflected Brownian motion with drift on a collection of 5 rays.

cution of the transaction and its final completion. As it is explained in McDonough (1997) and Padoa-Schioppa (2005), if a counterparty does not settle an obligation for the full value when due but at some unspecified time thereafter, the expected liquidity position of the payee could be affected. The settlement delay may force the payee to cover its cash-flow shortage by funding at short notice from other sources, which may result in a financial loss due to higher financing costs or to damage to its reputation. In more extreme cases it may be unable to cover its cash-flow shortage at any price, in which case it may be unable to meet its obligation to others. As the settlement delay is the major source of liquidity risk in the RTGS system, both the central bank and the participating banks are interested in the length of the delay. Previous research in Che and Dassios (2013) has shown that the Markov-type models are adequate for CHAPS, we will extend this model here to study the settlement delay. For bank A and bank i in CHAPS, we view the net balance between them as a reflected Brownian motion with drift. Assume that bank A has set a time limit d_i on the duration of settlement delay for bank i , and they are interested in the first time that the limit is exceeded. In practice, an individual bank could set multiple limits or even remove the limit on different types of counterparties. We reduce this problem to the calculation of the Parisian time of a reflected Brownian motion with drift on rays. For more details about the CHAPS, see Che (2011) and Soramäki et al. (2007).

The rest of this chapter is organised as follows. We construct the reflected Brownian motion with drift on rays in Section 3.1, then calculate the Laplace transform of the Parisian time in Section 3.2. An exact simulation algorithm to sample from the distribution of the Parisian time is provided in Section 3.3. We discuss the application of these results in Section 3.4.

3.1 Construction of the underlying process and the Parisian time

The underlying process $X(t)$ used in this chapter is exactly the ‘reflected Brownian motion with drift on rays’ constructed in Chapter 2. To avoid repetition, we refer the reader to Section 2.1 for the construction and special cases of the underlying process.

Next, we define the last zero time and excursion time length of $X(t)$ as $g(t) := \sup\{s \leq t \mid |X(s)| = 0\}$ and $U(t) := t - g(t)$. Then $U(t)$ represents the time length $X(t)$ has spent in the current ray since last time at the origin. On each ray S_i , there

is a threshold $d_i > 0$ for the excursion time length, our target is to find the first time that the threshold is exceeded by $U(t)$. Thus, we are interested in the Parisian time τ defined as

$$\begin{aligned}\tau_i &:= \inf\{t \geq 0 \mid U(t) \geq d_i, \Theta(t^-) = S_i\}, \text{ for } i = 1, \dots, n, \\ \tau &:= \min_{i=1, \dots, n} \tau_i.\end{aligned}\tag{3.1}$$

Note that $X(t)$ may make an excursion with infinite time length on a ray S_i if the drift μ_i on this ray is positive. But since our target is to study the Parisian time τ , we are only interested in the excursion time length up to d_i , even if the total length is infinite.

We need to calculate the excursion time length of $X(t)$, but the problem is there is no first excursion from zero; before any $t > 0$, the process has made an infinite number of small excursions away from the origin. To approximate the dynamic of a Brownian motion, Dassios and Wu (2010) introduced the ‘‘perturbed Brownian motion’’, we will extend this idea here.

For every $\epsilon > 0$, we define a perturbed process $X^\epsilon(t) = (|X^\epsilon(t)|, \Theta^\epsilon(t))$ on the system of rays S . On each ray S_i , $|X^\epsilon(t)|$ behaves as a reflected Brownian motion with drift μ_i , dispersion σ_i and starting from ϵ , as long as it does not return to the origin. Once at the origin, $X^\epsilon(t)$ not only chooses a new ray according to P , but also jumps to ϵ on the new ray. In other words, $X^\epsilon(t)$ has a perturbation of size ϵ at the origin which can be described as

$$\mathbb{P}(X^\epsilon(t) = (\epsilon, S_i) \mid |X^\epsilon(t^-)| = 0) = P_i, \quad i \in \{1, \dots, n\}.$$

Hence, we describe the behaviour of $X^\epsilon(t)$ as follows. The initial state of $X^\epsilon(t)$ is distributed as $\mathbb{P}(X^\epsilon(0) = (\epsilon, S_i)) = P_i$, $i = 1, \dots, n$. Then it behaves as a Brownian motion with drift μ_i , dispersion σ_i and starting from ϵ on ray S_i , as long as it does not return to the origin. Once at the origin, it instantaneously chooses a new ray according to P and jumps to ϵ on the new ray.

We define the Parisian time of $X^\epsilon(t)$ similarly as before. Let $g^\epsilon(t) := \sup\{s \leq t \mid |X^\epsilon(s)| = 0\}$ and $U^\epsilon(t) := t - g^\epsilon(t)$. We are interested in the Parisian time τ^ϵ defined as

$$\begin{aligned}\tau_i^\epsilon &:= \inf\{t \geq 0 \mid U^\epsilon(t) \geq d_i, \Theta^\epsilon(t^-) = S_i\}, \text{ for } i = 1, \dots, n, \\ \tau^\epsilon &:= \min_{i=1, \dots, n} \tau_i^\epsilon,\end{aligned}$$

As $\epsilon \rightarrow 0$, the perturbation at origin vanishes, and $X^\epsilon(t) \rightarrow X(t)$ in a pathwise sense, then $\tau^\epsilon \rightarrow \tau$ in distribution. Hence we will first derive the Laplace transform of τ^ϵ , then take the limit $\lim_{\epsilon \rightarrow 0} \mathbb{E}(e^{-\beta\tau^\epsilon})$ to calculate the Laplace transform of the Parisian time τ .

3.2 Laplace transform of τ

In this section, we derive the Laplace transform of the Parisian. For simplicity, we denote the symmetric function

$$\Psi(x) := 2\sqrt{\pi}x\Phi(\sqrt{2}x) - \sqrt{\pi}x + e^{-x^2}, \quad x \in \mathbb{R},$$

where $\Phi(\cdot)$ is the cumulative distribution function of standard normal distribution; and the constant

$$C_i := P_i \left(\frac{2}{\sqrt{2\pi\sigma_i^2 d_i}} \Psi \left(\frac{\mu_i \sqrt{d_i}}{\sqrt{2\sigma_i^2}} \right) + \frac{\mu_i}{\sigma_i^2} \right),$$

where μ_i , σ_i , P_i and d_i are defined in Section 3.1. For $\mu_i \in \mathbb{R}$, $\sigma_i \in \mathbb{R}^+$, $P_i \in (0, 1]$ and $d_i > 0$, we deduce from the definition that $C_i > 0$.

Theorem 3.2.1. *Let $X(t)$ be a reflected Brownian motion with drift on a system of rays S , where $\mu_i \in \mathbb{R}$, $\sigma_i \in \mathbb{R}^+$, $P_i \in (0, 1]$ and $d_i > 0$ are the drift, dispersion, entering probability and excursion time threshold of ray S_i , $i = 1, \dots, n$. For $\beta \geq 0$, the Laplace transform of the Parisian time τ is*

$$\mathbb{E}(e^{-\beta\tau}) = \frac{\sum_{i=1}^n e^{-\beta d_i} C_i}{\sum_{i=1}^n C_i + \sum_{i=1}^n P_i \int_0^{d_i} (1 - e^{-\beta v}) e^{-\frac{\mu_i^2}{2\sigma_i^2} v} \frac{1}{\sqrt{2\pi\sigma_i^2 v^3}} dv}, \quad (3.2)$$

and the expectation of τ is

$$\mathbb{E}(\tau) = \frac{\sum_{i=1}^n d_i C_i + \sum_{i=1}^n P_i \int_0^{d_i} e^{-\frac{\mu_i^2}{2\sigma_i^2} v} \frac{1}{\sqrt{2\pi\sigma_i^2 v}} dv}{\sum_{i=1}^n C_i}. \quad (3.3)$$

Proof. We prepare some preliminary formulas for the proof. From Section 3.1, we know $X^\epsilon(t)$ starts from ϵ on ray S_i , and behaves as a Brownian motion with drift μ_i and dispersion σ_i as long as it does not return to the origin. Let $g_i(\epsilon, t)$ be the

density of the first hitting time at 0 of such a Brownian motion, then

$$g_i(\epsilon, t) = \frac{\epsilon}{\sqrt{2\pi\sigma_i^2 t^3}} e^{-\frac{(\epsilon+\mu_i t)^2}{2\sigma_i^2 t}}, \text{ for } \mu_i \in \mathbb{R}, \sigma_i \in \mathbb{R}^+, \epsilon > 0, t > 0, i = 1, \dots, n.$$

We define the following functions in ϵ ,

$$L_i(\epsilon) := \int_0^{d_i} e^{-\beta t} g_i(\epsilon, t) dt \text{ and } U_i(\epsilon) := \int_{d_i}^{\infty} e^{-\beta d_i} g_i(\epsilon, t) dt,$$

and call them L_i and U_i for convenience. In their Laplace transforms respectively, L_i represents the excursion time length of $X^\epsilon(t)$ on ray S_i if it is shorter than the threshold d_i , and U_i represents the excursion time length if it is longer than d_i . In the latter case, we set the excursion time length to be d_i because we are only interested in the excursion up to the threshold.

These functions have the limits

$$\lim_{\epsilon \rightarrow 0} U_i(\epsilon) = 0 \text{ and } \lim_{\epsilon \rightarrow 0} L_i(\epsilon) = 1.$$

Moreover, we calculate the limits of their derivatives to be

$$\lim_{\epsilon \rightarrow 0} \left(\frac{d}{d\epsilon} U_i(\epsilon) \right) = e^{-\beta d_i} \left(\frac{2}{\sqrt{2\pi\sigma_i^2 d_i}} \Psi \left(\frac{\mu_i \sqrt{d_i}}{\sqrt{2\sigma_i^2}} \right) + \frac{\mu_i}{\sigma_i^2} \right), \quad (3.4)$$

$$\begin{aligned} & \lim_{\epsilon \rightarrow 0} \left(\frac{d}{d\epsilon} L_i(\epsilon) \right) \\ &= - \frac{2}{\sqrt{2\pi\sigma_i^2 d_i}} \Psi \left(\sqrt{\frac{\mu_i^2 d_i}{2\sigma_i^2} + \beta d_i} \right) - \frac{\mu_i}{\sigma_i^2} \\ &= - \left(\frac{2}{\sqrt{2\pi\sigma_i^2 d_i}} \Psi \left(\frac{\mu_i \sqrt{d_i}}{\sqrt{2\sigma_i^2}} \right) + \frac{\mu_i}{\sigma_i^2} \right) - \int_0^{d_i} (1 - e^{-\beta y}) e^{-\frac{\mu_i^2}{2\sigma_i^2} y} \frac{1}{\sqrt{2\pi\sigma_i^2 y^3}} dy. \end{aligned} \quad (3.5)$$

The last equation can be checked using $\Psi(x) = 1 + \int_0^1 (1 - e^{-x^2 v}) \frac{1}{2v^{3/2}} dv$, which is obtained by a direct calculation from the definition of $\Psi(x)$.

Now we study the Parisian time τ^ϵ . Define the sequence of random times

$$\zeta_0 = 0, \zeta_{m+1} = \inf\{t > \zeta_m \mid |X^\epsilon(t)| = 0\}, \text{ for } m \in \mathbb{N}_0$$

recursively, and the mutually exclusive events

$$C_m := \{\zeta_m \leq \tau^\epsilon < \zeta_{m+1}\}, \text{ for } m \in \mathbb{N}_0.$$

Then C_m denotes the event that the exceeding of threshold occurs during the $(m+1)$ -th excursion of $X^\epsilon(t)$ away from the origin. Next, we set $\{X^\epsilon(0) = (\epsilon, S_i)\}$ for an arbitrary but fixed i , and calculate the Laplace transforms $\mathbb{E}(e^{-\beta\tau^\epsilon} \mathbb{1}_{\{C_m\}} | X^\epsilon(0) = (\epsilon, S_i))$ for $m \in \mathbb{N}_0$.

For $m = 0$, we interpret C_0 as follows. Starting from ϵ on ray S_i , $X^\epsilon(t)$ spends more than d_i time before hitting the origin, hence the exceeding occurs during the first excursion. This is equivalent to the event that a Brownian motion with drift μ_i and dispersion σ_i spends more than d_i time to travel from ϵ to 0, which has probability $\int_{d_i}^\infty g_i(\epsilon, t)dt$. Thus $(\tau^\epsilon \mathbb{1}_{\{C_0\}} | X^\epsilon(0) = (\epsilon, S_i)) = d_i$, and

$$\mathbb{E}(e^{-\beta\tau^\epsilon} \mathbb{1}_{\{C_0\}} | X^\epsilon(0) = (\epsilon, S_i)) = \int_{d_i}^\infty e^{-\beta d_i} g_i(\epsilon, t)dt = U_i.$$

Next, we consider the event C_1 . In this case, the duration of the first excursion of $X^\epsilon(t)$ is shorter than d_i , and the Laplace transform of the duration is $\int_0^{d_i} e^{-\beta s} g_i(\epsilon, t)dt$. After the first excursion, $X^\epsilon(t)$ returns to the origin and jumps to (ϵ, S_k) with probability P_k , then exceeds the excursion time threshold d_k before returning to the origin. But the behaviour of $X^\epsilon(t)$ during the second excursion is similar to what we described for C_0 , with the index i replaced by k . Thus, we have

$$\begin{aligned} & \mathbb{E}(e^{-\beta\tau^\epsilon} \mathbb{1}_{\{C_1\}} | X^\epsilon(0) = (\epsilon, S_i)) \\ &= \left(\int_0^{d_i} e^{-\beta s} g_i(\epsilon, t)dt \right) \left(\sum_{k=1}^n P_k \mathbb{E}(e^{-\beta\tau^\epsilon} \mathbb{1}_{\{C_0\}} | X^\epsilon(0) = (\epsilon, S_k)) \right) \\ &= L_i \left(\sum_{k=1}^n P_k U_k \right). \end{aligned}$$

In the same way, we consider the event C_2 . In this case, the duration of the first excursion of $X^\epsilon(t)$ is shorter than d_i , with the Laplace transform $\int_0^{d_i} e^{-\beta s} g_i(\epsilon, t)dt$. After the first excursion, $X^\epsilon(t)$ returns to the origin and jumps to (ϵ, S_k) with probability P_k . Restarting from (ϵ, S_k) , $X^\epsilon(t)$ will exceed the excursion time threshold exactly during the second excursion (hence the third in total). But the behaviour of $X^\epsilon(t)$ during the second and third excursions is similar to what we described for

C_1 , with the index i replaced by k . Hence

$$\begin{aligned} & \mathbb{E} \left(e^{-\beta\tau^\epsilon} \mathbf{1}_{\{C_2\}} \mid X^\epsilon(0) = (\epsilon, S_i) \right) \\ &= \left(\int_0^{d_i} e^{-\beta s} g_i(\epsilon, t) dt \right) \left(\sum_{k=1}^n P_k \mathbb{E} \left(e^{-\beta\tau^\epsilon} \mathbf{1}_{\{C_1\}} \mid X^\epsilon(0) = (\epsilon, S_k) \right) \right) \\ &= L_i \left(\sum_{k=1}^n P_k L_k \left(\sum_{j=1}^n P_j U_j \right) \right) = L_i \left(\sum_{k=1}^n P_k L_k \right) \left(\sum_{j=1}^n P_j U_j \right). \end{aligned}$$

The same explanation applies to C_m for any positive integer m , i.e., the duration of the first excursion of $X^\epsilon(t)$ is shorter than d_i , after that $X^\epsilon(t)$ restarts from (ϵ, S_k) and exceeds the threshold exactly during the m -th excursion. Hence we deduce that

$$\mathbb{E} \left(e^{-\beta\tau^\epsilon} \mathbf{1}_{\{C_m\}} \mid X^\epsilon(0) = (\epsilon, S_i) \right) = L_i \left(\sum_{k=1}^n P_k \mathbb{E} \left(e^{-\beta\tau^\epsilon} \mathbf{1}_{\{C_{m-1}\}} \mid X^\epsilon(0) = (\epsilon, S_k) \right) \right).$$

This implies a recursive structure between the Laplace transforms of τ^ϵ conditioned on C_m and C_{m-1} , we solve for

$$\mathbb{E} \left(e^{-\beta\tau^\epsilon} \mathbf{1}_{\{C_m\}} \mid X^\epsilon(0) = (\epsilon, S_i) \right) = L_i \left(\sum_{k=1}^n P_k L_k \right)^{m-1} \left(\sum_{j=1}^n P_j U_j \right), \quad m = 1, 2, \dots$$

Since the exceeding of threshold may occur during any excursion of $X^\epsilon(t)$, we need to sum the result over $m \in \mathbb{N}_0$, this gives

$$\begin{aligned} & \mathbb{E} \left(e^{-\beta\tau^\epsilon} \mid X^\epsilon(0) = (\epsilon, S_i) \right) = \sum_{m=0}^{\infty} \mathbb{E} \left(e^{-\beta\tau^\epsilon} \mathbf{1}_{\{C_m\}} \mid X^\epsilon(0) = (\epsilon, S_i) \right) \\ &= U_i + \sum_{m=1}^{\infty} \left(L_i \left(\sum_{k=1}^n P_k L_k \right)^{m-1} \left(\sum_{j=1}^n P_j U_j \right) \right) = U_i + \frac{L_i \left(\sum_{j=1}^n P_j U_j \right)}{1 - \sum_{k=1}^n P_k L_k}, \end{aligned} \tag{3.6}$$

the last equation holds because for each k , $g_k(\epsilon, t)$ is a probability density function on $(0, \infty)$, so for any $\beta \geq 0$,

$$0 < \sum_{k=1}^n P_k L_k = \sum_{k=1}^n P_k \int_0^{d_k} e^{-\beta s} g_k(\epsilon, s) ds \leq \sum_{k=1}^n P_k \int_0^{d_k} g_k(\epsilon, s) ds < \sum_{k=1}^n P_k = 1.$$

Equation (3.6) boils down the Laplace transform of τ^ϵ to the initial state of $X^\epsilon(t)$, which is distributed as $\mathbb{P}(X^\epsilon(0) = (\epsilon, S_i)) = P_i$. Then we calculate the Laplace

transform of τ^ϵ to be

$$\begin{aligned}\mathbb{E}(e^{-\beta\tau^\epsilon}) &= \sum_{i=1}^n P_i \mathbb{E}(e^{-\beta\tau^\epsilon} \mid X^\epsilon(0) = (\epsilon, S_i)) \\ &= \sum_{i=1}^n P_i \left(U_i + \frac{L_i(\sum_{j=1}^n P_j U_j)}{1 - \sum_{k=1}^n P_k L_k} \right) = \frac{\sum_{i=1}^n P_i U_i(\epsilon)}{1 - \sum_{k=1}^n P_k L_k(\epsilon)}.\end{aligned}\tag{3.7}$$

As $\epsilon \rightarrow 0$, both numerator and denominator of the right hand side of (3.7) tend to 0, then we can calculate the limit $\lim_{\epsilon \rightarrow 0} \mathbb{E}(e^{-\beta\tau^\epsilon})$ using (3.4) and (3.5), and this gives $\mathbb{E}(e^{-\beta\tau})$. The expectation of τ is obtained by applying the moment generating function. \square

As in Section 3.1, $X(t)$ can be reduced to a Brownian motion with drift or a standard Brownian motion by choosing the parameters accordingly, then we can compare Theorem 3.2.1 with the results in the existing literature.

Remark 4. When $n = 2$, $\mu_1 = \mu \geq 0$, $\mu_2 = -\mu$, $\sigma_1 = \sigma_2 = 1$, $P_1 = P_2 = \frac{1}{2}$ and $d_1 > 0$, $d_2 > 0$, equation (3.2) becomes the Laplace transform of the two-sided Parisian time of a Brownian motion with drift

$$\mathbb{E}(e^{-\beta\tau}) = \frac{e^{-\beta d_1} \left(\sqrt{d_2} \Psi\left(\mu \sqrt{\frac{d_1}{2}}\right) + \mu \sqrt{\frac{d_1 d_2 \pi}{2}} \right) + e^{-\beta d_2} \left(\sqrt{d_1} \Psi\left(\mu \sqrt{\frac{d_2}{2}}\right) - \mu \sqrt{\frac{d_1 d_2 \pi}{2}} \right)}{\sqrt{d_2} \Psi\left(\sqrt{\left(\beta + \frac{\mu^2}{2}\right) d_1}\right) + \sqrt{d_1} \Psi\left(\sqrt{\left(\beta + \frac{\mu^2}{2}\right) d_2}\right)},$$

this is the main result of Dassios and Wu (2010). Moreover, for $n = 2$, $P_1 = P_2 = \frac{1}{2}$, $\mu_1 = \mu_2 = 0$, $\sigma_1 = \sigma_2 = 1$, we set $d_2 > 0$ and let $d_1 \rightarrow \infty$, then equation (3.2) gives the Laplace transform of the one-sided Parisian time of a standard Brownian motion

$$\mathbb{E}(e^{-\beta\tau}) \rightarrow \frac{1}{1 + 2\sqrt{\pi\beta d_2} \exp(\beta d_2) \Phi(\sqrt{2\beta d_2})},$$

this was derived in Section 8.4.1 of Chesney et al. (1997).

3.3 Exact simulation algorithm of the Parisian time

In this section we provide an exact simulation algorithm to sample from the distribution of the Parisian time τ . Our algorithm is based on the exact simulation schemes

of the truncated Lévy subordinator developed in Dassios et al. (2020). We refer to Algorithm 4.3 and 4.4 of Dassios et al. (2020) as $\text{AlgorithmI}(\cdot)$ and $\text{AlgorithmII}(\cdot, \cdot)$, their full steps are attached in Appendix B.

Algorithm 3.3.1. *Exact simulation algorithm of the Parisian time τ .*

1. Initialise $\mu_i, \sigma_i, P_i, d_i$ and calculate C_i for $i = 1, \dots, n$. Set $\lambda = \sum_{i=1}^n C_i$.
2. Generate a multinomial random variable I whose probability function is

$$\mathbb{P}(I = i) = \frac{C_i}{\sum_{j=1}^n C_j} \text{ for } i = 1, \dots, n,$$

via the following steps:

- (a) Generate a uniform random variable $U_1 \sim U[0, 1]$.
- (b) Set $\mathbb{P}(I = 0) = 0$. For $i = 1, \dots, n$, find the unique i such that

$$\sum_{j=0}^{i-1} \mathbb{P}(I = j) < U_1 \leq \sum_{j=0}^i \mathbb{P}(I = j),$$

then return $I = i$.

3. Generate a random variable τ^* via the following steps:

- (a) Generate an exponential random variable $T \sim \exp(\lambda)$ by setting $U_2 \sim U[0, 1]$, then return $T = -\frac{1}{\lambda} \ln(1 - U_2)$.
- (b) For each $i = 1, \dots, n$, generate the following subordinator:
 - If $\mu_i = 0$, generate a subordinator X_i by setting $\alpha = \frac{1}{2}$ and

$$X_i = \text{AlgorithmI} \left(\frac{TP_i}{\sqrt{2\pi\sigma_i^2 d_i}} \frac{\Gamma(1 - \alpha)}{\alpha} \right);$$

- If $\mu_i \neq 0$, generate a subordinator X_i by setting $\alpha = \frac{1}{2}$ and

$$X_i = \text{AlgorithmII} \left(\frac{TP_i}{\sqrt{2\pi\sigma_i^2 d_i}} \frac{\Gamma(1 - \alpha)}{\alpha}, \frac{\mu_i^2 d_i}{2\sigma_i^2} \right).$$

- (c) Set $\tau^* = \sum_{i=1}^n d_i X_i$.

4. Output $\tau = \tau^* + d_I$.

Proof. For simplicity, we denote by $M := \sum_{i=1}^n e^{-\beta d_i} C_i$ and $\lambda := \sum_{i=1}^n C_i$, then the Laplace transform (3.2) can be written as

$$\mathbb{E}(e^{-\beta\tau}) = \frac{M}{\lambda + \sum_{i=1}^n P_i \int_0^{d_i} (1 - e^{-\beta v}) e^{-\frac{\mu_i^2}{2\sigma_i^2} v} \frac{1}{\sqrt{2\pi\sigma_i^2 v^3}} dv}, \text{ for } \beta \geq 0.$$

Since $C_i > 0$ for $i = 1, \dots, n$, we know $\lambda > 0$, and the denominator of $\mathbb{E}(e^{-\beta\tau})$ is positive. This enables us to rewrite the Laplace transform in the integral form

$$\begin{aligned} & \mathbb{E}(e^{-\beta\tau}) \\ &= M \int_0^\infty \exp\left(-t \left(\lambda + \sum_{i=1}^n P_i \int_0^{d_i} (1 - e^{-\beta v}) e^{-\frac{\mu_i^2}{2\sigma_i^2} v} \frac{1}{\sqrt{2\pi\sigma_i^2 v^3}} dv\right)\right) dt \\ &= \frac{M}{\lambda} \int_0^\infty \lambda e^{-\lambda t} \exp\left(-\sum_{i=1}^n \frac{t P_i}{\sqrt{2\pi\sigma_i^2 d_i}} \int_0^1 (1 - e^{-\beta d_i z}) e^{-\frac{\mu_i^2 d_i}{2\sigma_i^2} z} \frac{1}{z^{3/2}} dz\right) dt. \end{aligned} \quad (3.8)$$

Equation (3.8) can be understood as a product of the Laplace transforms of two independent random variables, hence we can generate them separately, and view the Parisian time τ as their summation.

Denote by I a multinomial random variable with the probability function

$$\mathbb{P}(I = i) = \frac{C_i}{\sum_{j=1}^n C_j} \text{ for } i = 1, \dots, n,$$

then we can generate I using the inversion method for discrete random variable (see Devroye 1986 Section III.2), this becomes Step 2. Note that the random variable $d_I = \{d_1, \dots, d_n\}$ has the Laplace transform

$$\mathbb{E}(e^{-\beta d_I}) = \sum_{i=1}^n \left(e^{-\beta d_i} \frac{C_i}{\sum_{j=1}^n C_j} \right) = \frac{M}{\lambda}.$$

Next, we denote by τ^* the random variable whose Laplace transform is

$$\mathbb{E}(e^{-\beta\tau^*}) = \int_0^\infty \lambda e^{-\lambda t} \exp\left(-\sum_{i=1}^n \frac{t P_i}{\sqrt{2\pi\sigma_i^2 d_i}} \int_0^1 (1 - e^{-\beta d_i z}) e^{-\frac{\mu_i^2 d_i}{2\sigma_i^2} z} \frac{1}{z^{3/2}} dz\right) dt. \quad (3.9)$$

For each i , we interpret the expression

$$\exp\left(-\frac{tP_i}{\sqrt{2\pi\sigma_i^2d_i}}\int_0^1(1-e^{-\beta d_i z})e^{-\frac{\mu_i^2 d_i}{2\sigma_i^2}z}\frac{1}{z^{3/2}}dz\right) \quad (3.10)$$

as the Laplace transform of the random variable $d_i X_i(\frac{tP_i}{\sqrt{2\pi\sigma_i^2d_i}})$, where $X_i(\frac{tP_i}{\sqrt{2\pi\sigma_i^2d_i}})$ is a subordinator with truncated Lévy measure

$$v(dz) := e^{-\frac{\mu_i^2 d_i}{2\sigma_i^2}z}\frac{1}{z^{3/2}}\mathbb{1}_{\{0 < z < 1\}}dz$$

at time $\frac{tP_i}{\sqrt{2\pi\sigma_i^2d_i}}$. Comparing (3.10) with (B.1), we know $X_i(\cdot)$ can be generated via Algorithm 4.3 and 4.4 in Appendix B.

Moreover, (3.9) implies that $\tau^* \stackrel{\text{law}}{=} \sum_{i=1}^n d_i X_i(\frac{TP_i}{\sqrt{2\pi\sigma_i^2d_i}})$, where $T \sim \exp(\lambda)$ is an exponential random variable. Hence we generate T in Step 3(a), sample from $X_i(\frac{TP_i}{\sqrt{2\pi\sigma_i^2d_i}})$ in Step 3(b), and calculate τ^* via Step 3(c).

Finally, since $\mathbb{E}(e^{-\beta\tau}) = \mathbb{E}(e^{-\beta d_I})\mathbb{E}(e^{-\beta\tau^*})$, we have the representation $\tau \stackrel{\text{law}}{=} d_I + \tau^*$, where d_I and τ^* are independent, then τ can be generated via Step 4. \square

Next, we illustrate the accuracy and performance of the exact simulation algorithm with a numerical example. We set $n = 7$, and

$$\mu_1 = 0, \quad \mu_2 = 0.5, \quad \mu_3 = -0.3, \quad \mu_4 = 0, \quad \mu_5 = 0.2, \quad \mu_6 = 0, \quad \mu_7 = -0.1;$$

$$\sigma_1 = 1.5, \quad \sigma_2 = 2, \quad \sigma_3 = 1.3, \quad \sigma_4 = 1, \quad \sigma_5 = 2, \quad \sigma_6 = 1, \quad \sigma_7 = 1;$$

$$P_1 = 0.1, \quad P_2 = 0.2, \quad P_3 = 0.1, \quad P_4 = 0.2, \quad P_5 = 0.2, \quad P_6 = 0.1, \quad P_7 = 0.1;$$

$$d_1 = 1, \quad d_2 = 3, \quad d_3 = 2.5, \quad d_4 = 1.5, \quad d_5 = 1.5, \quad d_6 = 0.5, \quad d_7 = 2.5.$$

Using the exact simulation algorithm, we generate samples from the Parisian time and calculate their average. On the other hand, we use equation (3.3) to calculate the true expectation of τ to be 3.0534. Then we consider the following two standard measures for the associated error of the algorithm,

1. difference = sample average – true expectation
2. standard error = $\frac{\text{sample standard deviation}}{\sqrt{\text{number of samples}}}$

Table 3.1 reports the results, we see that the algorithm can achieve a high accuracy, and one has to generate more samples to decrease the standard error.

Table 3.1 Sample average and accuracy of the exact simulation algorithm.

Sample size	Sample average	Difference	Standard error
1000	3.0666	0.0132	0.0616
4000	3.0302	-0.0232	0.0304
16000	3.0470	-0.0065	0.0155
64000	3.0509	-0.0025	0.0077
256000	3.0520	-0.0014	0.0039
1024000	3.0538	0.0004	0.0019

In addition, we estimate the distribution function of the Parisian time. Using the exact simulation algorithm and the smoothing techniques (see Bowman and Azzalini, 1997), we get the estimated curve for the distribution function. On the other hand, we apply the Gaver-Stehfest method (see Cohen, 2007) to invert the Laplace transform $\frac{\mathbb{E}(e^{-\beta\tau})}{\beta}$ numerically. We set $\tilde{f}(\beta) := \frac{\mathbb{E}(e^{-\beta\tau})}{\beta}$ and calculate

$$f(t) \approx \frac{\ln(2)}{t} \sum_{k=1}^{2M} w_k \tilde{f}\left(\frac{k \ln(2)}{t}\right)$$

numerically, where the weights w_k are defined as

$$w_k := (-1)^{M+k} \sum_{j=\lceil (k+1)/2 \rceil}^{\min(k,M)} \frac{j^{M+1}}{M!} \binom{M}{j} \binom{2j}{j} \binom{j}{k-j},$$

and $\lceil x \rceil$ means the greatest integer less or equal to x . Then we obtain the inverted curve for the distribution function. These curves are provided in Figure 3.2, they show that the exact simulation algorithm provides a good approximation for the distribution of the Parisian time.

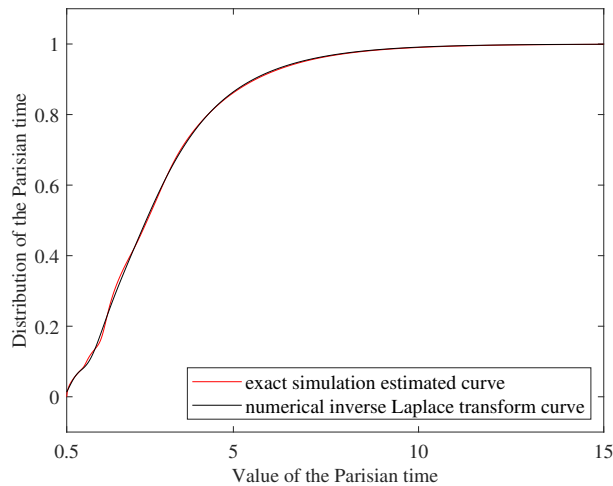


Figure 3.2 Inverted and numerical estimated curves of the distribution function.

We also illustrate the performance of the algorithm by recording the CPU time needed to generate these samples from the Parisian time. The experiment is implemented on an Intel Core i5-5200U CPU@2.20GHz processor, 8.00GB RAM, Windows 10, 64-bit Operating System and performed in Matlab R2019b. No parallel computing is used. Table 3.2 reports the results.

Table 3.2 CPU time of the exact simulation algorithm.

Sample size	CPU time (in seconds)
1000	0.201831
4000	0.725738
16000	3.080721
64000	12.214876
256000	52.715700
1024000	201.460605

3.4 Discussion

We can apply this model to study the settlement delay in CHAPS. For an individual bank A , we assume that there are n counterparties in the system, namely bank 1, bank 2, \dots , bank n . We also assume that bank A uses an internal queue to manage its outgoing payments, and once the current payment is settled, it has probability P_i to make another payment to bank i , $i = 1, \dots, n$. Let a reflected Brownian motion with drift μ_i and dispersion σ_i be the net balance between bank A and bank i . To avoid the excessive exposure to liquidity risk, a time limit d_i has been set for the duration of settlement delay between bank A and bank i . Both the central bank and the participating banks are interested in the first time that the limit is exceeded.

We model the net balance between bank A and the counterparties by the planar process $X(t)$, and view the first exceeding time as the Parisian time of $X(t)$. Using the results in the current chapter, we can sample from this first exceeding time and estimate its distribution function numerically. We remark that this approach can be adopted by both the policymaker in the central bank and the credit control departments of the participating banks to lay down decisive actions. For example, the central bank may use time-dependent transaction fees to provide incentives to earlier settlements. Alternatively, the participating banks may also learn to coordinate their payments over time, creating non-binding behavioural conventions or implicit contracts.

In particular, an empirical method has been developed in Denbee and Zimmerman (2012) to detect the apparent ‘free-riding’ in the RTGS system, referring to the

behaviour that the banks wait for incoming payments to fund subsequent outgoing payments and not supply an amount of liquidity to the system commensurate with the share of payments they are responsible for. Suppose the banks are required to hold buffers of liquid assets in order that they can make payments in a stress scenario, and the buffers are continuously calculated based on past activity. Banks may have an incentive to delay their payments so that the regulatory buffer will be reduced at subsequent recalibrations. The method in Denbee and Zimmerman (2012) could help to detect this behaviour and calibrate buffers independent of strategic actions. The study in the current chapter provides another point of view towards this method. We can estimate the distribution of the settlement delay and take this into consideration when calculating the buffers.

It is also possible to extend the model in the current chapter to the settlement systems other than CHAPS. For example, the structure of settlement delay in SPEI (Interbank Electronic Payment System operated by Banco de México) has been specified in Alexandrova-Kabadjova and Solis (2012) with real transactions data from April 7 to May 7, 2010. We may assume that the Markov model is adequate for SPEI, and use these data to calibrate the parameters of the model. Moreover, the observations in Alexandrova-Kabadjova and Solis (2012) suggest that low value payments do not increase the settlement delay in the system. This is reasonable under the assumption that the net balance between two banks follows a reflected Brownian motion with drift, because the process will make an infinite number of small excursions at the origin.

This chapter has focused on the model with one central bank (or agent) and several domestic participants, which is classified as a ‘within border payment system’ (see Bech et al., 2020). For a cross-border payment system, however, we need to consider a model containing two or more central banks, each with their own domestic participants. Assume that the system offers PVP (payment versus payment, see Bech et al., 2020) services, then the settlement delay may originate in any local system, and the first exceeding time of settlement delay of the whole system can be viewed as the joint distribution of the Parisian times of the local systems. To this end, we can collect the transaction data and calibrate the parameters of the model for each local system, then simulate the Parisian times for all the systems simultaneously. Then the minimal value of the sample is taken to be the first exceeding time of settlement delay of the whole system. This is a topic for future research, and the result would be beneficial on a global scale.

Also, our Brownian-type model reflects the random fluctuations of payments and delays, but the external events that can influence these are not taken into account.

For example, the operational risks related to computer and telecommunication system breakdown may increase the settlement delay, see Rochet and Tirole (1996) for the impact of computer problem of Bank of New York in 1985 and the San Francisco earthquake in 1989. More recently, many reports have suggested the impact of global pandemic in 2020 on the settlement systems. These might be interesting for a further study.

Chapter 4

Parisian time of a squared Bessel process with a linear excursion boundary and the pricing of moving Parisian options

4.1 Introduction

Let $(\Omega, \mathcal{F}, (\mathcal{F}_t)_{t \geq 0}, \mathcal{P})$ be a filtered probability space and Z_t be a squared Bessel process adapted to $(\mathcal{F}_t)_{t \geq 0}$. The squared Bessel process Z_t satisfies the following SDE

$$dZ_t = 2(1 - \alpha)dt + 2\sqrt{Z_t}dW_t, \quad Z_0 = 0, \quad 0 < \alpha < 1.$$

Set

$$g_t = \sup\{u \leq t | Z_u = 0\},$$

and denote by U_t the time elapsed since the last time zero can be achieved by the squared Bessel process

$$U_t = t - \sup\{u \leq t | Z_u = 0\}. \quad (4.1)$$

We are interested in studying the Parisian time defined as (see Fig. 4.1)

$$\tau = \inf\{t \geq 0 | U_t = a + bt\}, \quad a > 0, \quad 0 \leq b < 1. \quad (4.2)$$

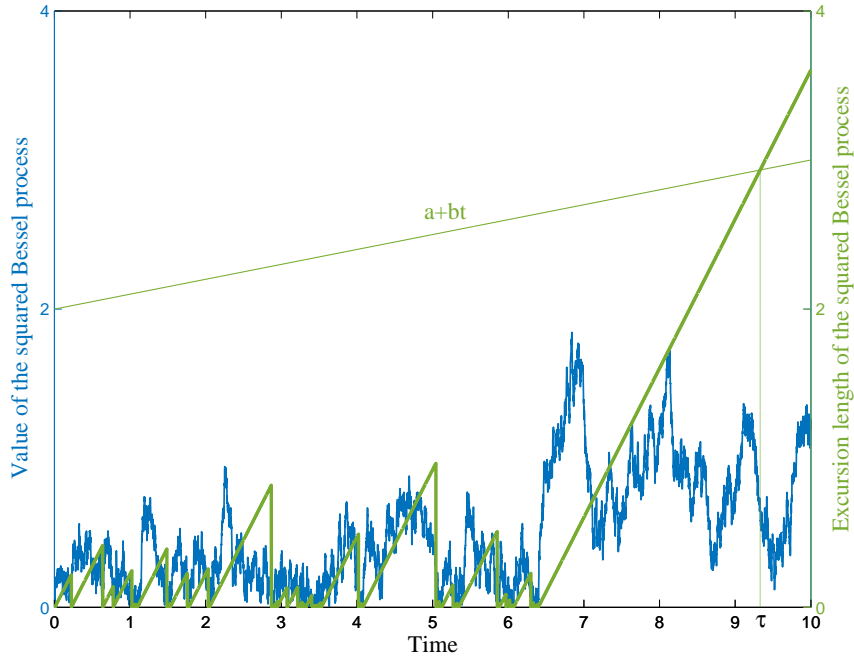


Figure 4.1 Definition of the Parisian time τ with a linear excursion boundary $a + bt$.

In this chapter, we focus on the non-trivial excursion boundary where $b > 0$, and use $b = 0$ to verify our results. By definition, τ is the first time that the excursion length of the squared Bessel process reaches a linear boundary $a + bt$. The definition of τ can be expressed as

$$\tau = \inf \left\{ t \geq 0 \mid \frac{U_t}{a + bt} = 1 \right\}, \quad a > 0, \quad 0 \leq b < 1, \quad (4.3)$$

where $b < 1$ because the excursion time length can not increase faster than the actual time. This expression motivates us to find the first hitting time at 1 of the ratio $\frac{U_t}{a + bt}$.

To study the distribution of the Parisian time τ , we need to find a martingale involving this ratio. From Jeanblanc et al. (2009), we know that a squared Bessel process is connected to a CIR process via a time change, and a martingale using the excursion length of the CIR process can be found in Dassios et al. (2019). We use these results to provide a variation of the Azéma martingale for the process $\frac{U_{s(t)}}{a + bs(t)}$, where $s(t)$ is a change of time. Our martingale reduces to the two-sided version of the martingale used in Chesney et al. (1997) when $\alpha = \frac{1}{2}$ and $b = 0$. The Azéma martingale can also be obtained by projecting another martingale onto the slow filtration which contains the zero points of the squared Bessel process, we will demonstrate the projection in this chapter.

The Azéma martingale enables us to study the distribution of the Parisian time τ . We derive a recursive formula for its probability density function. In addition, we develop an exact simulation algorithm to sample from the Parisian time distribution. Finally, we use the results to price the moving Parisian option.

This chapter will be organised as follows. Section 4.2 sets out some preliminary results on the time-changed squared Bessel process that will be used in other sections. Section 4.3 proves the extension of the Azéma martingale. Section 4.4 demonstrates the martingale projection. In Section 4.5, we obtain the recursive formula of the Parisian time density. Section 4.6 provides the exact simulation algorithm for sampling from the Parisian time distribution, we also give some numerical results in this section. In Section 4.7, we present details on pricing of moving Parisian options.

4.2 Preliminaries

In this section, we introduce the basic settings that will be applied throughout the chapter. Let Z_t be a squared Bessel process on the t -domain, then Z_t follows the SDE

$$dZ_t = 2(1 - \alpha)dt + 2\sqrt{Z_t}dW_t, \quad Z_0 = 0,$$

where we reparametrize with $\alpha := 1 - \frac{\delta}{2}$ and δ represents the dimension of the squared Bessel process. We consider in particular dimensions $0 < \delta < 2$, which corresponds to $0 < \alpha < 1$. In this case, the squared Bessel process returns to 0 in finite time almost surely and is instantaneously reflecting at 0.

We define a new variable s by

$$s := \frac{1}{b} \ln \left(\frac{b}{a}t + 1 \right) \quad \text{and} \quad t(s) = \frac{a}{b} (e^{bs} - 1), \quad \text{for } b > 0, \quad (4.4)$$

then Z_t can be written as $Z_{\frac{a}{b}(e^{bs}-1)}$, which is a time-changed squared Bessel process on the s -domain. We define the process Y_s on the s -domain by

$$Y_s := \frac{e^{-bs} Z_{t(s)}}{a} = \frac{e^{-bs} Z_{\frac{a}{b}(e^{bs}-1)}}{a}. \quad (4.5)$$

Using Ito's formula, Y_s is a CIR process satisfying the following SDE,

$$dY_s = 2((1 - \alpha) - kY_s)ds + 2\sqrt{Y_s}dW_s, \quad Y_0 = 0,$$

with $k = \frac{b}{2}$. Since $k > 0$ and $2k(1 - \alpha) > 0$, the CIR process Y_s hits 0 in finite time almost surely and the boundary 0 is instantaneously reflecting (see Jeanblanc et al. 2009).

From Dassios et al. (2019), we have some knowledge about the Azéma martingale and meander density of the CIR process Y_s , these are very useful for the study of our Parisian time τ . Hence it is more convenient for us to work on the s -domain.

We adopt the following notation. We use Z_s for a squared Bessel process on the s -domain, $\mathcal{F} = (\mathcal{F}_s)_{s \geq 0}$ is the filtration generated by Z_s . We also use U_s for the excursion length of the squared Bessel process Z_s , U_s is adapted to the filtration $\mathcal{F}_U = (\mathcal{F}_{U_s})_{s \geq 0}$. Similarly, we denote by $\mathcal{F}_Y = (\mathcal{F}_{Y_s})_{s \geq 0}$ the filtration generated by the CIR process Y_s . And we use U_s^Y for the excursion length of the CIR process, U_s^Y is adapted to the filtration $\mathcal{F}_{U^Y} = (\mathcal{F}_{U_s^Y})_{s \geq 0}$. Furthermore, we notice that the process U_t defined as (4.1) is adapted to the filtration $(\mathcal{F}_{U_t})_{t \geq 0}$, which contains the zero points of the squared Bessel process Z_t . From (4.5), we know that Z_t and Y_s have the same zero points, hence the filtration $(\mathcal{F}_{U_t})_{t \geq 0}$ contains the same information as $\mathcal{F}_{U^Y} = (\mathcal{F}_{U_s^Y})_{s \geq 0}$.

Next we define a stopping time σ on the s -domain by

$$\sigma = \inf \{s \geq 0, U_s = a + bs\} = \inf \left\{ s \geq 0, \frac{U_s}{a + bs} = 1 \right\}, \quad (4.6)$$

then it follows immediately that

$$\sigma \stackrel{\text{law}}{=} \frac{1}{b} \ln \left(\frac{b}{a} \tau + 1 \right). \quad (4.7)$$

In order to obtain the distributional properties of the Parisian time τ , we will first derive these properties for σ and then apply the transformation (4.7) to obtain the actual results on τ .

4.3 An extension of the Azéma martingale

Let \mathcal{F}_U be the filtration generated by U_s containing the zeros of the squared Bessel process Z_s , we consider a martingale involving the process $\frac{U_s}{a + bs}$ and adapted to \mathcal{F}_U . This result is an extension of the celebrated Azéma martingale.

Theorem 4.3.1 (Azéma martingale). *Let M_s be the process defined as*

$$M_s := e^{-\beta s} \left(1 + \left(1 - b \frac{U_s}{a + bs}\right)^{-\frac{\beta}{b}} \left(\frac{b \frac{U_s}{a+bs}}{1 - b \frac{U_s}{a+bs}}\right)^\alpha \int_0^{-\frac{1}{b} \ln(1 - b \frac{U_s}{a+bs})} \frac{\beta e^{-\beta v}}{(e^{bv} - 1)^\alpha} dv \right), \quad (4.8)$$

then M_s is a \mathcal{F}_U -martingale, where \mathcal{F}_U is the filtration generated by $(U_s)_{s \geq 0}$.

Proof. This is an extension of Theorem 3.1 in Dassios et al. (2019) with a changed time. We have proved that the process Y_s defined as (4.5) is a CIR process on the s -domain. By (4.5), Y_s and the time-changed squared Bessel process $Z_{\frac{a}{b}(e^{bs}-1)}$ have the same zeros; hence they share the same excursion time.

Let the process $R(s)$ be defined as

$$R(s) := -\frac{1}{b} \ln \left(1 - \frac{bU_{t(s)}}{a + bt(s)} \right) = -\frac{1}{b} \ln \left(1 - \frac{bU_{\frac{a}{b}(e^{bs}-1)}}{a + b\frac{a}{b}(e^{bs}-1)} \right),$$

where $U_{t(s)} := t(s) - g_{t(s)}$ is the excursion length of the squared Bessel process $Z_{t(s)}$. Notice that $U_{\frac{a}{b}(e^{bs}-1)} = 0$ results in $R(s) = 0$. Furthermore, since

$$U_{\frac{a}{b}(e^{bs}-1)} = \frac{a}{b}(e^{bs} - 1) - g_{\frac{a}{b}(e^{bs}-1)},$$

we have

$$R(s) = -\frac{1}{b} \ln \left(1 - \frac{b(\frac{a}{b}(e^{bs} - 1) - g_{\frac{a}{b}(e^{bs}-1)})}{a + b\frac{a}{b}(e^{bs} - 1)} \right) = s + \frac{-\ln \left(a + bg_{\frac{a}{b}(e^{bs}-1)} \right) + \ln(a)}{b}.$$

While the time-changed squared Bessel process $Z_{\frac{a}{b}(e^{bs}-1)}$ is non-zero, its last zero time $g_{\frac{a}{b}(e^{bs}-1)}$ remains unchanged, and $R(s)$ evolves linearly at rate 1 on the s -domain; When $Z_{\frac{a}{b}(e^{bs}-1)}$ hits zero, which is equivalent to Y_s hitting zero, $g_{\frac{a}{b}(e^{bs}-1)} = \frac{a}{b}(e^{bs} - 1)$. And as a result, $R(s) = 0$. In conclusion, $R(s)$ evolves linearly at rate 1 and jumps back to 0 when Y_s hits zero, therefore $R(s)$ represents the excursion length of the CIR process Y_s .

On the other hand, for a CIR process Y_t defined as

$$dY_t = 2((1 - \alpha) - kY_t)dt + 2\sqrt{Y_t}dW_t,$$

denote by U_t^Y its excursion length at time t , then from Dassios et al. (2019) we know

that

$$e^{-\beta t} \left(1 + e^{\beta U_t^Y} (e^{2kU_t^Y} - 1)^\alpha \int_0^{U_t^Y} \frac{\beta e^{-\beta v}}{(e^{2kv} - 1)^\alpha} dv \right) \quad (4.9)$$

is a \mathcal{F}_{U^Y} -martingale, where the filtration \mathcal{F}_{U^Y} is generated by $(U_t^Y)_{t \geq 0}$ and contains the zeros of the CIR process Y_t . By setting $k = \frac{1}{2}b$, substituting U_t^Y with $R(s)$ and t with s , we conclude that (4.8) is a \mathcal{F}_U -martingale. \square

4.4 A martingale projection onto the filtration \mathcal{F}_U

In this section, we introduce a martingale involving the process $\frac{Z_s}{a+bs}$ and adapted to the full filtration \mathcal{F} . Furthermore, we show that the projection of this martingale onto the restricted filtration \mathcal{F}_U is exactly the martingale M_s we obtained in Theorem 4.3.1. This section also provides an alternative proof for Theorem 4.3.1.

Proposition 4.4.1 (Martingale projection). *Let M_s^Z be the process defined by*

$$M_s^Z := e^{-\beta s} \Phi \left(\frac{\beta}{b}, 1 - \alpha, \frac{b}{2} \frac{Z_s}{a + bs} \right)$$

then M_s^Z is a \mathcal{F} -martingale. Furthermore, projecting this martingale onto the filtration \mathcal{F}_{U_s} gives

$$\mathbb{E}(M_s^Z | \mathcal{F}_{U_s}) = M_s, \quad (4.10)$$

where $\Phi(a, b, x)$ is the Kummer function of the first kind, \mathcal{F} is the filtration generated by $(Z_s)_{s \geq 0}$, and M_s is the \mathcal{F}_U -martingale defined as (4.8).

Proof. We first present a martingale projection result based on the CIR process Y_s , then we show that (4.10) is a time and space changed version of the CIR result.

Let Y_s be defined as (4.5), the infinitesimal generator of Y_s is

$$\mathcal{A}f(s, y) = \frac{\partial f}{\partial s} + 2((1 - \alpha) - ky) \frac{\partial f}{\partial y} + 2y \frac{\partial^2 f}{\partial y^2}. \quad (4.11)$$

In order to find a martingale involving Y_s , we consider the partial differential equation (see Revuz and Yor, 1999)

$$\frac{\partial f}{\partial s} + 2((1 - \alpha) - ky) \frac{\partial f}{\partial y} + 2y \frac{\partial^2 f}{\partial y^2} = 0. \quad (4.12)$$

Assume its solution has the format $f(s, y) = e^{-\beta s}g(y)$, then solving the partial differential equation reduces to solving the ordinary differential equation with the reflecting boundary condition (see Mandl 1968 pp. 13, 67 for a proof of the reflecting boundary condition)

$$-\beta g(y) + 2((1-\alpha) - ky)g'(y) + 2yg''(y) = 0, \quad g(0) = 1, \quad \lim_{y \rightarrow 0} y^{1-\alpha}g'(y) = 0. \quad (4.13)$$

This is an extended confluent hypergeometric equation, in general it has two linearly independent solutions, but only one solution follows the boundary condition. We use $\Phi(a, b, x)$ for the Kummer function of the first kind, then we solve for

$$g(y) = \Phi\left(\frac{\beta}{2k}, 1 - \alpha, ky\right)$$

Thus the process M_s^Y defined as

$$M_s^Y := e^{-\beta s} \Phi\left(\frac{\beta}{2k}, 1 - \alpha, kY_s\right)$$

is a \mathcal{F}_Y -martingale, where \mathcal{F}_Y is the filtration generated by $(Y_s)_{s \geq 0}$.

Denote by U_s^Y the excursion length of Y_s , and \mathcal{F}_{U^Y} the filtration generated by $(U_s^Y)_{s \geq 0}$. Next we consider the projection of the martingale M_s^Y onto the filtration \mathcal{F}_{U^Y} . From Dassios et al. (2019) we know that the meander of the CIR process Y_s has the probability density function

$$p(u, y) = \mathbb{P}(Y_s \in dy | U_s^Y = u) = \frac{k}{1 - e^{-2ku}} e^{-\frac{k}{1 - e^{-2ku}} y}.$$

For simplicity we denote

$$k(u) := \int_0^\infty g(y)p(u, y)dy, \quad (4.14)$$

then integrating both sides of equation (4.13) with respect to $p(u, y)$ gives

$$-\beta k(u) + g(0) \frac{2\alpha k}{1 - e^{-2ku}} - \frac{2\alpha k}{1 - e^{-2ku}} k(u) + k'(u) = 0.$$

From integration by parts we have

$$k(0) = \lim_{u \rightarrow 0} k(u) = \lim_{u \rightarrow 0} \int_0^\infty g(y) \frac{k}{1 - e^{-2ku}} e^{-\frac{k}{1 - e^{-2ku}} y} dy = g(0),$$

hence by applying the CIR meander, the ordinary differential equation in (4.13) becomes

$$-\beta k(u) + k'(u) + \frac{2\alpha k}{1 - e^{-2ku}} (k(0) - k(u)) = 0, \quad k(0) = 1. \quad (4.15)$$

Notice that there is one boundary condition here because we only care about the Kummer function of the first kind, i.e., the second boundary condition in (4.13) must hold throughout the discussion.

But (4.15) admits to the following partial differential equation,

$$\frac{\partial h}{\partial s} + \frac{\partial h}{\partial u} + \frac{2\alpha k}{1 - e^{-2ku}} (h(s, 0) - h(s, u)) = 0, \quad (4.16)$$

with the assumption that the solution has the format $h(s, u) = e^{-\beta s} k(u)$. Notice that the left side of (4.16) is exactly the infinitesimal generator of U_s^Y . In order to find a martingale involving U_s^Y , we solve (4.15) for

$$k(u) = 1 + e^{\beta u} (e^{2ku} - 1)^\alpha \int_0^u \frac{\beta e^{-\beta v}}{(e^{2kv} - 1)^\alpha} dv.$$

Then we have that the process $M_s^{U^Y}$ defined as

$$M_s^{U^Y} := e^{-\beta s} \left(1 + e^{\beta U_s^Y} (e^{2kU_s^Y} - 1)^\alpha \int_0^{U_s^Y} \frac{\beta e^{-\beta v}}{(e^{2kv} - 1)^\alpha} dv \right),$$

is a \mathcal{F}_{U^Y} -martingale. Combining M_s^Y , $M_s^{U^Y}$ and (4.14), we conclude that

$$\mathbb{E}(M_s^Y | \mathcal{F}_{U_s^Y}) = M_s^{U^Y},$$

this provides us a martingale projection result for the CIR process.

Now we proceed to prove Proposition 4.4.1, let X_t be the process defined as

$$X_t = \frac{Z_t}{a + bt},$$

the infinitesimal generator of X_t is

$$\mathcal{A}f(t, x) = \frac{\partial f}{\partial t} + \frac{2(1 - \alpha) - bx}{a + bt} \frac{\partial f}{\partial x} + \frac{2x}{a + bt} \frac{\partial^2 f}{\partial x^2}.$$

In order to find a martingale involving X_t , we consider the partial differential equation

$$\frac{\partial f}{\partial t} + \frac{2(1 - \alpha) - bx}{a + bt} \frac{\partial f}{\partial x} + \frac{2x}{a + bt} \frac{\partial^2 f}{\partial x^2} = 0,$$

it has the same solution as

$$(a + bt) \frac{\partial f}{\partial t} + (2(1 - \alpha) - bx) \frac{\partial f}{\partial x} + 2x \frac{\partial^2 f}{\partial x^2} = 0. \quad (4.17)$$

Apply the time change (4.4), we rewrite (4.17) as

$$\frac{\partial f}{\partial s} + (2(1 - \alpha) - bx) \frac{\partial f}{\partial x} + 2x \frac{\partial^2 f}{\partial x^2} = 0. \quad (4.18)$$

Note that (4.18) is same as (4.12) with $k = \frac{b}{2}$, hence the process M_s^Z defined as

$$M_s^Z := e^{-\beta s} \Phi \left(\frac{\beta}{b}, 1 - \alpha, \frac{b}{2} \frac{Z_s}{a + bs} \right)$$

is a \mathcal{F}_s -martingale, where \mathcal{F}_s is the filtration generated by $(Z_s)_{s \geq 0}$.

Similarly, we define the process X_t^U via

$$X_t^U = \frac{U_t}{a + bt},$$

the infinitesimal generator of X_t^U is

$$\mathcal{A}f(t, x) = \frac{\partial f}{\partial t} + \frac{1 - bx}{a + bt} \frac{\partial f}{\partial x} + \frac{\alpha}{x(a + bt)} (f(t, 0) - f(t, x)).$$

In order to find a martingale involving X_t^U , we consider the partial differential equation

$$\frac{\partial f}{\partial t} + \frac{1 - bx}{a + bt} \frac{\partial f}{\partial x} + \frac{\alpha}{x(a + bt)} (f(t, 0) - f(t, x)) = 0,$$

it has the same solution as

$$(a + bt) \frac{\partial f}{\partial t} + (1 - bx) \frac{\partial f}{\partial x} + \frac{\alpha}{x} (f(t, 0) - f(t, x)) = 0. \quad (4.19)$$

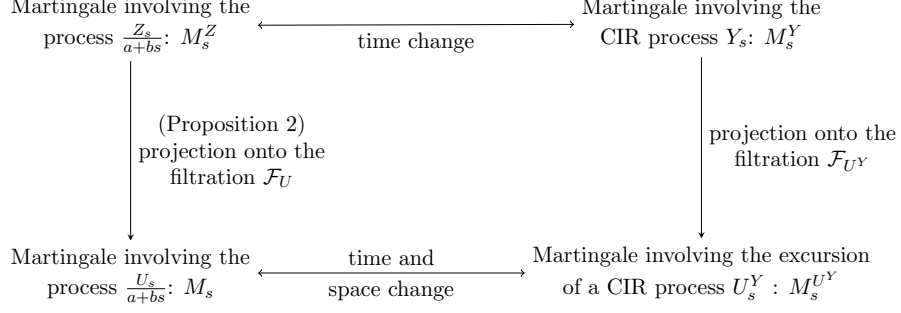


Figure 4.2 Sketch of the proof of Proposition 2.

Apply the time change and define a new variable $u := -\frac{1}{b} \ln(1 - bx)$. We rewrite (4.19) as

$$\frac{\partial f}{\partial s} + \frac{\partial f}{\partial u} + \frac{\alpha b}{1 - e^{-bu}}(f(s, 0) - f(s, u)) = 0. \quad (4.20)$$

Note that (4.20) is same as (4.16) with $k = \frac{b}{2}$, hence the process M_s defined as

$$M_s := e^{-\beta s} \left(1 + \left(1 - b \frac{U_s}{a + bs}\right)^{-\frac{\beta}{b}} \left(\frac{b \frac{U_s}{a + bs}}{1 - b \frac{U_s}{a + bs}}\right)^\alpha \int_0^{-\frac{1}{b} \ln(1 - b \frac{U_s}{a + bs})} \frac{\beta e^{-\beta v}}{(e^{bv} - 1)^\alpha} dv \right),$$

is a \mathcal{F}_U -martingale, where \mathcal{F}_U is the filtration generated by $(U_s)_{s \geq 0}$. This provides us an alternative proof for Theorem 1.

We have obtained the projection from M_s^Y to $M_s^{U^Y}$. Since (4.18) is same as (4.12) and (4.20) is same as (4.16), the projection (4.10) follows immediately, and the proposition is proved. \square

Remark 5. We give a graphical representation of the proof in Figure 2. It was shown in Dassios and Lim (2019) that the projection of the Kennedy martingale (see Kennedy 1976b, Nguyen-Ngoc and Yor 2005) onto the restricted filtration gives a variation of the Azéma martingale. Just like Dassios and Lim (2019), the projection related to the Azéma type martingale is also of interest here. Inspired by this, we provide the martingale which is adapted to the full filtration \mathcal{F} and has the projection M_s in Proposition 4.4.1.

Furthermore, in the proof of Theorem 4.3.1, we used the fact that (4.9) is a martingale. The martingale property of (4.9) was proved by Dassios et al. (2019), but the associated projection was not provided there. In the proof of Proposition 4.4.1, we provide another approach to the martingale property of (4.9), and present the associated projection. Hence we complete the discussion about the Azéma type martingale (4.9) in the current chapter.

4.5 Distributional properties of the Parisian time

In this section, we study the distributional properties of the Parisian time τ . Due to the time change we have made, we will first derive these properties for the stopping time σ and then apply the transformation (4.7) to obtain the actual results on τ .

4.5.1 Laplace transform for the stopping time

We apply the optional stopping theorem on the martingale M_s to obtain the Laplace transform of the stopping time σ .

Lemma 4.5.1 (Laplace transform). *The Laplace transform of σ is*

$$\mathbb{E}(e^{-\beta\sigma}) = \frac{1}{1 + (1-b)^{-\frac{\beta}{b}} \left(\frac{b}{1-b}\right)^\alpha \int_0^{-\frac{1}{b} \ln(1-b)} \frac{\beta e^{-\beta v}}{(e^{bv}-1)^\alpha} dv}.$$

Proof. Since $\frac{U_{s \wedge \sigma}}{a+b(s \wedge \sigma)} \leq 1$ and M_s is an increasing function in $\frac{U_{s \wedge \sigma}}{a+b(s \wedge \sigma)}$, we have $|M_{s \wedge \sigma}| \leq K$ for some constant K for all s . Thus optional stopping theorem and dominated convergence theorem applies, and we have

$$\mathbb{E}(M_\sigma) = \mathbb{E}(\lim_{s \rightarrow \infty} M_{s \wedge \sigma}) = M_0 = 1.$$

Hence

$$\mathbb{E} \left(e^{-\beta\sigma} \left(1 + (1-b)^{-\frac{\beta}{b}} \left(\frac{b}{1-b}\right)^\alpha \int_0^{-\frac{1}{b} \ln(1-b)} \frac{\beta e^{-\beta v}}{(e^{bv}-1)^\alpha} dv \right) \right) = 1,$$

the lemma is proved. □

Next, we calculate the moments of τ using the following method.

Remark 6 (Finiteness of moments). *Consider a special case of Lemma 4.5.1, when $\beta = -b$ we know*

$$\mathbb{E}(e^{b\sigma}) = \frac{1}{1 + (1-b) \left(\frac{b}{1-b}\right)^\alpha \int_0^{-\frac{1}{b} \ln(1-b)} \frac{-be^{bv}}{(e^{bv}-1)^\alpha} dv} = \frac{1-\alpha}{1-\alpha-b}.$$

By setting $\sigma = \frac{1}{b} \ln(\frac{b}{a}\tau + 1)$, we obtain the mean of τ ,

$$\mathbb{E}(\tau) = \frac{a}{1-\alpha-b},$$

hence τ has finite mean only for $0 \leq b < 1 - \alpha$. When $\alpha = \frac{1}{2}$ and $b = 0$, $\mathbb{E}(\tau) = 2a$, this corresponds to the mean of the Parisian time of reflected Brownian motion with a constant excursion boundary $D = a$ (see Chesney et al. 1997). Next we set $\beta = -2b$, then Lemma 4.5.1 implies

$$\mathbb{E}(e^{2b\sigma}) = \frac{1}{1 + (1-b)^2 \left(\frac{b}{1-b}\right)^\alpha \int_0^{-\frac{1}{b} \ln(1-b)} \frac{-2be^{2bv}}{(e^{bv}-1)^\alpha} dv} = \frac{(2-\alpha)(1-\alpha)}{(2-\alpha)(1-\alpha) - 2b(2-b-\alpha)}.$$

By setting $\sigma = \frac{1}{b} \ln\left(\frac{b}{a}\tau + 1\right)$, we obtain the second moment of τ ,

$$\mathbb{E}(\tau^2) = \frac{2a^2(1-b)}{[(2-\alpha)(1-\alpha) - 2b(2-b-\alpha)](1-\alpha-b)},$$

hence τ has finite second moment only for $0 \leq b < \frac{1}{2}(2-\alpha - \sqrt{\alpha(2-\alpha)})$. In general, by setting $\beta = -nb$, we can calculate the n -th moment of τ and derive the range of b where the moment is finite.

In the calculation above, we have taken β to be a negative number. It seems that we do not need $\beta \geq 0$ for the existence of the Laplace transform of σ , because for any fixed $\beta \in \mathbb{R}$, we can always find the bound K in the proof of Lemma 4.5.1. And from the numerical implementation in the next subsection, we believe the moments are correct. But the use of negative β still needs a further study.

4.5.2 Density of the Parisian time

We obtain a recursive expression for the density of the Parisian time τ , the expression involves only a finite sum.

Theorem 4.5.2 (Recursive density). *Let $f_\tau(t)$ be the probability density function of the Parisian time τ , we have*

$$f_\tau(t) = \frac{1}{a+bt} \sum_{i=0}^{n-1} (-1)^i L_i \left(\frac{1}{b} \ln \left(\frac{b}{a}t + 1 \right) - \left(-\frac{1}{b} \ln(1-b) \right) \right),$$

for

$$\frac{a}{b} \left(\frac{1}{(1-b)^n} - 1 \right) < t \leq \frac{a}{b} \left(\frac{1}{(1-b)^{n+1}} - 1 \right), \quad n = 1, 2, \dots,$$

where $L_i(t)$ is defined recursively as follows:

$$L_0(t) = \left(\frac{1-b}{b} \right)^\alpha \frac{b \sin(\alpha\pi)}{\pi} (1 - e^{-bt})^{\alpha-1}, \quad \text{for } t > 0,$$

$$L_{i+1}(t) = \int_{-\frac{1}{b} \ln(1-b)}^{t-i(-\frac{1}{b} \ln(1-b))} L_i(t-s) \frac{b \sin(\alpha\pi)}{\pi} \frac{(1 - \frac{1}{1-b} e^{-bs})^\alpha}{(1 - e^{-bs})(\frac{b}{1-b})^\alpha} ds,$$

$$\text{for } t > (i+1) \left(-\frac{1}{b} \ln(1-b) \right).$$

Proof. See Appendix C. □

Remark 7. By setting $a = 1$ and taking the limit $b \rightarrow 0$, τ reduces to the Parisian time of a squared Bessel process with constant excursion boundary $D = 1$, then Lemma 4.5.1 and Theorem 4.5.2 become the main results of Dassios et al. (2019). Furthermore, by setting $\alpha = \frac{1}{2}$, τ reduces to the Parisian time of a reflected Brownian motion with constant excursion boundary $D = 1$, Lemma 4.5.1 becomes the Laplace transform used in Chesney et al. (1997), and Theorem 4.5.2 become the main results of Dassios and Lim (2017).

4.6 Exact simulation

In this section, we develop an exact simulation algorithm for the Parisian time τ , the algorithm is based on the compound geometric representation of the Laplace transform we obtained in Lemma 4.5.1. We also present some numerical experiments to illustrate the performance of our simulation algorithm.

4.6.1 Exact simulation algorithm

We provide a compound geometric representation for the Laplace transform of the stopping time σ , this representation will lead to the exact simulation algorithm.

Lemma 4.6.1 (Compound geometric representation). *The Laplace transform of the stopping time σ can be written as*

$$\mathbb{E}(e^{-\beta\sigma}) = \frac{p(e^{-(-\frac{1}{b} \ln(1-b))})^\beta \int_0^{-\frac{1}{b} \ln(1-b)} e^{-\beta u} f_0(u) du}{1 - (1-p)(e^{-(-\frac{1}{b} \ln(1-b))})^\beta \int_0^{-\frac{1}{b} \ln(1-b)} e^{-\beta u} f(u) du},$$

where we define

$$p = \frac{bM}{\pi \csc(\pi\alpha)(e^{b(-\frac{1}{b} \ln(1-b))} - 1)^\alpha}, \tag{4.21}$$

$$f_0(u) = \frac{(1 - e^{-bu})^{\alpha-1}}{M},$$

$$f(u) = \frac{1}{E} \int_u^{-\frac{1}{b} \ln(1-b)} \frac{\alpha b e^{b(u + (-\frac{1}{b} \ln(1-b)) - s)} (1 - e^{-bs})^{\alpha-1} (e^{b(-\frac{1}{b} \ln(1-b))} - 1)^\alpha}{(e^{b(u + (-\frac{1}{b} \ln(1-b)) - s)} - 1)^{\alpha+1}} ds,$$

and

$$M = \int_0^{-\frac{1}{b} \ln(1-b)} \frac{1}{(1 - e^{-bs})^{1-\alpha}} ds, \quad (4.22)$$

$$E = \int_0^{-\frac{1}{b} \ln(1-b)} \left(\frac{(e^{b(-\frac{1}{b} \ln(1-b))} - 1)^\alpha}{(e^{b(-\frac{1}{b} \ln(1-b)) - s} - 1)^\alpha} - 1 \right) \frac{1}{(1 - e^{-bs})^{1-\alpha}} ds. \quad (4.23)$$

Furthermore, $f_0(u)$ and $f(u)$ are well-defined probability density functions over $u \in [0, -\frac{1}{b} \ln(1-b)]$.

Proof. See Appendix C. □

Then we have the following exact simulation algorithm for the Parisian time τ .

Algorithm 4.6.2 (Exact simulation algorithm). *The simulation algorithm for the Parisian time τ is the following:*

1. Generate a geometric random variable G with

$$\mathbb{P}(G = g) = p(1-p)^g,$$

where $g = 0, 1, 2, \dots$, and p is defined in (4.21).

2. Generate a random variable T_0 using the A/R scheme (see Glasserman, 2004) by the following steps

- (a) Generate \bar{T}_0 by setting

$$\bar{T}_0 = \left(-\frac{1}{b} \ln(1-b) \right) U_1^{\frac{1}{\alpha}}, \quad U_1 \sim U[0, 1];$$

- (b) Generate a standard uniform random variable $V_1 \sim U[0, 1]$, if

$$V_1 \leq \frac{(1 - e^{-b\bar{T}_0})^{\alpha-1}}{b^{\alpha-1} (-\frac{1}{b} \ln(1-b))^{1-\alpha}} \bar{T}_0^{1-\alpha},$$

then accept \bar{T}_0 and then set $\sigma_0 = \bar{T}_0 + (-\frac{1}{b} \ln(1-b))$; Otherwise reject this candidate and go back to step 2.(a).

3. For $G = g$, generate the sequence of independent and identical distributed random variables $\{T_i\}_{i=1,2,\dots,g}$ via the following steps,

(a) Numerically maximising

$$C(s) = \left(\frac{(e^{b(-\frac{1}{b}\ln(1-b))} - 1)^\alpha}{(e^{b(-\frac{1}{b}\ln(1-b)-s)} - 1)^\alpha} - 1 \right) (1 - e^{-bs})^{\alpha-1} \left(-\frac{1}{b} \ln(1-b) - s \right)^{1-\alpha},$$

record the optimal s^* and set $C = C(s^*)$.

(b) Generate \bar{S} by setting

$$\bar{S} = \left(-\frac{1}{b} \ln(1-b) \right) (1 - U_2^{\frac{1}{\alpha}}), \quad U_2 \sim U[0, 1].$$

(c) Generate a standard uniform random variable $V_2 \sim U[0, 1]$, if

$$V_2 \leq \frac{1}{C} \frac{\left(\frac{(e^{b(-\frac{1}{b}\ln(1-b))} - 1)^\alpha}{(e^{b(-\frac{1}{b}\ln(1-b)-\bar{S})} - 1)^\alpha} - 1 \right) (1 - e^{-b\bar{S}})^{\alpha-1}}{\left(-\frac{1}{b} \ln(1-b) - \bar{S} \right)^{\alpha-1}},$$

then accept \bar{S} ; Otherwise reject this candidate and go back to step 3.(a).

(d) With the accepted \bar{S} , generate T_i by setting

$$T_i = \bar{S} - \left(-\frac{1}{b} \ln(1-b) \right) + \frac{1}{b} \ln \left(\left[\frac{(e^{b(-\frac{1}{b}\ln(1-b))} - 1)^\alpha}{\frac{(e^{b(-\frac{1}{b}\ln(1-b))} - 1)^\alpha}{(e^{b(-\frac{1}{b}\ln(1-b)-\bar{S})} - 1)^\alpha} - U_3 \left(\frac{(e^{b(-\frac{1}{b}\ln(1-b))} - 1)^\alpha}{(e^{b(-\frac{1}{b}\ln(1-b)-\bar{S})} - 1)^\alpha} - 1 \right)} \right]^{\frac{1}{\alpha}} + 1 \right),$$

where $U_3 \sim U[0, 1]$, and then set $\sigma_i = T_i + (-\frac{1}{b} \ln(1-b))$.

4. Set $\sigma = \sigma_0 + \dots + \sigma_n$, return $\tau = \frac{\alpha}{b}(e^{b\sigma} - 1)$.

Proof. See Appendix C. □

4.6.2 Numerical illustration

In this section, we illustrate the performance of our exact simulation algorithm via numerical examples. We estimate the mean and standard deviation of the Parisian

time τ under the parameter settings $\alpha = \frac{1}{2}$, $a = 1$, $b = \{0.01, 0.1, 0.2, 0.3, 0.4, 0.5\}$, with the sample size 10^6 . From Remark 6 we know for $\alpha = \frac{1}{2}$, τ has finite mean only when $0 \leq b < 0.5$, and finite standard deviation only when $0 \leq b < \frac{3}{4} - \frac{\sqrt{3}}{4} \approx 0.3170$, hence we restrict b to the interval $[0, 0.5]$. We also know that when $b = 0$, the excursion boundary becomes a constant $D = a$, and in this case the Parisian time has mean $2a$ and standard deviation $\frac{2\sqrt{3}}{3}a$. Since our algorithm is designed for $b > 0$, we take $b = 0.01$ and compare the estimations to the case of $b = 0$.

Table 4.1 Estimated mean and standard deviation of the Parisian time τ based on parameter settings $\alpha = \frac{1}{2}$, $a = 1$, $b = \{0.01, 0.1, 0.2, 0.3, 0.4, 0.5\}$ and sample size 10^6 .

	Sample average	True expectation	Sample standard deviation	True standard deviation
$b = 0.01$	2.0402	2.0408	1.2036	1.2024
$b = 0.1$	2.5004	2.5000	1.8289	1.8233
$b = 0.2$	3.3365	3.3333	3.5231	3.4752
$b = 0.3$	5.0051	5.0000	11.2083	14.4338
$b = 0.4$	9.9263	10.0000	183.4117	∞
$b = 0.5$	58.3532	∞	9134.6000	∞

Table 4.1 reports the simulation results. We see that the estimations are very close to the true values when b is small. While $b = 0.3$ is close to the boundary of the range where the standard deviation exists, hence the estimation shows a higher level of error. When $b = 0.4$, the standard deviation does not exist, and when $b = 0.5$, both the mean and the standard deviation do not exist.

In addition, since Algorithm 4.6.2 is based on the exact simulation of the stopping time σ (see Step 4. of the algorithm), we carry out separate numerical experiments for the distribution function of σ . Using the exact simulation algorithm and the smoothing techniques (see Bowman and Azzalini 1997), we get the estimated curve for the distribution function. On the other hand, we apply the Gaver-Stehfest method (see Cohen 2007) to invert the Laplace transform $\frac{\mathbb{E}(e^{-\beta\sigma})}{\beta}$ numerically and obtain the inverted curve for the distribution function. The estimated and inverted curves are provided in Figure 4.3a, Figure 4.3b and Figure 4.3c, showing that our algorithm provides a good simulation for the stopping time σ , and hence a good simulation for the Parisian time τ , because τ is just a transform of σ .

4.7 Application: Pricing moving Parisian options

In this section, we use our results to price the two-sided moving Parisian options. It is called a ‘moving’ option because unlike the traditional Parisian options, the

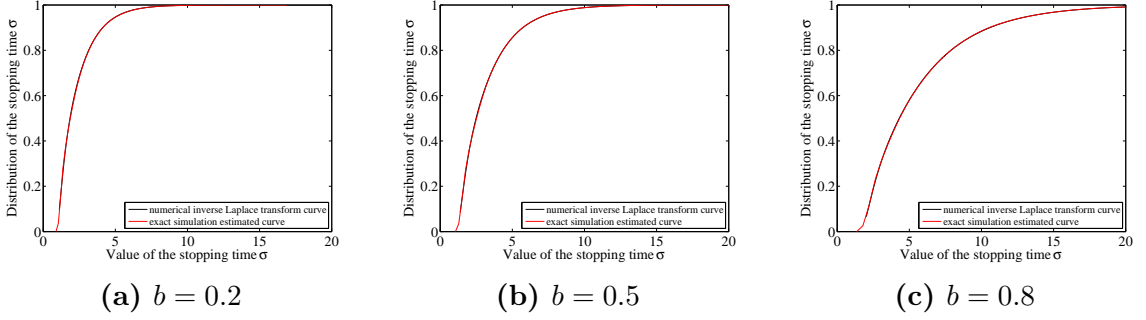


Figure 4.3 Distribution function curves of σ with $\alpha = \frac{1}{2}$ and $b = \{0.2, 0.5, 0.8\}$.

excursion boundary of our option is a function of time. In the option pricing problem, it is the Parisian time of a reflected Brownian motion that matters. For this reason, we take $\alpha = \frac{1}{2}$ in this section, which reduces the squared Bessel process Z_t to a square of reflected Brownian motion. But a reflected Brownian motion has the same excursion time as its square, hence the Parisian time τ is reduced to the first time that the excursion length of a reflected Brownian motion hits a linear boundary. This is also the reason for the option to be called ‘two-sided’: Our Parisian time results are for the squared Bessel process, and in particular, the reflect Brownian motion. On the other hand, the option pricing problem is based on a standard Brownian motion, which could be either positive or negative, and the excursion length of the standard Brownian motion will accumulate in both cases. Hence it is equivalent to consider the excursion of a reflected Brownian motion, in other words, we treat the positive and negative excursions of the standard Brownian motion in the same manner.

Let S_t be the price process of the underlying asset which follows a geometric Brownian motion, the owner of a moving Parisian option receives a payoff $h(S_T)$ only if the price process S_t has an excursion away from the predetermined barrier L which is of length greater or equal to $D = a + bt$ before the expiration time T . For a two-sided moving Parisian option, the owner will receive the payoff when either the underlying makes an excursion above the barrier or an excursion below the barrier of length D .

Let \mathcal{Q} denote the risk neutral probability measure. The dynamic of S under \mathcal{Q} is

$$dS_t = S_t(rdt + \sigma dW_t), \quad S_0 = x,$$

where W_t is a standard Brownian motion under \mathcal{Q} , and r and σ are positive constants. For simplicity, assume zero dividends. Let K denote the strike price of the

option and we introduce the notation

$$m = \frac{1}{\sigma} \left(r - \frac{\sigma^2}{2} \right),$$

so that the asset price $S_t = xe^{\sigma(mt+W_t)}$. Also define

$$g_t^S = \inf\{s \leq t | S_s = L\},$$

to be the last time the asset price reaches L before time t , and

$$\tau_D^S = \inf\{t \geq 0 | t - g_t^S \geq D\}.$$

Thus, τ_D^S denotes the first time that the excursion length of the process S away from the barrier L reaches level D . In our case the excursion boundary is linear, hence we set $D = a + bt$. To emphasise the effect of the linear boundary, we also let $L = x$.

The price of the moving Parisian option with initial underlying price x , maturity T , strike price K , payoff function $h(s)$, and parameters K, L, D, r fixed, is

$$P(x, T) = \mathbb{E}_{\mathcal{Q}} \left(e^{-rT} h(xe^{\sigma(mT+W_T)}) I_{\{\tau_D^S < T\}} \right).$$

We introduce a new probability measure \mathcal{P} , which makes $Z_t = W_t + mt$ a standard Brownian motion under \mathcal{P} . Applying Girsanov's theorem, we have

$$\begin{aligned} P(x, T) &= \mathbb{E}_{\mathcal{P}} \left(e^{-\frac{1}{2}m^2T + mZ_T} e^{-rT} h(xe^{\sigma(mT+W_T)}) I_{\{\tau < T\}} \right) \\ &= \mathbb{E}_{\mathcal{P}} \left(e^{-(r+\frac{1}{2}m^2)T} e^{mZ_T} h(xe^{\sigma Z_T}) I_{\{\tau < T\}} \right). \end{aligned} \tag{4.24}$$

Thus, we propose two methods to price the moving Parisian option with a certain payoff function $h(s)$. The first is using Monte Carlo simulation based on $P(x, T)$. In Table 4.2, we present numerical examples of the moving Parisian call option ($h(s) = (s - K)^+$) for a range of parameters a, b , and x . After one year (52 weeks), the boundary has been increased by the length of b years in total, making it harder for the excursion length to reach the boundary. We observe that the price decreases when the excursion boundary increase, i.e. a and b increase.

Alternatively, we can use explicit expressions for the expectation (4.24) to obtain numerical prices for the moving Parisian option. We denote by \mathcal{F}_t^Z the filtration generated by the Brownian motion $(Z_t)_{t \geq 0}$, then τ is a \mathcal{F}_t^Z -stopping time, and by

Table 4.2 Price of the two-sided moving Parisian call option with $K = 90$ under parameter setting $r = 0.05$, $\sigma = 0.2$, $T = 1$ year (assumed to be 52 weeks), $D = (a + bt)$ year, $a = \frac{4}{52}, \frac{8}{52}$, $b = 0.1, 0.2, 0.4$, $x = 80, 82, 84, 86, 88, 90$.

S_0	$D = \frac{4}{52} + 0.1t$	$D = \frac{4}{52} + 0.2t$	$D = \frac{8}{52} + 0.2t$	$D = \frac{8}{52} + 0.4t$
80	4.2076	4.0839	4.0745	3.6619
82	5.0362	4.9490	4.9429	4.3865
84	5.9673	5.9552	5.7534	5.1881
86	7.0574	7.0305	6.7648	6.0227
88	8.1885	8.1652	7.9085	6.8857
90	9.4036	9.3819	8.9880	7.7386

the strong Markov property of Brownian motion,

$$\begin{aligned} P(x, T) &= \mathbb{E}_{\mathcal{P}} \left(\mathbb{E}_{\mathcal{P}} \left(e^{-(r+\frac{1}{2}m^2)T} e^{mZ_T} h(xe^{\sigma Z_T}) I_{\{\tau < T\}} \mid \mathcal{F}_\tau \right) \right) \\ &= e^{-(r+\frac{1}{2}m^2)T} \mathbb{E}_{\mathcal{P}} \left(I_{\{\tau < T\}} \int_{-\infty}^{\infty} e^{my} h(xe^{\sigma y}) \frac{1}{\sqrt{2\pi(T-\tau)}} e^{-\frac{(y-Z_\tau)^2}{2(T-\tau)}} dy \right). \end{aligned}$$

We can then think of Z_τ as a Brownian meander, because it is a Brownian motion starting from 0 and conditioned to stay away from 0 up to time $a + b\tau$. We denote the density of Z_τ by $v(dz)$, then we have (see Yor 1997)

$$v(dz) = \frac{-z}{2(a+b\tau)} e^{-\frac{z^2}{2(a+b\tau)}} I_{\{z < 0\}} dz + \frac{z}{2(a+b\tau)} e^{-\frac{z^2}{2(a+b\tau)}} I_{\{z > 0\}} dz,$$

hence

$$\begin{aligned} P(x, T) &= e^{-(r+\frac{1}{2}m^2)T} \int_0^T f_\tau(t) \int_{-\infty}^{\infty} \int_{-\infty}^{\infty} e^{my} h(xe^{\sigma y}) \frac{1}{\sqrt{2\pi(T-t)}} e^{-\frac{(y-z)^2}{2(T-t)}} dy v(dz) dt \\ &= e^{-(r+\frac{1}{2}m^2)T} \int_0^T f_\tau(t) \int_0^{\infty} \int_{-\infty}^{\infty} e^{my} h(xe^{\sigma y}) \frac{1}{\sqrt{2\pi(T-t)}} e^{-\frac{(y-z)^2}{2(T-t)}} dy \frac{z}{2(a+bt)} e^{-\frac{z^2}{2(a+bt)}} dz dt \\ &\quad + e^{-(r+\frac{1}{2}m^2)T} \int_0^T f_\tau(t) \int_{-\infty}^0 \int_{-\infty}^{\infty} e^{my} h(xe^{\sigma y}) \frac{1}{\sqrt{2\pi(T-t)}} e^{-\frac{(y-z)^2}{2(T-t)}} dy \frac{-z}{2(a+bt)} e^{-\frac{z^2}{2(a+bt)}} dz dt, \end{aligned}$$

where $f_\tau(t)$ denotes the density of the Parisian time given by Theorem 4.5.2. For a

moving Parisian call option with the payoff function $h(s) = (s - K)^+$, the price is

$$\begin{aligned}
& P(x, T) \\
&= \int_0^T f_\tau(t) \int_0^\infty \int_\eta^\infty e^{my} (xe^{\sigma y} - K) \frac{1}{\sqrt{2\pi(T-t)}} e^{-\frac{(y-z)^2}{2(T-t)}} dy \frac{z}{2(a+bt)} e^{-\frac{z^2}{2(a+bt)}} dz dt \\
&\quad + \int_0^T f_\tau(t) \int_{-\infty}^0 \int_\eta^\infty e^{my} (xe^{\sigma y} - K) \frac{1}{\sqrt{2\pi(T-t)}} e^{-\frac{(y-z)^2}{2(T-t)}} dy \frac{-z}{2(a+bt)} e^{-\frac{z^2}{2(a+bt)}} dz dt \\
&= \int_0^T f_\tau(t) \int_0^\infty (\rho(z) + \rho(-z)) \frac{z}{2(a+bt)} e^{-\frac{z^2}{2(a+bt)}} dz dt,
\end{aligned}$$

where we have denoted by $\eta := \frac{1}{\sigma} \ln\left(\frac{K}{x}\right)$, and

$$\begin{aligned}
\rho(z) &:= \int_\eta^\infty e^{my} (xe^{\sigma y} - K) \frac{1}{\sqrt{2\pi(T-t)}} e^{-\frac{(y-z)^2}{2(T-t)}} dy \\
&= xe^{z(m+\sigma) + \frac{1}{2}(T-t)(m+\sigma)^2} \left[1 - \Phi\left(\frac{\eta - [z + (T-t)(m+\sigma)]}{\sqrt{T-t}}\right) \right] \\
&\quad + Ke^{zm + \frac{1}{2}(T-t)m^2} \left[1 - \Phi\left(\frac{\eta - [z + (T-t)m]}{\sqrt{T-t}}\right) \right].
\end{aligned}$$

Chapter 5

Exact simulation of two-parameter Poisson-Dirichlet random variables

5.1 Introduction

The two-parameter Poisson-Dirichlet distribution is a probability distribution on the set of decreasing positive sequences with sum 1. It can be defined in terms of independent Beta random variables as the following.

Definition 5.1.1 (Definition 1 of Pitman and Yor 1997). *For $0 \leq \alpha < 1$ and $\theta > -\alpha$, suppose that a probability $\mathbb{P}_{\alpha, \theta}$ governs independent random variables \tilde{Y}_i such that \tilde{Y}_i has Beta($1 - \alpha, \theta + i\alpha$) distribution. Let*

$$\tilde{V}_1 = \tilde{Y}_1, \quad \tilde{V}_i = (1 - \tilde{Y}_1) \dots (1 - \tilde{Y}_{i-1}) \tilde{Y}_i \quad (i \geq 2)$$

and let $V_1 \geq V_2 \geq \dots$ be the ranked values of the \tilde{V}_i . Define the Poisson-Dirichlet distribution with parameters (α, θ) , abbreviated $PD(\alpha, \theta)$, to be the $\mathbb{P}_{\alpha, \theta}$ distribution of (V_i) .

Moreover, results of McCloskey (1965), Perman et al. (1992) and Pitman (1996) show that under the $\mathbb{P}_{\alpha, \theta}$ governing, the sequence $\{\tilde{V}_i\}_{i \geq 1}$ is a size-biased permutation of $\{V_i\}_{i \geq 1}$, i.e., the same sequence presented in a random order $(V_{\sigma_1}, V_{\sigma_2}, \dots)$, where $\mathbb{P}(\sigma_1 = i) = V_i$, and for k distinct indices i_1, \dots, i_k ,

$$\mathbb{P}(\sigma_k = i_k \mid \sigma_1 = i_1, \dots, \sigma_{k-1} = i_{k-1}) = \frac{V_{i_k}}{1 - (V_{i_1} + \dots + V_{i_{k-1}})}.$$

An index i with bigger ‘size’ V_i tends to appear earlier in the permutation, hence the name size-biased. Based on the size-biased permutation, Engen (2013) proposed a residual allocation model for $\{\tilde{V}_i\}_{i \geq 1}$.

The $PD(\alpha, \theta)$ distribution extends the one-parameter family of Poisson-Dirichlet distribution introduced by Kingman (1975) and denoted by $PD(0, \theta)$, $\theta > 0$. It also generalises the family of distributions denoted by $PD(\alpha, 0)$, which can be interpreted in terms of the ranked lengths of excursion intervals between zeros of a recurrent Bessel process, see Pitman and Yor (1992). We refer the reader to Pitman and Yor (1997) for the motivation and a collection of existing results of the Poisson-Dirichlet distribution. In particular, Pitman and Yor (1997) includes the distributional properties of $PD(\alpha, 0)$ and its connection to random processes, we will use these properties throughout the chapter.

Despite its long history of research, the simulation method for $PD(\alpha, \theta)$ is less attended and we found no exact method in the literature. When $\alpha = 0$, $PD(0, \theta)$ can be approximated by a Dirichlet distribution, see Section 9.3 of Kingman (1993) and Proposition 5 of Pitman and Yor (1997). An approximation method for $PD(\alpha, \theta)$ with a general value of α is proposed in Al Labadi and Zarepour (2014).

In this chapter we develop two exact simulation algorithms for the first n components, (V_1, V_2, \dots, V_n) , of the $PD(\alpha, \theta)$ distribution. The following trivial simulation algorithm is obtained immediately from Definition 5.1.1. However, this is only an approximation.

Algorithm 5.1.2 (Trivial algorithm). *The approximation algorithm for the random vector (V_1, V_2, \dots, V_n) is the following.*

-
1. Initialise α , θ and n , select a positive integer $m \gg n$ (for example $m = 5n$).
 2. For $i = 1, 2, \dots, m$, generate independent Beta random variables

$$\tilde{Y}_i \sim \text{Beta}(1 - \alpha, \theta + i\alpha).$$

3. Set $\tilde{V}_1 = \tilde{Y}_1$, and for each $i = 2, \dots, m$, set

$$\tilde{V}_i = (1 - \tilde{Y}_1) \dots (1 - \tilde{Y}_{i-1}) \tilde{Y}_i.$$

4. Sort $\{\tilde{V}_i\}_{i=1, \dots, m}$ in a descending order and let $V_1 \geq V_2 \geq \dots \geq V_m$ be the ranked values of $\{\tilde{V}_i\}_{i=1, \dots, m}$.

5. Truncate the sequence $\{V_i\}_{i=1,\dots,m}$ at the first n components, then (V_1, V_2, \dots, V_n) is an approximation of the first n components of the $PD(\alpha, \theta)$ distribution.

Proof. This follows Definition 5.1.1 directly. \square

As $m \rightarrow \infty$, Algorithm 5.1.2 coincides with the definition of the $PD(\alpha, \theta)$ distribution, but in practice m can only take a finite value, so this algorithm is a non-exact approximation for (V_1, V_2, \dots, V_n) .

The rest of the chapter is organised as follows. In Section 5.2 we provide two decompositions in law for the components of the $PD(\alpha, \theta)$ distribution, these decompositions will lead to the exact simulation algorithms directly. In Section 5.3 we present the main results, namely the subordinator algorithm and the compound geometric representation algorithm to sample from the $PD(\alpha, \theta)$ distribution. Numerical examples and their discussions are given in Section 5.4.

5.2 Decompositions of $1/V_k$ under $\mathbb{P}_{\alpha, \theta}$

Denote by (V_1, V_2, \dots, V_n) the first n components of the $PD(\alpha, \theta)$ distribution. In this section, we provide two decompositions for $1/V_k$, $k = 1, \dots, n$ under the probability measure $\mathbb{P}_{\alpha, \theta}$. These decompositions will lead to the exact simulation algorithms. For simplicity, we make the convention throughout the chapter that $\prod_{j=n}^{n-1} a_j = 1$. The following lemma provides a preliminary result that will be used in the proof of the main results.

Lemma 5.2.1 (Existing results under $\mathbb{P}_{\alpha, 0}$). *Denote by τ_t a stable subordinator with Lévy measure $C\alpha x^{-\alpha-1}\mathbf{1}_{\{x>0\}}dx$ for $0 < \alpha < 1$, and Δ_k the ranked jumps of τ_t , such that $\Delta_1 > \Delta_2 > \dots$ and $\tau_t = \sum_{k=1}^{\infty} \Delta_k$. Then for every $C > 0$ and $t > 0$, the random vector*

$$\left(\frac{\Delta_1}{\tau_t}, \frac{\Delta_2}{\tau_t}, \dots \right) \text{ has } PD(\alpha, 0) \text{ distribution.}$$

Moreover, let $V_k := \frac{\Delta_k}{\tau_t}$ be the k -th component of the $PD(\alpha, 0)$ distribution, then for $k = 1, \dots, n$, the decomposition

$$\frac{1}{V_k} \stackrel{\text{law}}{=} \left(1 + \left(R_1 + R_1 R_2 + \dots + \prod_{j=1}^{n-1} R_j \right) + \left(\prod_{j=1}^{n-1} R_j \right) \Sigma_n \right) \prod_{j=1}^{k-1} R_j^{-1} \quad (5.1)$$

holds under the probability measure $\mathbb{P}_{\alpha,0}$, where $R_j := V_{j+1}/V_j = \Delta_{j+1}/\Delta_j$, and $\Sigma_n | \Delta_1, \dots, \Delta_n$ is a subordinator with truncated Lévy measure $C\alpha x^{-\alpha-1} \mathbb{1}_{\{0 < x < 1\}} dx$ at time $t\Delta_1^{-\alpha} (\prod_{j=1}^{n-1} R_j^{-\alpha})$.

Proof. For the distribution of the random vector $(\frac{\Delta_1}{\tau_t}, \frac{\Delta_2}{\tau_t}, \dots)$, see Proposition 6 of Pitman and Yor (1997). We now proceed to prove the decomposition (5.1) under $\mathbb{P}_{\alpha,0}$. Denote by

$$\Sigma_n := \frac{\tau_t - \Delta_1 - \dots - \Delta_n}{\Delta_n}$$

and $R_j := \Delta_{j+1}/\Delta_j$, it follows that

$$\begin{aligned} \frac{1}{V_1} &= \frac{\tau_t}{\Delta_1} = 1 + \frac{\Delta_2 + \dots + \Delta_n}{\Delta_1} + \frac{\Delta_n}{\Delta_1} \Sigma_n \\ &= 1 + \left(R_1 + R_1 R_2 + \dots + \prod_{j=1}^{n-1} R_j \right) + \left(\prod_{j=1}^{n-1} R_j \right) \Sigma_n, \end{aligned}$$

and the decomposition for $1/V_k$, $k = 2, \dots, n$ is given by $V_k = V_1 \prod_{j=1}^{k-1} R_j$.

Moreover, from the proof of Proposition 11 in Pitman and Yor (1997) (see also the calculations in Kingman 1975 and Perman 1993), we know the Laplace transform of $\Sigma_n | \Delta_1, \dots, \Delta_n$ is

$$\begin{aligned} \mathbb{E} \left(e^{-\beta \Sigma_n} | \Delta_1, \dots, \Delta_n \right) &= e^{-t\Delta_n^{-\alpha} \int_0^1 (1-e^{-\beta x}) C\alpha x^{-\alpha-1} dx} \\ &= e^{-t\Delta_1^{-\alpha} (\prod_{j=1}^{n-1} R_j^{-\alpha}) \int_0^1 (1-e^{-\beta x}) C\alpha x^{-\alpha-1} dx}, \end{aligned}$$

this is the Lévy-Khintchine representation (see Kyprianou 2006) of a subordinator with truncated Lévy measure $C\alpha x^{-\alpha-1} \mathbb{1}_{\{0 < x < 1\}}$ at time $t\Delta_1^{-\alpha} (\prod_{j=1}^{n-1} R_j^{-\alpha})$, then the Lemma is proved. \square

Next, we present the decomposition for the first n components of the $PD(\alpha, \theta)$ distribution, this result will permit us to use the subordinator algorithm developed in Dassios et al. (2020). Without loss of generality, we set $t = 1$ and $C = 1$ in the rest of the chapter.

Theorem 5.2.2. *Let (V_1, V_2, \dots, V_n) be the first n components of the $PD(\alpha, \theta)$ distribution, then for every $k = 1, \dots, n$, the decomposition*

$$\frac{1}{V_k} \stackrel{law}{=} \left(1 + \left(R_1 + R_1 R_2 + \dots + \prod_{j=1}^{n-1} R_j \right) + \left(\prod_{j=1}^{n-1} R_j \right) \Sigma_n \right) \prod_{j=1}^{k-1} R_j^{-1}$$

holds under the probability measure $\mathbb{P}_{\alpha,\theta}$, where $(\Delta_1^{-\alpha}, R_1, \dots, R_{n-1}, \Sigma_n)$ has the joint density

$$g(w, r_1, \dots, r_{n-1}, x) := \frac{\frac{\Gamma(\theta+1)}{\Gamma(\frac{\theta}{\alpha}+1)} \Gamma(1-\alpha) \frac{\theta}{\alpha} f_{\Sigma_n} \left(x \mid w \prod_{j=1}^{n-1} r_j^{-\alpha} \right) \alpha^{n-1} w^{\frac{\theta}{\alpha}+n-1} e^{-w \prod_{j=1}^{n-1} r_j^{-\alpha}} \left(\prod_{j=1}^{n-1} r_j^{-(n-j)\alpha-1} \right)}{\left(1 + \left(r_1 + r_1 r_2 + \dots + \prod_{j=1}^{n-1} r_j \right) + \left(\prod_{j=1}^{n-1} r_j \right) x \right)^\theta},$$

and $f_{\Sigma_n} \left(x \mid w \prod_{j=1}^{n-1} r_j^{-\alpha} \right)$ denotes the density of a subordinator with truncated Lévy measure $\alpha x^{-\alpha-1} \mathbb{1}_{\{0 < x < 1\}} dx$ at time $w \prod_{j=1}^{n-1} r_j^{-\alpha}$, for $w > 0$, $0 < r_j < 1$, $j = 1, \dots, n-1$ and $x > 0$.

Proof. This theorem is an analogue of Lemma 5.2.1 with a changed probability measure. Denote by H the non-negative product measurable function

$$H(x_1, \dots, x_n) := e^{-\beta_1 \frac{1}{x_1}} \dots e^{-\beta_n \frac{1}{x_n}},$$

where $\beta_k \geq 0$ and $0 < x_k < 1$, for $k = 1, \dots, n$. From Proposition 14 of Pitman and Yor (1997), we know

$$\mathbb{E}_{\alpha,\theta}(H(V_1, \dots, V_n)) = c_{\alpha,\theta} \mathbb{E}_{\alpha,0}(\tau_t^{-\theta} H(V_1, \dots, V_n)),$$

where

$$c_{\alpha,\theta} = C \frac{\theta}{\alpha} \frac{\Gamma(\theta+1)}{\Gamma(\frac{\theta}{\alpha}+1)} \Gamma(1-\alpha) \frac{\theta}{\alpha}. \quad (5.2)$$

Since $V_1 = \Delta_1/\tau_t$ under $\mathbb{P}_{\alpha,0}$, we set $\tau_t^{-\theta} = \Delta_1^{-\theta} V_1^\theta$, then

$$\mathbb{E}_{\alpha,\theta}(H(V_1, \dots, V_n)) = c_{\alpha,\theta} \mathbb{E}_{\alpha,0}(\Delta_1^{-\theta} V_1^\theta H(V_1, \dots, V_n)). \quad (5.3)$$

From Lemma 24 of Pitman and Yor (1997), we know that under the probability measure $\mathbb{P}_{\alpha,0}$, $\Delta_1^{-\alpha}$ has a standard exponential distribution. Conditioning on $\Delta_1^{-\alpha}$, we have

$$\begin{aligned} \mathbb{E}_{\alpha,0}(\Delta_1^{-\theta} V_1^\theta H(V_1, \dots, V_n)) &= \int_0^\infty \mathbb{E}_{\alpha,0}(\Delta_1^{-\theta} V_1^\theta H(V_1, \dots, V_n) \mid \Delta_1^{-\alpha}) e^{-w} dw \\ &= \int_0^\infty \mathbb{E}_{\alpha,0}(V_1^\theta H(V_1, \dots, V_n) \mid \Delta_1^{-\alpha}) w^{\frac{\theta}{\alpha}} e^{-w} dw. \end{aligned}$$

Moreover, the joint density of $R_1, \dots, R_{n-1} \mid \Delta_1^{-\alpha} = w$ under $\mathbb{P}_{\alpha,0}$ is given by Lemma

3.2 of James (2019) (see Appendix D),

$$f_{R_1, \dots, R_{n-1}}(r_1, \dots, r_{n-1} \mid \Delta_1^{-\alpha} = w) := \alpha^{n-1} w^{n-1} e^w e^{-w \prod_{j=1}^{n-1} r_j^{-\alpha}} \prod_{j=1}^{n-1} r_j^{-(n-j)\alpha-1}, \quad (5.4)$$

for $0 < r_j < 1$, $j = 1, \dots, n-1$. Thus, conditioning on R_1, \dots, R_{n-1} , we have

$$\begin{aligned} & \mathbb{E}_{\alpha,0} (\Delta_1^{-\theta} V_1^\theta H(V_1, \dots, V_n)) \\ &= \int_0^\infty \int_0^1 \cdots \int_0^1 \mathbb{E}_{\alpha,0} (V_1^\theta H(V_1, \dots, V_n) \mid \Delta_1^{-\alpha}, R_1, \dots, R_{n-1}) \\ & \quad \times f_{R_1, \dots, R_{n-1}}(r_1, \dots, r_{n-1} \mid w) w^{\frac{\theta}{\alpha}} e^{-w} dr_1 \dots dr_{n-1} dw. \end{aligned}$$

We also denote by $f_{\Sigma_n}(x \mid w \prod_{j=1}^{n-1} r_j^{-\alpha})$ the density of a subordinator with truncated Lévy measure $\alpha x^{-\alpha-1} \mathbb{1}_{\{0 < x < 1\}} dx$ at time $w \prod_{j=1}^{n-1} r_j^{-\alpha}$. Then, conditioning on Σ_n leads to

$$\begin{aligned} & \mathbb{E}_{\alpha,0} (\Delta_1^{-\theta} V_1^\theta H(V_1, \dots, V_n)) \\ &= \int_0^\infty \int_0^1 \cdots \int_0^1 \int_0^\infty \mathbb{E}_{\alpha,0} (V_1^\theta H(V_1, \dots, V_n) \mid \Delta_1^{-\alpha}, R_1, \dots, R_{n-1}, \Sigma_n) \\ & \quad \times f_{\Sigma_n} \left(x \mid w \prod_{j=1}^{n-1} r_j^{-\alpha} \right) f_{R_1, \dots, R_{n-1}}(r_1, \dots, r_{n-1} \mid w) w^{\frac{\theta}{\alpha}} e^{-w} dx dr_1 \dots dr_{n-1} dw. \end{aligned}$$

From Lemma 5.2.1, we know (V_1, \dots, V_n) is determined by $(\Delta_1^{-\alpha}, R_1, \dots, R_{n-1}, \Sigma_n)$ under the probability measure $\mathbb{P}_{\alpha,0}$. Using the decomposition (5.1), we get

$$\begin{aligned} & \mathbb{E}_{\alpha,0} (\Delta_1^{-\theta} V_1^\theta H(V_1, \dots, V_n)) \\ &= \int_0^\infty \int_0^1 \cdots \int_0^1 \int_0^\infty \prod_{k=1}^n e^{-\beta_k (1 + (r_1 + r_1 r_2 + \cdots + \prod_{j=1}^{n-1} r_j) + (\prod_{j=1}^{n-1} r_j) x) \prod_{j=1}^{k-1} r_j^{-1}} \\ & \quad \times \frac{f_{\Sigma_n} \left(x \mid w \prod_{j=1}^{n-1} r_j^{-\alpha} \right) f_{R_1, \dots, R_{n-1}}(r_1, \dots, r_{n-1} \mid w) w^{\frac{\theta}{\alpha}} e^{-w}}{\left(1 + \left(r_1 + r_1 r_2 + \cdots + \prod_{j=1}^{n-1} r_j \right) + \left(\prod_{j=1}^{n-1} r_j \right) x \right)^\theta} dx dr_1 \dots dr_{n-1} dw. \end{aligned}$$

Taking this into (5.3) and using the expressions of $f_{R_1, \dots, R_{n-1}}(r_1, \dots, r_{n-1} \mid \Delta_1^{-\alpha} = w)$

and $\overline{c_{\alpha,\theta}}$, we obtain the joint Laplace transform of $(\frac{1}{V_1}, \dots, \frac{1}{V_n})$ under $\mathbb{P}_{\alpha,\theta}$,

$$\begin{aligned} & \mathbb{E}_{\alpha,\theta} \left(e^{-\beta_1 \frac{1}{V_1}} \dots e^{-\beta_n \frac{1}{V_n}} \right) \\ &= \int_0^\infty \int_0^1 \dots \int_0^1 \int_0^\infty \prod_{k=1}^n e^{-\beta_k (1 + (r_1 + r_1 r_2 + \dots + \prod_{j=1}^{n-1} r_j) + (\prod_{j=1}^{n-1} r_j) x) \prod_{j=1}^{k-1} r_j^{-1}} \\ & \times \frac{\frac{\Gamma(\theta+1)}{\Gamma(\frac{\theta}{\alpha}+1)} \Gamma(1-\alpha)^{\frac{\theta}{\alpha}} f_{\Sigma_n} \left(x \mid w \prod_{j=1}^{n-1} r_j^{-\alpha} \right) \alpha^{n-1} w^{\frac{\theta}{\alpha}+n-1} e^{-w \prod_{j=1}^{n-1} r_j^{-\alpha}} \left(\prod_{j=1}^{n-1} r_j^{-(n-j)\alpha-1} \right)}{\left(1 + \left(r_1 + r_1 r_2 + \dots + \prod_{j=1}^{n-1} r_j \right) + \left(\prod_{j=1}^{n-1} r_j \right) x \right)^\theta} \\ & dx dr_1 \dots dr_{n-1} dw, \end{aligned}$$

and the theorem is a direct consequence of this result. \square

The next theorem gives another decomposition for the components of $PD(\alpha, \theta)$, which will permit us to use a faster simulation algorithm when θ/α is a positive integer.

Theorem 5.2.3. *Let (V_1, V_2, \dots, V_n) be the first n components of the $PD(\alpha, \theta)$ distribution. If $\theta > 0$ and θ/α is a positive integer, then for every $k = 1, \dots, n$, the decomposition*

$$\frac{1}{V_k} \stackrel{\text{law}}{=} \left(1 + R_1 + R_1 R_2 + \dots + \prod_{j=1}^{n-1} R_j \right) \prod_{j=1}^{k-1} R_j^{-1} + \sum_{i=1}^{\frac{\theta}{\alpha}+n} \left(\left(\prod_{j=k}^{n-1} R_j \right) \left(\sum_{j=0}^{N^{(i)}} T_j^{(i)} \right) \right)$$

holds under the probability measure $\mathbb{P}_{\alpha,\theta}$, where (Z, R_1, \dots, R_{n-1}) has the joint density

$$\begin{aligned} m(z, r_1, \dots, r_{n-1}) &:= \frac{\Gamma(\theta+1) \Gamma(1-\alpha)^{\frac{\theta}{\alpha}}}{\Gamma(\theta)} z^{\theta-1} \left(\prod_{j=1}^{n-1} (j\alpha + \theta) r_j^{j\alpha + \theta - 1} \right) \\ & \times \frac{e^{-z(1+r_1+r_1 r_2+\dots+\prod_{j=1}^{n-1} r_j)}}{\left(1 + \int_0^1 (1 - e^{-z(\prod_{j=1}^{n-1} r_j)x}) \alpha x^{-\alpha-1} dx \right)^{\frac{\theta}{\alpha}+n}}, \end{aligned}$$

for $z > 0$ and $0 < r_j < 1$, $j = 1, 2, \dots, n-1$. Moreover, let A be defined as

$$A = A(Z, R_1, \dots, R_{n-1}) := \int_0^1 e^{-Z(\prod_{j=1}^{n-1} R_j)(v+1)} \frac{v^{-\alpha} - v^\alpha}{v+1} dv; \quad (5.5)$$

then for $i = 1, 2, \dots, \theta/\alpha + n$, $N^{(i)} \in \{0, 1, 2, \dots\}$ are independent and identical

geometric random variables with parameter q , where

$$q = q(Z, R_1, \dots, R_{n-1}) := 1 - \frac{A}{\pi \csc(\pi\alpha)}. \quad (5.6)$$

Furthermore, for every $i = 1, 2, \dots, \theta/\alpha + n$, $T_0^{(i)} \in (0, 1)$ is a random variable with density

$$h_0(x | Z, R_1, \dots, R_{n-1}) = \frac{e^{-Z(\prod_{j=1}^{n-1} R_j)x} x^{\alpha-1}}{\int_0^1 e^{-Z(\prod_{j=1}^{n-1} R_j)y} y^{\alpha-1} dy} \quad \text{for } 0 < x < 1; \quad (5.7)$$

and $T_1^{(i)}, T_2^{(i)}, \dots$ are independent and identically distributed random variables with $T_j^{(i)} \stackrel{\mathcal{D}}{=} G + 1$, $j = 1, 2, \dots, N^{(i)}$, where $G \in (0, 1)$ is a random variable with density

$$h(u | Z, R_1, \dots, R_{n-1}) = \frac{e^{-Z(\prod_{j=1}^{n-1} R_j)(u+1)} \frac{u^{-\alpha-u}}{u+1}}{A} \quad \text{for } 0 < u < 1. \quad (5.8)$$

Proof. From equation (5.3), we know that

$$\begin{aligned} \mathbb{E}_{\alpha, \theta} \left(\prod_{k=1}^n e^{-\beta_k \frac{1}{V_k}} \right) &= c_{\alpha, \theta} \mathbb{E}_{\alpha, 0} \left(\Delta_1^{-\theta} V_1^\theta \prod_{k=1}^n e^{-\beta_k \frac{1}{V_k}} \right) \\ &= c_{\alpha, \theta} \mathbb{E}_{\alpha, 0} \left(\Delta_1^{-\theta} V_1^\theta \prod_{k=1}^n e^{-\beta_k \frac{1}{V_1 (\prod_{j=1}^{k-1} R_j^{-1})}} \right), \end{aligned}$$

where $R_j := V_{j+1}/V_j$ and $c_{\alpha, \theta}$ is defined as (5.2).

Since $\theta > 0$ and $V_1 > 0$, the Gamma density implies $V_1^\theta = \int_0^\infty \frac{1}{\Gamma(\theta)} z^{\theta-1} e^{-\frac{z}{V_1}} dz$, then

$$\mathbb{E}_{\alpha, \theta} \left(\prod_{k=1}^n e^{-\beta_k \frac{1}{V_k}} \right) = c_{\alpha, \theta} \mathbb{E}_{\alpha, 0} \left(\Delta_1^{-\theta} \left(\int_0^\infty \frac{1}{\Gamma(\theta)} z^{\theta-1} e^{-\frac{z}{V_1}} dz \right) \prod_{k=1}^n e^{-\beta_k \frac{1}{V_1 (\prod_{j=1}^{k-1} R_j^{-1})}} \right). \quad (5.9)$$

As in the proof of Theorem 5.2.2, we condition on $(\Delta_1^{-\alpha}, R_1, \dots, R_{n-1})$ under $\mathbb{P}_{\alpha, 0}$,

then

$$\begin{aligned}
& \mathbb{E}_{\alpha,0} \left(\Delta_1^{-\theta} \left(\int_0^\infty \frac{1}{\Gamma(\theta)} z^{\theta-1} e^{-\frac{z}{\sqrt{v_1}}} dz \right) \prod_{k=1}^n e^{-\beta_k \frac{1}{\sqrt{v_1}} (\prod_{j=1}^{k-1} R_j^{-1})} \right) \\
&= \int_0^\infty \int_0^1 \cdots \int_0^1 \mathbb{E}_{\alpha,0} \left(\int_0^\infty \frac{1}{\Gamma(\theta)} z^{\theta-1} e^{-\frac{z}{\sqrt{v_1}}} dz \prod_{k=1}^n e^{-\beta_k \frac{1}{\sqrt{v_1}} (\prod_{j=1}^{k-1} r_j^{-1})} \mid \Delta_1^{-\alpha}, R_1, \dots, R_{n-1} \right) \\
&\quad \times f_{R_1, \dots, R_{n-1}}(r_1, \dots, r_{n-1} \mid w) w^{\frac{\theta}{\alpha}} e^{-w} dr_1 \dots dr_{n-1} dw \\
&= \int_0^\infty \int_0^1 \cdots \int_0^1 \int_0^\infty \frac{1}{\Gamma(\theta)} z^{\theta-1} \mathbb{E}_{\alpha,0} \left(e^{-(z + \sum_{k=1}^n \beta_k (\prod_{j=1}^{k-1} r_j^{-1})) \frac{1}{\sqrt{v_1}}} \mid \Delta_1^{-\alpha}, R_1, \dots, R_{n-1} \right) dz \\
&\quad \times \alpha^{n-1} w^{\frac{\theta}{\alpha} + n-1} e^{-w \prod_{j=1}^{n-1} r_j^{-\alpha}} \left(\prod_{j=1}^{n-1} r_j^{-(n-j)\alpha-1} \right) dr_1 \dots dr_{n-1} dw,
\end{aligned}$$

where $f_{R_1, \dots, R_{n-1}}(r_1, \dots, r_{n-1} \mid w)$ is given in (5.4).

Using the decomposition (5.1) for $\frac{1}{\sqrt{v_1}}$ under the probability measure $\mathbb{P}_{\alpha,0}$, we get

$$\begin{aligned}
& \mathbb{E}_{\alpha,0} \left(\Delta_1^{-\theta} \left(\int_0^\infty \frac{1}{\Gamma(\theta)} z^{\theta-1} e^{-\frac{z}{\sqrt{v_1}}} dz \right) \prod_{k=1}^n e^{-\beta_k \frac{1}{\sqrt{v_1}} (\prod_{j=1}^{k-1} R_j^{-1})} \right) \\
&= \int_0^\infty \int_0^1 \cdots \int_0^1 \int_0^\infty \frac{1}{\Gamma(\theta)} z^{\theta-1} e^{-(z + \sum_{k=1}^n \beta_k (\prod_{j=1}^{k-1} r_j^{-1})) (1+r_1+r_1 r_2+\dots+\prod_{j=1}^{n-1} r_j)} \\
&\quad \times \mathbb{E}_{\alpha,0} \left(e^{-(z + \sum_{k=1}^n \beta_k (\prod_{j=1}^{k-1} r_j^{-1})) (\prod_{j=1}^{n-1} r_j)^{\Sigma_n}} \mid \Delta_1^{-\alpha}, R_1, \dots, R_{n-1} \right) dz \\
&\quad \times \alpha^{n-1} w^{\frac{\theta}{\alpha} + n-1} e^{-w \prod_{j=1}^{n-1} r_j^{-\alpha}} \left(\prod_{j=1}^{n-1} r_j^{-(n-j)\alpha-1} \right) dr_1 \dots dr_{n-1} dw.
\end{aligned}$$

The distribution of $\Sigma_n \mid \Delta_1^{-\alpha}, R_1, \dots, R_{n-1}$ under $\mathbb{P}_{\alpha,0}$ has been specified in Lemma 5.2.1, hence we can calculate its Laplace transform using the Lévy-Khintchine representation,

$$\begin{aligned}
& \mathbb{E}_{\alpha,0} \left(\Delta_1^{-\theta} \left(\int_0^\infty \frac{1}{\Gamma(\theta)} z^{\theta-1} e^{-\frac{z}{\sqrt{v_1}}} dz \right) \prod_{k=1}^n e^{-\beta_k \frac{1}{\sqrt{v_1}} (\prod_{j=1}^{k-1} R_j^{-1})} \right) \\
&= \int_0^\infty \int_0^1 \cdots \int_0^1 \int_0^\infty \frac{1}{\Gamma(\theta)} z^{\theta-1} e^{-(z + \sum_{k=1}^n \beta_k (\prod_{j=1}^{k-1} r_j^{-1})) (1+r_1+r_1 r_2+\dots+\prod_{j=1}^{n-1} r_j)} \\
&\quad \times e^{-w (\prod_{j=1}^{n-1} r_j)^{-\alpha}} \int_0^1 (1-e^{-(z + \sum_{k=1}^n \beta_k (\prod_{j=1}^{k-1} r_j^{-1})) (\prod_{j=1}^{n-1} r_j)^x})^{\alpha} x^{\alpha-1} dx dz \\
&\quad \times \alpha^{n-1} w^{\frac{\theta}{\alpha} + n-1} e^{-w \prod_{j=1}^{n-1} r_j^{-\alpha}} \left(\prod_{j=1}^{n-1} r_j^{-(n-j)\alpha-1} \right) dr_1 \dots dr_{n-1} dw.
\end{aligned}$$

Next, we carry out the integral with respect to w using a Gamma density; it follows

that

$$\begin{aligned}
& \mathbb{E}_{\alpha,0} \left(\Delta_1^{-\theta} \left(\int_0^\infty \frac{1}{\Gamma(\theta)} z^{\theta-1} e^{-\frac{z}{\tilde{V}_1}} dz \right) \prod_{k=1}^n e^{-\beta_k \frac{1}{\tilde{V}_1} (\prod_{j=1}^{k-1} R_j^{-1})} \right) \\
&= \int_0^1 \cdots \int_0^1 \int_0^\infty \frac{1}{\Gamma(\theta)} z^{\theta-1} e^{-(z+\sum_{k=1}^n \beta_k (\prod_{j=1}^{k-1} r_j^{-1})) (1+r_1+r_1 r_2+\cdots+\prod_{j=1}^{n-1} r_j)} \\
&\quad \times \frac{\Gamma(\frac{\theta}{\alpha} + n) \alpha^{n-1} \left(\prod_{j=1}^{n-1} r_j^{j\alpha+\theta-1} \right)}{\left(1 + \int_0^1 (1 - e^{-(z+\sum_{k=1}^n \beta_k (\prod_{j=1}^{k-1} r_j^{-1})) (\prod_{j=1}^{n-1} r_j)^x}) \alpha x^{-\alpha-1} dx \right)^{\frac{\theta}{\alpha}+n}} dz dr_1 \cdots dr_{n-1}.
\end{aligned} \tag{5.10}$$

We focus on the fraction in the integrand, denoted by

$$I := \frac{1}{1 + \int_0^1 (1 - e^{-(z+\sum_{k=1}^n \beta_k (\prod_{j=1}^{k-1} r_j^{-1})) (\prod_{j=1}^{n-1} r_j)^x}) \alpha x^{-\alpha-1} dx}.$$

For the denominator of I , we integrate by parts; then we multiply both the numerator and denominator of I by $\int_0^1 e^{-(z+\sum_{k=1}^n \beta_k (\prod_{j=1}^{k-1} r_j^{-1})) (\prod_{j=1}^{n-1} r_j)^x} x^{\alpha-1} dx$. We also divide both the numerator and denominator of I by $\pi \csc(\pi\alpha)$, it follows that

$$\begin{aligned}
I &= \frac{\int_0^1 e^{-(z+\sum_{k=1}^n \beta_k (\prod_{j=1}^{k-1} r_j^{-1})) (\prod_{j=1}^{n-1} r_j)^x} x^{\alpha-1} dx}{\pi \csc(\pi\alpha) - \int_0^1 e^{-(z+\sum_{k=1}^n \beta_k (\prod_{j=1}^{k-1} r_j^{-1})) (\prod_{j=1}^{n-1} r_j)^{u+1}} \frac{u^{-\alpha-u\alpha}}{u+1} du} \\
&= \frac{\frac{B}{\pi \csc(\pi\alpha)} \frac{1}{(1-\frac{A}{\pi \csc(\pi\alpha)})} \left(1 - \frac{A}{\pi \csc(\pi\alpha)}\right) \int_0^1 e^{-\sum_{k=1}^n \beta_k (\prod_{j=k}^{n-1} r_j)^x} \frac{e^{-z(\prod_{j=1}^{n-1} r_j)^x} x^{\alpha-1}}{B} dx}{1 - \frac{A}{\pi \csc(\pi\alpha)} \int_0^1 e^{-\sum_{k=1}^n \beta_k (\prod_{j=k}^{n-1} r_j)^{u+1}} \frac{e^{-z(\prod_{j=1}^{n-1} r_j)^{u+1}} \frac{u^{-\alpha-u\alpha}}{u+1}}{A} du},
\end{aligned}$$

where we have defined

$$\begin{aligned}
A &= A(z, r_1, \dots, r_{n-1}) := \int_0^1 e^{-z(\prod_{j=1}^{n-1} r_j)^{v+1}} \frac{v^{-\alpha} - v^\alpha}{v+1} dv, \\
B &= B(z, r_1, \dots, r_{n-1}) := \int_0^1 e^{-z(\prod_{j=1}^{n-1} r_j)^y} y^{\alpha-1} dy.
\end{aligned}$$

Also, let q , $h_0(x \mid z, r_1, \dots, r_{n-1})$ and $h(u \mid z, r_1, \dots, r_{n-1})$ be defined as (5.6), (5.7)

and (5.8), then I can be written as

$$\begin{aligned} I &= \frac{B}{\pi \csc(\pi\alpha) - A} \times \frac{q \int_0^1 e^{-\sum_{k=1}^n \beta_k (\prod_{j=k}^{n-1} r_j)^x} h_0(x \mid z, r_1, \dots, r_{n-1}) dx}{1 - (1-q) \int_0^1 e^{-\sum_{k=1}^n \beta_k (\prod_{j=k}^{n-1} r_j)^{(u+1)}} h(u \mid z, r_1, \dots, r_{n-1}) du} \\ &= \frac{1}{1 + \int_0^1 (1 - e^{-z(\prod_{j=1}^{n-1} r_j)^x}) \alpha x^{-\alpha-1} dx} \times \mathbb{E} \left(e^{-\sum_{k=1}^n \beta_k (\prod_{j=k}^{n-1} r_j)^{(\sum_{j=0}^N T_j)}} \right), \end{aligned}$$

where $N \in \{0, 1, 2, \dots\}$ is a geometric random variable with parameter q . Taking this back to equation (5.10) and using equation (5.9), we get the joint Laplace transform of $(\frac{1}{V_1}, \dots, \frac{1}{V_n})$ under $\mathbb{P}_{\alpha, \theta}$,

$$\begin{aligned} &\mathbb{E}_{\alpha, \theta} \left(e^{-\beta_1 \frac{1}{V_1}} \dots e^{-\beta_n \frac{1}{V_n}} \right) \\ &= \int_0^1 \dots \int_0^1 \int_0^\infty e^{-\sum_{k=1}^n \beta_k (\prod_{j=1}^{k-1} r_j^{-1}) (1+r_1+r_1 r_2+\dots+\prod_{j=1}^{n-1} r_j)} \\ &\quad \times \left(\mathbb{E} \left(e^{-\sum_{k=1}^n \beta_k (\prod_{j=k}^{n-1} r_j)^{(\sum_{j=0}^N T_j)}} \right) \right)^{\frac{\theta}{\alpha}+n} \frac{\Gamma(\theta+1) \Gamma(1-\alpha)^{\frac{\theta}{\alpha}}}{\Gamma(\theta)} z^{\theta-1} \\ &\quad \times \frac{\left(\prod_{j=1}^{n-1} (j\alpha + \theta) r_j^{j\alpha+\theta-1} \right) e^{-z(1+r_1+r_1 r_2+\dots+\prod_{j=1}^{n-1} r_j)}}{\left(1 + \int_0^1 (1 - e^{-z(\prod_{j=1}^{n-1} r_j)^x}) \alpha x^{-\alpha-1} dx \right)^{\frac{\theta}{\alpha}+n}} dz dr_1 \dots dr_{n-1}, \end{aligned}$$

and the theorem is a direct consequence of this result. \square

5.3 Exact simulation algorithms

We start this section with introducing the subordinator algorithm for the random vector (V_1, \dots, V_n) . We call it the ‘‘subordinator algorithm’’ because it is based on the exact simulation algorithm of truncated subordinator. It is Algorithm 4.3 of Dassios et al. (2020), which we refer to as Algorithm (α, t) and attach the full steps in Appendix B.

Algorithm 5.3.1 (Subordinator algorithm). *For $\alpha \in (0, 1)$ and $\theta \geq 0$, the exact simulation algorithm for (V_1, V_2, \dots, V_n) is the following.*

-
1. Initialise $\alpha \in (0, 1)$, $\theta \geq 0$ and $n \geq 2$.
 2. Sample from the random vector $(R_1, \dots, R_{n-1}, Y, \Sigma_n)$ via the following steps.

(a) Generate a Gamma random variable Y by setting

$$Y \sim \text{Gamma}\left(\frac{\theta}{\alpha} + n, 1\right).$$

(b) For $j = 1, \dots, n-1$, generate a Beta random variable R_j by setting

$$R_j \sim \text{Beta}(j\alpha + \theta, 1).$$

(c) Generate a truncated subordinator Σ_n by setting

$$\Sigma_n = \text{Algorithm}(\alpha, \Gamma(1 - \alpha)Y).$$

(d) Set $V \sim U[0, 1]$, if

$$V \leq \frac{1}{\left(1 + R_1 + R_1 R_2 + \dots + \prod_{j=1}^{n-1} R_j + \left(\prod_{j=1}^{n-1} R_j\right) \Sigma_n\right)^\theta},$$

accept these candidates and go to Step 3; Otherwise go back to Step 2(a).

3. For $k = 1, \dots, n$ output

$$V_k = \frac{1}{\left(1 + R_1 + R_1 R_2 + \dots + \prod_{j=1}^{n-1} R_j + \left(\prod_{j=1}^{n-1} R_j\right) \Sigma_n\right)} \prod_{j=1}^{k-1} R_j$$

Proof. We apply the acceptance rejection method to sample from the random vector $(\Delta_1^{-\alpha}, R_1, \dots, R_{n-1}, \Sigma_n)$ given in Theorem 5.2.2 with the envelope

$$g^*(r_1, \dots, r_{n-1}, y, x) := \left(\prod_{j=1}^{n-1} (j\alpha + \theta) r_j^{j\alpha + \theta - 1} \right) \frac{1}{\Gamma(\frac{\theta}{\alpha} + n)} y^{\frac{\theta}{\alpha} + n - 1} e^{-y} f_{\Sigma_n}(x | y) dx dy dr_1 \dots dr_{n-1},$$

where $f_{\Sigma_n}(x | y)$ denotes the density of a subordinator with truncated Lévy measure $\alpha x^{-\alpha-1} \mathbf{1}_{\{0 < x < 1\}} dx$ at time y , for $x > 0$, $y > 0$ and $0 < r_j < 1$, $j = 1, \dots, n-1$. To sample from the envelope, we generate independent $\text{Gamma}(\frac{\theta}{\alpha} + n, 1)$ and $\text{Beta}(j\alpha + \theta, 1)$ random variables in Step 2(a, b), then simulate the subordinator via Step 2(c).

To justify the acceptance rejection algorithm, we re-parametrize the envelope with a new variable $w := y \prod_{j=1}^{n-1} r_j^\alpha$, $w > 0$, then we have

$$g^*(w, r_1, \dots, r_{n-1}, x) = f_{\Sigma_n} \left(x \mid w \prod_{j=1}^{n-1} r_j^{-\alpha} \right) \frac{\alpha^{n-1}}{\Gamma(\frac{\theta}{\alpha} + 1)} w^{\frac{\theta}{\alpha} + n - 1} e^{-w(\prod_{j=1}^{n-1} r_j^{-\alpha})} \\ \times \left(\prod_{j=1}^{n-1} r_j^{-(n-j)\alpha - 1} \right) dx dw dr_1 \dots dr_{n-1}.$$

Since $\theta \geq 0$, we know

$$\sup_{w>0, 0<r_1<1, \dots, 0<r_{n-1}<1, x>0} \frac{g(w, r_1, \dots, r_{n-1}, x)}{g^*(w, r_1, \dots, r_{n-1}, x)} \\ = \sup_{w>0, 0<r_1<1, \dots, 0<r_{n-1}<1, x>0} \frac{\Gamma(\theta + 1)\Gamma(1 - \alpha)^{\frac{\theta}{\alpha}}}{\left(1 + \left(r_1 + r_1 r_2 + \dots + \prod_{j=1}^{n-1} r_j \right) + \left(\prod_{j=1}^{n-1} r_j \right) x \right)^\theta} \\ = \Gamma(\theta + 1)\Gamma(1 - \alpha)^{\frac{\theta}{\alpha}},$$

then we accept the candidates via Step 2(d). □

Next, we consider a special case when $\theta > 0$ and θ/α is a positive integer, and develop the compound geometric representation algorithm for the random vector (V_1, \dots, V_n) .

Algorithm 5.3.2 (Compound geometric representation algorithm). *For $\alpha \in (0, 1)$ and $\theta > 0$, if θ/α is a positive integer, the exact simulation algorithm for (V_1, V_2, \dots, V_n) is the following.*

1. Initialise $\alpha \in (0, 1)$, $\theta > 0$ and $n \geq 2$.
2. Sample from the random vector (Z, R_1, \dots, R_{n-1}) via the following steps.
 - (a) Generate a Gamma random variable Z by setting

$$Z \sim \text{Gamma}(\theta, 1).$$

- (b) For $j = 1, 2, \dots, n - 1$, generate a Beta random variable R_j by setting

$$R_j \sim \text{Beta}(j\alpha + \theta, 1).$$

(c) Set $V \sim U[0, 1]$, if

$$V \leq \frac{e^{-Z(R_1 + R_1 R_2 + \dots + \prod_{j=1}^{n-1} R_j)}}{\left(1 + \int_0^1 (1 - e^{-Z(\prod_{j=1}^{n-1} R_j)x}) \alpha x^{-\alpha-1} dx\right)^{\frac{\theta}{\alpha} + n}},$$

accept these candidates; otherwise go back to Step 2(a).

With the accepted candidates, calculate A and q numerically by setting

$$A = \int_0^1 e^{-Z(\prod_{j=1}^{n-1} R_j)(v+1)} \frac{v^{-\alpha} - v^\alpha}{v+1} dv \quad \text{and} \quad q = 1 - \frac{A}{\pi \csc(\pi\alpha)},$$

then go to Step 3.

3. For every $i = 1, 2, \dots, \theta/\alpha + n$, execute the following Step (a), (b) and (c):

(a) Generate a geometric random variable $N^{(i)}$ by setting

$$N^{(i)} \sim \text{Geometric}(q).$$

(b) Generate a random variable $T_0^{(i)}$ via the following Step i. and ii.:

i. Generate a Beta random variable T_0^* by setting

$$T_0^* \sim \text{Beta}(\alpha, 1).$$

ii. Set $V \sim U[0, 1]$, if

$$V \leq e^{-Z(\prod_{j=1}^{n-1} R_j)T_0^*},$$

accept this candidate and set $T_0^{(i)} = T_0^*$; otherwise go back to 3.b.(i).

(c) If $N^{(i)} > 0$, generate $T_j^{(i)}$ by executing the following Step i. and ii. for every $j = 1, 2, \dots, N^{(i)}$; otherwise skip this step:

i. Generate a random variable G^* whose density is

$$h^*(u) = \frac{1}{\frac{\pi}{\sin(\alpha\pi)} - \frac{1}{\alpha}} \frac{u^{-\alpha} - u^\alpha}{u+1} \quad \text{for } 0 < u < 1,$$

using the algorithm provided in Appendix E.

ii. Set $V \sim U[0, 1]$, if

$$V \leq e^{-Z(\prod_{j=1}^{n-1} R_j)G^*},$$

accept this candidate and set $G = G^*$, then set $T_j^{(i)} = G+1$; otherwise go back to 3.c.(i).

4. For $k = 1, 2, \dots, n$, output

$$V_k = \frac{1}{\left(1 + R_1 + \dots + \prod_{j=1}^{n-1} R_j\right) \prod_{j=1}^{k-1} R_j^{-1} + \sum_{i=1}^{\frac{\theta}{\alpha} + n} \left(\left(\prod_{j=k}^{n-1} R_j\right) \left(\sum_{j=0}^{N^{(i)}} T_j^{(i)}\right) \right)}$$

Proof. We apply the acceptance rejection method to sample from the random vector (Z, R_1, \dots, R_{n-1}) given in Theorem 5.2.3 with the envelope

$$m^*(z, r_1, \dots, r_{n-1}) := \left(\prod_{j=1}^{n-1} (j\alpha + \theta) r_j^{j\alpha + \theta - 1} \right) \frac{1}{\Gamma(\theta)} z^{\theta-1} e^{-z},$$

for $z > 0$ and $0 < r_j < 1$, $j = 1, \dots, n-1$. To sample from the envelope, we generate independent $\text{Gamma}(\theta, 1)$ and $\text{Beta}(j\alpha + \theta, 1)$ random variables via Step 2(a-b). Since $\frac{\theta}{\alpha} + n > 0$, we know

$$\begin{aligned} & \sup_{z>0, 0<r_1<1, \dots, 0<r_{n-1}<1} \frac{m(z, r_1, \dots, r_{n-1})}{m^*(z, r_1, \dots, r_{n-1})} \\ &= \sup_{z>0, 0<r_1<1, \dots, 0<r_{n-1}<1} \frac{\Gamma(\theta + 1) \Gamma(1 - \alpha) \frac{\theta}{\alpha} e^{-z(r_1 + r_1 r_2 + \dots + \prod_{j=1}^{n-1} r_j)}}{\left(1 + \int_0^1 (1 - e^{-z(\prod_{j=1}^{n-1} r_j)x}) \alpha x^{-\alpha-1} dx\right)^{\frac{\theta}{\alpha} + n}} \\ &= \Gamma(\theta + 1) \Gamma(1 - \alpha) \frac{\theta}{\alpha}, \end{aligned}$$

then we accept the candidates via Step 2(c).

Next, we use the acceptance rejection method to sample from $T_0^{(i)}$ with the envelope $h_0^*(x) := \alpha x^{\alpha-1}$, for $0 < x < 1$. Since

$$\begin{aligned} \sup_{0<x<1} \frac{h_0(x | Z, R_1, \dots, R_{n-1})}{h_0^*(x)} &= \sup_{0<x<1} \frac{e^{-Z(\prod_{j=1}^{n-1} R_j)x}}{\alpha \int_0^1 e^{-Z(\prod_{j=1}^{n-1} R_j)y} y^{\alpha-1} dy} \\ &= \frac{1}{\alpha \int_0^1 e^{-Z(\prod_{j=1}^{n-1} R_j)y} y^{\alpha-1} dy} \end{aligned}$$

we accept the candidate via Step 3.b.(ii).

We also use the acceptance rejection method to sample from G with the envelope

$$h^*(u) = \frac{1}{\frac{\pi}{\sin(\alpha\pi)} - \frac{1}{\alpha}} \frac{u^{-\alpha} - u^\alpha}{u + 1} \quad \text{for } 0 < u < 1,$$

note that we can sample from $h^*(u)$ using the algorithm given in Appendix E. Since

$$\begin{aligned} \sup_{0 < u < 1} \frac{h(u \mid Z, R_1, \dots, R_{n-1})}{h^*(u)} &= \sup_{0 < u < 1} \frac{\frac{1}{A} e^{-Z(\prod_{j=1}^{n-1} R_j)(u+1)}}{\frac{1}{\frac{\pi}{\sin(\alpha\pi)} - \frac{1}{\alpha}}} \\ &= \frac{1}{A} \left(\frac{\pi}{\sin(\alpha\pi)} - \frac{1}{\alpha} \right) e^{-Z(\prod_{j=1}^{n-1} R_j)}, \end{aligned}$$

we accept the candidate via Step 3.c.(ii). □

5.4 Numerical results

In this section we present some numerical results for Algorithm 5.3.1 and 5.3.2. We will use the expectation and covariance of (V_1, \dots, V_n) as benchmarks to illustrate the accuracy of these algorithms. The complexity of the algorithms are also considered. The following theorem gives an expression for the moments of V_n .

Theorem 5.4.1 (Proposition 17 of Pitman and Yor 1997). *Let V_n be the n -th component of the $PD(\alpha, \theta)$ distribution. For $p > 0$,*

$$\mathbb{E}_{\alpha, \theta}(V_n^p) = \frac{\Gamma(1 - \alpha)^{\frac{\theta}{\alpha}} \Gamma(\theta + 1) \Gamma(\frac{\theta}{\alpha} + n)}{\Gamma(n) \Gamma(\theta + p) \Gamma(\frac{\theta}{\alpha} + 1)} \int_0^\infty t^{p+\theta-1} e^{-t} \frac{\phi_\alpha(t)^{n-1}}{\psi_\alpha(t)^{\frac{\theta}{\alpha}+n}} dt,$$

where

$$\phi_\alpha(\lambda) := \alpha \int_1^\infty e^{-\lambda x} x^{-\alpha-1} dx \quad \text{and} \quad \psi_\alpha(\lambda) := \Gamma(1 - \alpha) \lambda^\alpha + \phi_\alpha(\lambda).$$

Proof. See Proposition 17 of Pitman and Yor (1997). □

Next, we derive an expression for $\mathbb{E}_{\alpha, \theta}(V_m V_n)$.

Theorem 5.4.2 (Covariance). *For positive integers m and n , such that $1 \leq m \leq n$,*

let V_m and V_n be the m -th and n -th components of the $PD(\alpha, \theta)$ distribution, then

$$\begin{aligned} & \mathbb{E}_{\alpha, \theta}(V_m V_n) \\ &= \frac{\Gamma(\theta + 1) \Gamma(1 - \alpha) \frac{\theta}{\alpha} \Gamma(\frac{\theta}{\alpha} + n) \alpha^{n-1}}{\Gamma(\frac{\theta}{\alpha} + 1)} \int_0^1 \cdots \int_0^1 \int_0^\infty \frac{y^{\theta+1} e^{-y}}{\Gamma(\theta + 2)} \left(\prod_{j=1}^{m-1} r_j^{\theta+j\alpha+1} \right) \left(\prod_{j=m}^{n-1} r_j^{\theta+j\alpha} \right) \\ & \quad \times \frac{e^{-y(r_1+r_1r_2+\cdots+\prod_{j=1}^{n-1} r_j)}}{\left(1 + \int_0^1 (1 - e^{-y(\prod_{j=1}^{n-1} r_j)x}) \alpha x^{-\alpha-1} dx \right)^{\frac{\theta}{\alpha}+n}} dy dr_1 \dots dr_{n-1}. \end{aligned}$$

Proof. Since $(V_m V_n)^{-1} > 0$, we know $\int_0^\infty (V_m V_n)^{-1} e^{-(V_m V_n)^{-1} \beta} d\beta = 1$; it follows that

$$\mathbb{E}_{\alpha, \theta}(V_m V_n) = \mathbb{E}_{\alpha, \theta} \left(\int_0^\infty e^{-\frac{\beta}{V_m V_n}} d\beta \right) = \int_0^\infty \mathbb{E}_{\alpha, \theta} \left(e^{-\frac{\beta}{V_m V_n}} \right) d\beta. \quad (5.11)$$

We concentrate on the integrand first. As in the proof of Theorem 5.2.2, we change the probability measure to $\mathbb{P}_{\alpha, 0}$ using (5.3) and condition on $(\Delta_1^{-\alpha}, R_1, \dots, R_{n-1})$, then

$$\begin{aligned} \mathbb{E}_{\alpha, \theta} \left(e^{-\frac{\beta}{V_m V_n}} \right) &= c_{\alpha, \theta} \int_0^\infty \int_0^1 \cdots \int_0^1 \mathbb{E}_{\alpha, 0} \left(V_1^\theta e^{-\frac{\beta}{V_m V_n}} \mid \Delta_1^{-\alpha}, R_1, \dots, R_{n-1} \right) \\ & \quad \times \alpha^{n-1} w^{\frac{\theta}{\alpha}+n-1} e^{-w \prod_{j=1}^{n-1} r_j^{-\alpha}} \left(\prod_{j=1}^{n-1} r_j^{-(n-j)\alpha-1} \right) dr_1 \dots dr_{n-1} dw. \end{aligned}$$

Using the decomposition (5.1) for V_1 , V_m and V_n under $\mathbb{P}_{\alpha, 0}$, we get

$$\begin{aligned} & \mathbb{E}_{\alpha, \theta} \left(e^{-\frac{\beta}{V_m V_n}} \right) \\ &= c_{\alpha, \theta} \int_0^\infty \int_0^1 \cdots \int_0^1 \\ & \quad \mathbb{E}_{\alpha, 0} \left(\frac{e^{-\beta(1+(r_1+\cdots+\prod_{j=1}^{n-1} r_j)+(\prod_{j=1}^{n-1} r_j) \Sigma_n)^2 (\prod_{j=1}^{m-1} r_j^{-1}) (\prod_{j=1}^{n-1} r_j^{-1})}}{\left(1 + (r_1 + r_1 r_2 + \cdots + \prod_{j=1}^{n-1} r_j) + (\prod_{j=1}^{n-1} r_j) \Sigma_n \right)^\theta} \mid \Delta_1^{-\alpha}, R_1, \dots, R_{n-1} \right) \\ & \quad \times \alpha^{n-1} w^{\frac{\theta}{\alpha}+n-1} e^{-w \prod_{j=1}^{n-1} r_j^{-\alpha}} \left(\prod_{j=1}^{n-1} r_j^{-(n-j)\alpha-1} \right) dr_1 \dots dr_{n-1} dw. \end{aligned}$$

Taking this into (5.11) and calculating the integration with respect to β , we have

$$\begin{aligned}
& \mathbb{E}_{\alpha,\theta}(V_m V_n) \\
&= c_{\alpha,\theta} \int_0^\infty \int_0^1 \cdots \int_0^1 \\
& \mathbb{E}_{\alpha,0} \left(\frac{\left(\prod_{j=1}^{m-1} r_j \right) \left(\prod_{j=1}^{n-1} r_j \right)}{\left(1 + \left(r_1 + r_1 r_2 + \cdots + \prod_{j=1}^{n-1} r_j \right) + \left(\prod_{j=1}^{n-1} r_j \right) \Sigma_n \right)^{\theta+2}} \mid \Delta_1^{-\alpha}, R_1, \dots, R_{n-1} \right) \\
& \times \alpha^{n-1} w^{\frac{\theta}{\alpha} + n - 1} e^{-w \prod_{j=1}^{n-1} r_j^{-\alpha}} \left(\prod_{j=1}^{n-1} r_j^{-(n-j)\alpha-1} \right) dr_1 \dots dr_{n-1} dw.
\end{aligned}$$

Since $\theta+2 > 0$, we use a Gamma density to rewrite the denominator of the expression inside the conditional expectation, then rearrange the terms; it follows that

$$\begin{aligned}
& \mathbb{E}_{\alpha,\theta}(V_m V_n) \\
&= c_{\alpha,\theta} \int_0^\infty \int_0^1 \cdots \int_0^1 \left(\prod_{j=1}^{m-1} r_j \right) \left(\prod_{j=1}^{n-1} r_j \right) \int_0^\infty \frac{1}{\Gamma(\theta+2)} y^{\theta+1} \\
& \times e^{-y(1+r_1+r_1 r_2+\cdots+\prod_{j=1}^{n-1} r_j)} \mathbb{E}_{\alpha,0} \left(e^{-y(\prod_{j=1}^{n-1} r_j) \Sigma_n} \mid \Delta_1^{-\alpha}, R_1, \dots, R_{n-1} \right) dy \\
& \times \alpha^{n-1} w^{\frac{\theta}{\alpha} + n - 1} e^{-w \prod_{j=1}^{n-1} r_j^{-\alpha}} \left(\prod_{j=1}^{n-1} r_j^{-(n-j)\alpha-1} \right) dr_1 \dots dr_{n-1} dw.
\end{aligned}$$

Then we calculate the Laplace transform of $\Sigma_n \mid \Delta_1^{-\alpha}, R_1, \dots, R_{n-1}$ using the Lévy-Khintchine representation given in Lemma 5.2.1,

$$\begin{aligned}
& \mathbb{E}_{\alpha,\theta}(V_m V_n) \\
&= c_{\alpha,\theta} \int_0^\infty \int_0^1 \cdots \int_0^1 \left(\prod_{j=1}^{m-1} r_j \right) \left(\prod_{j=1}^{n-1} r_j \right) \int_0^\infty \frac{1}{\Gamma(\theta+2)} y^{\theta+1} \\
& \times e^{-y(1+r_1+r_1 r_2+\cdots+\prod_{j=1}^{n-1} r_j)} e^{-w(\prod_{j=1}^{n-1} r_j^{-\alpha}) \int_0^1 (1-e^{-y(\prod_{j=1}^{n-1} r_j)^x}) \alpha x^{-\alpha-1} dx} dy \\
& \times \alpha^{n-1} w^{\frac{\theta}{\alpha} + n - 1} e^{-w \prod_{j=1}^{n-1} r_j^{-\alpha}} \left(\prod_{j=1}^{n-1} r_j^{-(n-j)\alpha-1} \right) dr_1 \dots dr_{n-1} dw.
\end{aligned}$$

Finally, we carry out the integration with respect to w using a Gamma density and

rearrange the terms; it follows that

$$\begin{aligned} & \mathbb{E}_{\alpha,\theta}(V_m V_n) \\ &= \frac{\Gamma(\theta + 1)\Gamma(1 - \alpha)\frac{\theta}{\alpha}\Gamma(\frac{\theta}{\alpha} + n)\alpha^{n-1}}{\Gamma(\frac{\theta}{\alpha} + 1)} \int_0^1 \cdots \int_0^1 \int_0^\infty \frac{y^{\theta+1}e^{-y}}{\Gamma(\theta + 2)} \left(\prod_{j=1}^{m-1} r_j^{\theta+j\alpha+1} \right) \left(\prod_{j=m}^{n-1} r_j^{\theta+j\alpha} \right) \\ & \quad \times \frac{e^{-y(r_1+r_1r_2+\cdots+\prod_{j=1}^{n-1} r_j)}}{\left(1 + \int_0^1 (1 - e^{-y(\prod_{j=1}^{n-1} r_j)x}) \alpha x^{-\alpha-1} dx \right)^{\frac{\theta}{\alpha}+n}} dy dr_1 \dots dr_{n-1}, \end{aligned}$$

and the theorem is proved. \square

Next, we present numerical results of the algorithms.

5.4.1 Sample average

We illustrate the accuracy of our algorithms by comparing the expectation to the sample average. Consider the first 10 components, (V_1, \dots, V_{10}) , of the $PD(\alpha, \theta)$ distribution. We use Theorem 5.4.1 to calculate $\mathbb{E}_{\alpha,\theta}(V_k)$, $k = 1, \dots, 10$ numerically. Then we generate samples from the random vector using Algorithm 5.1.2, 5.3.1 and 5.3.2, and calculate the sample average of V_k . The results are recorded in Table 5.1, 5.2 and 5.3, we see from the tables that the algorithms can generate exact samples of the random vector.

5.4.2 Covariance

We also present numerical results for the covariance between different components of the random vector (V_1, \dots, V_5) , for simplicity we focus on $\mathbb{E}_{\alpha,\theta}(V_m V_n)$ only. We use Theorem 5.4.2 to calculate $\mathbb{E}_{\alpha,\theta}(V_m V_n)$ for $1 \leq m \leq n \leq 5$ numerically, then generate samples from $V_m V_n$ using Algorithm 5.1.2, 5.3.1 and 5.3.2 and calculate their averages. The results are recorded in Table 5.4, 5.5 and 5.6, the tables show that our algorithms are accurate in estimating the covariance.

5.4.3 Complexity

We are also interested in the complexity of the algorithms, which indicates how many resources the algorithms will costume. Instead of CPU times, we first consider

the total number of random variables generated by the algorithms, because it is consistent and does not depend on the performance of the computer.

From the definition we know the complexity of Algorithm 5.1.2 is m , that is, the algorithm will generate m number of Beta random variables in total. In the previous subsection we have taken $n = 10$ and $m = 50$.

We record the average number of random variables generated by Algorithm 5.3.1 and 5.3.2 for (V_1, \dots, V_{10}) in Table 5.7 and 5.8. From the tables we see that when θ/α is an integer and relatively large, Algorithm 5.3.2 has a lower complexity than Algorithm 5.3.1, this is because the truncated subordinator is not involved in Algorithm 5.3.2.

5.4.4 CPU time

We record the CPU times of Algorithm 5.1.2, 5.3.1 and 5.3.2 for 10^4 samples of (V_1, \dots, V_{10}) in Table 5.9, 5.10 and 5.11. The experiments are implemented on an AMD Ryzen 7 4800U CPU@1.80GHz processor, 16.00GB RAM, Windows 10, 64-bit Operating System and performed in Matlab R2019b. The tables show that when applicable, the compound geometric representation algorithm is preferable in general.

Table 5.1 Expectation and sample average of V_k , $k = 1, \dots, 10$ for $\alpha = \frac{1}{3}$ and $\theta = \frac{1}{3}$, the sample size is 10^5 . For the trivial algorithm $n = 10$ and $m = 50$.

	V_1	V_2	V_3	V_4	V_5	V_6	V_7	V_8	V_9	V_{10}
expectation	0.6273	0.1695	0.0729	0.0386	0.0230	0.0149	0.0102	0.0073	0.0054	0.0041
trivial algorithm	0.6265	0.1700	0.0737	0.0393	0.0235	0.0154	0.0106	0.0076	0.0057	0.0043
subordinator algorithm	0.6273	0.1696	0.0734	0.0391	0.0235	0.0153	0.0105	0.0076	0.0056	0.0043
compound algorithm	0.6282	0.1695	0.0732	0.0390	0.0234	0.0153	0.0105	0.0076	0.0056	0.0043

Table 5.2 Expectation and sample average of V_k , $k = 1, \dots, 10$ for $\alpha = \frac{1}{3}$ and $\theta = \frac{1}{5}$, the sample size is 10^5 . For the trivial algorithm $n = 10$ and $m = 50$. The compound geometric representation algorithm is not applicable because θ/α is not an integer.

	V_1	V_2	V_3	V_4	V_5	V_6	V_7	V_8	V_9	V_{10}
expectation	0.6727	0.1598	0.0648	0.0332	0.0195	0.0125	0.0085	0.0061	0.0046	0.0035
trivial algorithm	0.6715	0.1592	0.0648	0.0331	0.0194	0.0124	0.0084	0.0060	0.0044	0.0033
subordinator algorithm	0.6725	0.1589	0.0647	0.0330	0.0193	0.0123	0.0084	0.0060	0.0044	0.0033
Algorithm compound	N/A									

Table 5.3 Expectation and sample average of V_k , $k = 1, \dots, 10$ for $\alpha = \frac{2}{3}$ and $\theta = \frac{4}{3}$, the sample size is 10^5 . For the trivial algorithm $n = 10$ and $m = 50$.

	V_1	V_2	V_3	V_4	V_5	V_6	V_7	V_8	V_9	V_{10}
expectation	0.2873	0.1204	0.0718	0.0492	0.0364	0.0284	0.0231	0.0195	0.0169	0.0150
trivial algorithm	0.2879	0.1204	0.0721	0.0498	0.0372	0.0292	0.0237	0.0197	0.0166	0.0142
subordinator algorithm	0.2879	0.1205	0.0724	0.0500	0.0374	0.0294	0.0240	0.0200	0.0171	0.0148
Algorithm compound	0.2875	0.1205	0.0723	0.0500	0.0374	0.0295	0.0240	0.0200	0.0171	0.0148

Table 5.4 Expectation and sample average of $V_m V_n$, $1 \leq m \leq n \leq 5$ for $\alpha = \frac{1}{2}$ and $\theta = \frac{1}{2}$ with the trivial algorithm, the sample size is 10^5 . The data are in the format (a, b) where a represents the expectation and b represents the sample average.

	V_1	V_2	V_3	V_4	V_5
V_1	0.2830, 0.2841	0.0686, 0.0687	0.0324, 0.0322	0.0192, 0.0191	0.0129, 0.0127
V_2		0.0329, 0.0330	0.0149, 0.0147	0.0086, 0.0085	0.0057, 0.0056
V_3			0.0090, 0.0090	0.0052, 0.0052	0.0034, 0.0034
V_4				0.0036, 0.0036	0.0023, 0.0023
V_5					0.0017, 0.0017

Table 5.5 Expectation and sample average of $V_m V_n$, $1 \leq m \leq n \leq 5$ for $\alpha = \frac{1}{2}$ and $\theta = \frac{1}{2}$ with the subordinator algorithm, the sample size is 10^5 . The data are in the format (a, b) where a represents the expectation and b represents the sample average.

	V_1	V_2	V_3	V_4	V_5
V_1	0.2830, 0.2837	0.0686, 0.0688	0.0324, 0.0321	0.0192, 0.0191	0.0129, 0.0127
V_2		0.0329, 0.0331	0.0149, 0.0147	0.0086, 0.0085	0.0057, 0.0057
V_3			0.0090, 0.0091	0.0052, 0.0052	0.0034, 0.0034
V_4				0.0036, 0.0036	0.0023, 0.0023
V_5					0.0017, 0.0017

Table 5.6 Expectation and sample average of $V_m V_n$, $1 \leq m \leq n \leq 5$ for $\alpha = \frac{1}{2}$ and $\theta = \frac{1}{2}$ with the compound geometric representation algorithm, the sample size is 10^5 . The data are in the format (a, b) where a represents the expectation and b represents the sample average.

	V_1	V_2	V_3	V_4	V_5
V_1	0.2830, 0.2830	0.0686, 0.0685	0.0324, 0.0323	0.0192, 0.0191	0.0129, 0.0127
V_2		0.0329, 0.0330	0.0149, 0.0148	0.0086, 0.0086	0.0057, 0.0057
V_3			0.0090, 0.0091	0.0052, 0.0052	0.0034, 0.0034
V_4				0.0036, 0.0036	0.0023, 0.0023
V_5					0.0017, 0.0017

Table 5.7 Average number of random numbers (rounding to the nearest integer) generated by the subordinator algorithm for (V_1, \dots, V_{10}) , the sample size is 10^4 . The data are in the format $a + b + c$ where a, b, c represent the number of uniform, Gamma and Beta random variables respectively.

	$\theta = 0.3$	$\theta = 0.5$	$\theta = 1.0$	$\theta = 1.5$	$\theta = 1.6$
$\alpha = 0.3$	175+56+10	216+69+12	421+134+21	952+304+44	1144+365+52
$\alpha = 0.4$	177+55+11	224+70+13	458+144+24	1076+339+53	1302+410+63
$\alpha = 0.5$	192+59+11	251+77+14	537+166+28	1355+418+67	1664+514+80
$\alpha = 0.8$	435+123+15	647+183+21	1993+565+62	7336+2081+217	9650+2737+283

Table 5.8 Average number of random numbers (rounding to the nearest integer) generated by the compound geometric representation algorithm for (V_1, \dots, V_{10}) , the sample size is 10^4 . The data are in the format $a + b + c + d$ where a, b, c, d represent the number of uniform, Gamma, Beta and geometric random variables respectively.

	$\theta = 0.3$	$\theta = 0.5$	$\theta = 1.0$	$\theta = 1.5$	$\theta = 1.6$
$\alpha = 0.3$	16+1+24+11	N/A	N/A	25+5+62+15	N/A
$\alpha = 0.4$	N/A	N/A	N/A	N/A	30+7+82+14
$\alpha = 0.5$	N/A	26+2+32+11	29+3+47+12	36+7+87+13	N/A
$\alpha = 0.8$	N/A	N/A	N/A	N/A	115+30+318+12

Table 5.9 CPU time (in seconds) of the trivial algorithm for (V_1, \dots, V_{10}) , the sample size is 10^4 .

	$\theta = 0.3$	$\theta = 0.5$	$\theta = 1.0$	$\theta = 1.5$	$\theta = 1.6$
$\alpha = 0.3$	0.628853	0.698557	0.656535	0.667601	0.583066
$\alpha = 0.4$	0.572390	0.583742	0.570028	0.603642	0.553737
$\alpha = 0.5$	0.651893	0.557833	0.545066	0.561283	0.587276
$\alpha = 0.8$	0.545630	0.560253	0.558486	0.579318	0.610685

Table 5.10 CPU time (in seconds) of the subordinator algorithm for (V_1, \dots, V_{10}) , the sample size is 10^4 .

	$\theta = 0.3$	$\theta = 0.5$	$\theta = 1.0$	$\theta = 1.5$	$\theta = 1.6$
$\alpha = 0.3$	2.919347	3.407936	5.905766	12.709555	16.287444
$\alpha = 0.4$	4.129321	6.928111	11.446559	23.492180	25.992863
$\alpha = 0.5$	8.535146	10.143674	15.590900	31.600125	38.378702
$\alpha = 0.8$	18.097517	26.450564	85.147071	283.616955	372.585268

Table 5.11 CPU time (in seconds) of the compound geometric representation algorithm for (V_1, \dots, V_{10}) , the sample size is 10^4 .

	$\theta = 0.3$	$\theta = 0.5$	$\theta = 1.0$	$\theta = 1.5$	$\theta = 1.6$
$\alpha = 0.3$	7.394960	N/A	N/A	10.042571	N/A
$\alpha = 0.4$	N/A	N/A	N/A	N/A	12.311978
$\alpha = 0.5$	N/A	10.326533	11.250926	13.745608	N/A
$\alpha = 0.8$	N/A	N/A	N/A	N/A	42.778541

Chapter 6

Epilogue

In conclusion, this thesis contains several themes. Firstly, we derive the Laplace transform of the first hitting time of the Walsh Brownian motion on spider. Two methods are provided to invert this Laplace transform, which enable us to study the density and distribution functions. The Parisian time of the reflected Brownian motion with drift on rays is also considered. We provide the Laplace transform and exact simulation algorithm for the Parisian time. Moreover, we study the Parisian time of a squared Bessel process with a linear excursion boundary. The distributional properties and exact simulation algorithm are studied. These results are used to price moving Parisian options. Finally, we provide two decompositions for the components of the two-parameter Poisson-Dirichlet distribution, and propose the exact simulation algorithms for this distribution.

This thesis inspires us to work on the following topic in the future:

- In Chapter 2, we invert the Laplace transform (2.10) using the Bromwich integral (see Proof of Theorem 2.3.2 in Appendix A). This method could be generalised to the Laplace transform (2.6), and the result will enable us to study the density of the first hitting time of a reflected Brownian motion with drift on rays. Due to the existence of the drift term, the use of Bromwich integral is not straightforward. We need to focus on the singularities of the Laplace transform (2.6). We also plan to develop an exact simulation algorithm for the first hitting time whose Laplace transform is (2.6). This result can be used to price more complicated barrier options; it also has potential applications in physics and biology.
- In Chapter 3, we mention the application of the Parisian time in the real-time gross settlement system. In fact, we could construct a general framework

which reflects the liquidity management in RTGS under realistic settings. The daily payment data will be used to study how liquidity is managed in practice, and to estimate the parameters of the model. This research will link the mathematical theory to the methods employed in industry, and contribute to the stability of the interbank payment system.

- In Chapter 4, we study the Parisian time of a squared Bessel process with a linear excursion boundary, and provide a Azéma martingale relating to the Parisian time. In fact, the linear boundary could be generalised to other types of boundaries. Instead of the ratio $\frac{U_t}{a+bt}$, we could focus on $\frac{U_t}{f(t)}$ where $f(t)$ is a function satisfying certain conditions. We could write down the corresponding PDE and seek for other explicit solutions. This method will lead us to a general framework for the Parisian time of a squared Bessel process with an arbitrary boundary.
- In Chapter 5, the exact simulation algorithm for the two-parameter Poisson-Dirichlet distribution has been established. We plan to develop its application in Bayesian statistics, as well as in the capital distribution curve.

Appendix A

Proofs of the main results in

Chapter 2

Proof of Lemma 2.3.1. We notice that the Laplace transform (2.10) has the limit $\lim_{\beta \rightarrow 0} \mathbb{E}(e^{\beta\tau}) = 1$, hence $\beta = 0$ is not a pole of (2.10). We also know that $\sinh(b_k\sqrt{2\beta}) \neq 0$ for $b_k > 0$ and $\beta \in \mathbb{R} \setminus \{0\}$, hence the numerator part $\sum_{k=1}^n P_k \frac{1}{\sinh(b_k\sqrt{2\beta})}$ will not contribute to any pole of the Laplace transform. For this reason, the poles of (2.10) are equivalent to the roots of its denominator.

We look for the solutions of the equation

$$\sum_{k=1}^n P_k \frac{1}{\sqrt{2\beta}} \frac{\cosh(b_k\sqrt{2\beta})}{\sinh(b_k\sqrt{2\beta})} = 0. \quad (\text{A.1})$$

Using the inverse Laplace transform (see Borodin and Salminen 1996 Appendix 2.11) and the general Theta function transformation (see Bellman 1961 Section 19), we know

$$\mathcal{L}^{-1} \left(\frac{\cosh(b_k\sqrt{2\beta})}{\sqrt{2\beta} \sinh(b_k\sqrt{2\beta})} \right) = \frac{1}{\sqrt{2\pi t}} \sum_{n=-\infty}^{\infty} e^{-\frac{2b_k^2(2n+1)^2}{t}} = \frac{1}{2b_k} \sum_{n=-\infty}^{\infty} e^{-n^2\pi^2 \frac{t}{2b_k^2}}, \quad t > 0.$$

Then we invert both sides of (A.1), this gives

$$\sum_{k=1}^n \frac{P_k}{2b_k} \int_0^{\infty} e^{-\beta t} \sum_{n=-\infty}^{\infty} e^{-n^2\pi^2 \frac{t}{2b_k^2}} dt = 0. \quad (\text{A.2})$$

We assume that the roots of (A.2) have the format $x + iy$, for $x, y \in \mathbb{R}$, then

$$\sum_{k=1}^n \frac{P_k}{2b_k} \int_0^\infty e^{-xt} (\cos(yt) - i \sin(yt)) \sum_{n=-\infty}^\infty e^{-n^2 \pi^2 \frac{t}{2b_k^2}} dt = 0.$$

For the imaginary component of the equation, we calculate the integral

$$\int_0^\infty e^{-xt} \sin(yt) e^{-n^2 \pi^2 \frac{t}{2b_k^2}} dt = \frac{y}{\left(x + n^2 \pi^2 \frac{1}{2b_k^2}\right)^2 + y^2},$$

hence we must have $y = 0$, for otherwise the imaginary component cannot be zero. This means the roots are real numbers. Next, we set $\beta = x$ in equation (A.1), then we have

$$\sum_{k=1}^n \frac{P_k}{\sqrt{2x}} \coth(b_k \sqrt{2x}) = 0.$$

Since $\coth(x) > 0$ for $x \in \mathbb{R}^+$, this equation cannot hold for any positive real x , this means x must be negative real numbers. We denote by $-\beta^*$ the roots of equation (A.1), where $\beta^* > 0$, then we have

$$\sum_{k=1}^n P_k \cot(b_k \sqrt{2\beta^*}) = 0. \quad (\text{A.3})$$

Next, we proceed to solve equation (A.3) under the assumption that the upper boundaries $\{b_i\}_{i=1, \dots, n}$ are integers. For any positive integer n , the multiple-angle formula implies

$$\cot(n\theta) = \frac{\sum_{k \text{ even}} (-1)^{\frac{k}{2}} \binom{n}{k} \tan(\theta)^k}{\sum_{k \text{ odd}} (-1)^{\frac{k-1}{2}} \binom{n}{k} \tan(\theta)^k}.$$

Then, equation (A.3) can be written as

$$\begin{aligned} \sum_{k=1}^n P_k \cot(b_k \sqrt{2\beta^*}) &= \sum_{i=1}^n P_i \frac{\sum_{k \text{ even}} (-1)^{\frac{k}{2}} \binom{b_i}{k} \tan(\sqrt{2\beta^*})^k}{\sum_{k \text{ odd}} (-1)^{\frac{k-1}{2}} \binom{b_i}{k} \tan(\sqrt{2\beta^*})^k} \\ &= \frac{\sum_{i=1}^n P_i \left(\sum_{k \text{ even}} (-1)^{\frac{k}{2}} \binom{b_i}{k} y^k \prod_{j=\{1, \dots, n\} \setminus \{i\}} \left(\sum_{k \text{ odd}} (-1)^{\frac{k-1}{2}} \binom{b_j}{k} y^k \right) \right)}{\prod_{i=1}^n \left(\sum_{k \text{ odd}} (-1)^{\frac{k-1}{2}} \binom{b_i}{k} y^k \right)} = 0, \end{aligned} \quad (\text{A.4})$$

where we denote by $y := \tan(\sqrt{2\beta^*})$. Note that $y = 0$ is not a solution to this

equation, for otherwise equation (A.3) cannot hold. For this reason, we only need to consider the numerator part of (A.4):

$$\sum_{i=1}^n P_i \left(\sum_{k \text{ even}} (-1)^{\frac{k}{2}} \binom{b_i}{k} y^k \prod_{j=\{1, \dots, n\} \setminus \{i\}} \left(\sum_{k \text{ odd}} (-1)^{\frac{k-1}{2}} \binom{b_j}{k} y^k \right) \right) = 0.$$

This approach is also sufficient when $\{b_i\}_{i=1, \dots, n}$ are rational numbers. Let c_i and d_i be positive integers, such that $b_i = \frac{c_i}{d_i}$, for $i = 1, \dots, n$, then

$$b_i \sqrt{2\beta^*} = \frac{c_i}{d_i} \sqrt{2\beta^*} = c_i \left(\prod_{j=\{1, \dots, n\} \setminus \{i\}} d_j \right) \theta,$$

where we denote by $\theta := \frac{1}{d_1 \dots d_n} \sqrt{2\beta^*}$. Since $c_i \left(\prod_{j=\{1, \dots, n\} \setminus \{i\}} d_j \right)$ is a positive integer, we can replace $b_i \sqrt{2\beta^*}$ by $c_i \left(\prod_{j=\{1, \dots, n\} \setminus \{i\}} d_j \right) \theta$ in equation (A.3), and follow the rest of the proof. Then the lemma is proved. \square

Proof of Theorem 2.3.2. The poles of the Laplace transform (2.10) have been derived in Lemma 2.3.1, we first show that they are simple poles (see Lang 2013). The denominator of (2.10) has the derivative:

$$\frac{d}{d\beta} \left(\sum_{k=1}^n P_k \frac{\cosh(b_k \sqrt{2\beta})}{\sinh(b_k \sqrt{2\beta})} \right) = \frac{1}{\sqrt{2\beta}} \sum_{k=1}^n P_k b_k \left(1 - \frac{\cosh^2(b_k \sqrt{2\beta})}{\sinh^2(b_k \sqrt{2\beta})} \right),$$

and the limits of this derivative at the poles are non-zero, i.e.,

$$\lim_{\beta \rightarrow -\beta^*} \frac{d}{d\beta} \left(\sum_{k=1}^n P_k \frac{\cosh(b_k \sqrt{2\beta})}{\sinh(b_k \sqrt{2\beta})} \right) = \frac{1}{i\sqrt{2\beta^*}} \sum_{k=1}^n P_k b_k \left(1 + \frac{\cos^2(b_k \sqrt{2\beta^*})}{\sin^2(b_k \sqrt{2\beta^*})} \right) \neq 0,$$

this implies that $-\beta^*$ are simple poles.

Next, we introduce an explicit inverse method for the Laplace transform (2.10). Denote by $\hat{f}(\beta)$ the Laplace transform (2.10), and $f(t)$ its inverse. From the Bromwich integral (see Arfken and Weber 2001 Section 20.10), we know

$$f(t) = \frac{1}{2\pi i} \int_{-i\infty}^{+i\infty} e^{\beta t} \hat{f}(\beta) d\beta.$$

This integral can be calculated via the residue theorem, that is,

$$f(t) = \sum_{-\beta^*} \text{Res} \left(e^{\beta t} \hat{f}(\beta), -\beta^* \right).$$

Since the poles of (2.10) are simple poles, we can calculate the residues by evaluating the limit

$$\text{Res} \left(e^{\beta t} \hat{f}(\beta), -\beta^* \right) = \lim_{\beta \rightarrow -\beta^*} \left((\beta - (-\beta^*)) e^{\beta t} \hat{f}(\beta) \right),$$

it follows that

$$f(t) = \sum_{-\beta^*} e^{-\beta^* t} \frac{\sum_{k=1}^n P_k \frac{\sqrt{2\beta^*}}{\sin(b_k \sqrt{2\beta^*})}}{\sum_{k=1}^n P_k b_k + \sum_{k=1}^n P_k b_k \frac{\cos^2(b_k \sqrt{2\beta^*})}{\sin^2(b_k \sqrt{2\beta^*})}}.$$

For the distribution function, we integrate $f(t)$ over $(0, t)$, and the theorem is proved. □

Appendix B

Exact simulation of truncated subordinator

In this appendix we attach the Algorithm 4.3 and 4.4 of Dassios et al. (2020), these algorithms exactly generate samples from the truncated subordinator $Z(t)$ with Laplace transform

$$\mathbb{E}(e^{-vZ(t)}) = \exp\left(-\frac{\alpha t}{\Gamma(1-\alpha)} \int_0^1 (1-e^{-vz}) \frac{e^{-\eta z}}{z^{\alpha+1}} dz\right). \quad (\text{B.1})$$

We first present two ancillary algorithms, namely Algorithm 4.1 and 4.2 of Dassios et al. (2020).

Lemma B.1 (Algorithm 4.1 of Dassios et al. 2020). *Exact simulation of (T, W) .*

1. Set $\xi = \Gamma(1-\alpha)^{-1}$; $A_0 = (1-\alpha)\alpha^{\frac{\alpha}{1-\alpha}}$.
2. minimise $C(\lambda) = A_0 e^{\xi \frac{1}{\alpha} \lambda^{1-\frac{1}{\alpha}} \alpha(1-\alpha)^{\frac{1}{\alpha}-1}} (A_0 - \lambda)^{\alpha-2}$.
3. record critical value λ^* ; set $C = C(\lambda^*)$.
4. repeat {
 5. sample $U \sim U[0, \pi]$; $U_1 \sim U[0, 1]$,
 6. set $Y = 1 - U_1^{\frac{1}{1-\alpha}}$; $A_U = [\sin^\alpha(\alpha U) \sin^{1-\alpha}((1-\alpha)U) / \sin(U)]^{\frac{1}{1-\alpha}}$,
 7. sample $R \sim \Gamma(2-\alpha, A_U - \lambda)$; $V \sim U[0, 1]$.
 8. if $(V \leq A_U e^{\xi R^{1-\alpha} Y^\alpha} e^{-\lambda^* R} (A_U - \lambda^*)^{\alpha-2} Y^{\alpha-1} (1 - (1-Y)^\alpha) / C)$, break.

9. }
10. sample $U_2 \sim U[0, 1]$,
11. set $T = R^{1-\alpha}Y^\alpha$; $W = Y - 1 + [(1 - Y)^{-\alpha} - U_2((1 - Y)^{-\alpha} - 1)]^{-\frac{1}{\alpha}}$.
12. return (T, W) .

Lemma B.2 (Algorithm 4.2 of Dassios et al. 2020). *Exact simulation of $\{Z(t)|T > t\}$.*

1. sample $U_1 \sim U[0, \pi]$; set $A_{U_1} = [\sin^\alpha(\alpha U_1) \sin^{1-\alpha}((1 - \alpha)U_1) / \sin(U_1)]^{\frac{1}{1-\alpha}}$.
2. repeat {
3. sample $U_2 \sim U[0, 1]$; set $Z = \left[-\frac{\log(U_2)}{A_{U_1} t^{\frac{1}{1-\alpha}}} \right]^{-\frac{1-\alpha}{\alpha}}$.
4. if $(Z < 1)$, break.
5. }
6. return Z .

Next we provide the Algorithm 4.3 and 4.4 of Dassios et al. (2020).

Theorem B.3 (Algorithm 4.3 of Dassios et al. 2020). *Exact simulation of the subordinator $Z(t)$ when $\eta = 0$. The input is t .*

1. set $Z = 0$; $S = 0$.
2. repeat {
3. sample (T, W) via Algorithm 4.1; set $S = S + T$, $Z = Z + 1 + W$.
4. if $(S > t)$, break.
5. }
6. set $Z_{S-T} = Z - 1 - W$; sample $Z_{t-(S-T)}$ via Algorithm 4.2.
7. return $Z_{S-T} + Z_{t-(S-T)}$.

Theorem B.4 (Algorithm 4.4 of Dassios et al. 2020). *Exact simulation of the subordinator $Z(t)$ when $\eta > 0$. The inputs are (t, η) .*

1. repeat {

2. *sample Z_t via Algorithm 4.3; $V \sim U[0, 1]$.*
3. *if ($V \leq \exp(-\eta Z_t)$), break.*
4. *}*
5. *return Z_t .*

Proof. For the proof as well as the motivation of the algorithms above, see Dassios et al. (2020). □

Appendix C

Proofs of the main results in

Chapter 4

Proof of Theorem 4.5.2. Using integral by parts for its denominator, we rewrite the Laplace transform of σ obtained in Lemma 5.1 as

$$\begin{aligned}
 & \mathbb{E}(e^{-\beta\sigma}) \\
 &= \frac{1}{1 + (1-b)^{-\frac{\beta}{b}} \left(\frac{b}{1-b}\right)^\alpha \int_0^{-\frac{1}{b} \ln(1-b)} \frac{\beta e^{-\beta v}}{(e^{bv}-1)^\alpha} dv} \\
 &= \frac{(1-b)^{\frac{\beta}{b}}}{1 + \left(\frac{b}{1-b}\right)^\alpha \int_0^{-\frac{1}{b} \ln(1-b)} (1-e^{-\beta v}) \alpha b (e^{bv}-1)^{-(\alpha+1)} e^{bv} dv} \\
 &= \frac{(1-b)^{\frac{\beta}{b}}}{\left(\frac{b}{1-b}\right)^\alpha \int_0^\infty \beta e^{-\beta v} (e^{bv}-1)^{-\alpha} dv + \left(\frac{b}{1-b}\right)^\alpha \int_{-\frac{1}{b} \ln(1-b)}^\infty e^{-\beta v} \alpha b (e^{bv}-1)^{-(\alpha+1)} e^{bv} dv} \\
 &= \frac{(1-b)^{\frac{\beta}{b}}}{\left(\frac{b}{1-b}\right)^\alpha \frac{\Gamma(\frac{\beta}{b} + \alpha) \Gamma(-\alpha + 1)}{\Gamma(\frac{\beta}{b})} + \left(\frac{b}{1-b}\right)^\alpha \int_{-\frac{1}{b} \ln(1-b)}^\infty e^{-\beta v} \alpha b (e^{bv}-1)^{-(\alpha+1)} e^{bv} dv}.
 \end{aligned}$$

Then the negative binomial expansion implies

$$\begin{aligned}
 & \mathbb{E}(e^{-\beta\sigma}) \\
 &= \frac{(1-b)^{\frac{\beta}{b}}}{\left(\frac{b}{1-b}\right)^\alpha} \frac{\Gamma(\frac{\beta}{b})}{\Gamma(\frac{\beta}{b} + \alpha) \Gamma(-\alpha + 1)} \\
 & \quad \times \sum_{i=0}^{\infty} (-1)^i \left(\frac{\Gamma(\frac{\beta}{b})}{\Gamma(\frac{\beta}{b} + \alpha) \Gamma(-\alpha + 1)} \int_{-\frac{1}{b} \ln(1-b)}^\infty e^{-\beta v} \alpha b (e^{bv}-1)^{-(\alpha+1)} e^{bv} dv \right)^i.
 \end{aligned}$$

Next, we denote by

$$\hat{L}_i(\beta) = \frac{\Gamma(\frac{\beta}{b})}{\Gamma(\frac{\beta}{b} + \alpha)\Gamma(-\alpha + 1)} \left(\frac{\Gamma(\frac{\beta}{b})}{\Gamma(\frac{\beta}{b} + \alpha)\Gamma(-\alpha + 1)} \int_{-\frac{1}{b}\ln(1-b)}^{\infty} e^{-\beta v} \alpha b (e^{bv} - 1)^{-(\alpha+1)} e^{bv} dv \right)^i.$$

Since $\hat{L}_1(\beta) \rightarrow 0$ as $\beta \rightarrow \infty$, and $\hat{L}_1(\beta)$ is continuous and decreasing in β , there exists some $\beta^* > 0$ such that the infinite series summation is valid for all $\beta > \beta^*$. Furthermore, we have the following Laplace inversion

$$\mathcal{L}_s^{-1} \left\{ \frac{\Gamma(\frac{\beta}{b})}{\Gamma(\frac{\beta}{b} + \alpha)\Gamma(-\alpha + 1)} \right\} = \frac{b \sin(\alpha\pi)}{\pi} (1 - e^{-bs})^{\alpha-1}.$$

Then, we can use the convolution method to invert the product of two Laplace transforms

$$\begin{aligned} & \mathcal{L}_s^{-1} \left\{ \frac{\Gamma(\frac{\beta}{b})}{\Gamma(\frac{\beta}{b} + \alpha)\Gamma(-\alpha + 1)} \int_{-\frac{1}{b}\ln(1-b)}^{\infty} e^{-\beta v} \alpha b (e^{bv} - 1)^{-(\alpha+1)} e^{bv} dv \right\} \\ &= \frac{b \sin(\alpha\pi)}{\pi} \alpha b \int_{-\frac{1}{b}\ln(1-b)}^s (1 - e^{-b(s-v)})^{\alpha-1} (e^{bv} - 1)^{-(\alpha+1)} e^{bv} I_{\{s > -\frac{1}{b}\ln(1-b)\}} dv \\ &= \frac{b \sin(\alpha\pi) \alpha}{\pi} I_{\{s > -\frac{1}{b}\ln(1-b)\}} \int_{\frac{1}{1-b}}^{e^{bs}} (1 - e^{-bs}x)^{\alpha-1} (x-1)^{-(\alpha+1)} dx \\ &= \frac{b \sin(\alpha\pi)}{\pi} I_{\{s > -\frac{1}{b}\ln(1-b)\}} \frac{(1 - \frac{1}{1-b}e^{-bs})^\alpha}{(1 - e^{-bs})(\frac{b}{1-b})^\alpha}. \end{aligned}$$

Also notice that

$$\frac{(1-b)^{\frac{\beta}{b}}}{(\frac{b}{1-b})^\alpha} = \left(\frac{1-b}{b}\right)^\alpha (e^{-\frac{1}{b}\ln(1-b)})^{-\beta}.$$

Hence, inverting the Laplace transform in each term of $\mathbb{E}(e^{-\beta\sigma})$, we get the probability density function of σ . Finally we invert the time change

$$\mathbb{P}(\tau = t) = \frac{1}{a + bt} \mathbb{P} \left(\sigma = \frac{1}{b} \ln \left(\frac{b}{a} t + 1 \right) \right),$$

and obtain the probability density function of the Parisian time τ . □

Proof of Lemma 4.6.1. The Laplace transform of the stopping time σ can be written as

$$\mathbb{E}(e^{-\beta\sigma}) = \frac{(e^{-(-\frac{1}{b}\ln(1-b))})^\beta}{(e^{-(-\frac{1}{b}\ln(1-b))})^\beta + (\frac{b}{1-b})^\alpha \int_0^{-\frac{1}{b}\ln(1-b)} \beta e^{-\beta v} (e^{bv} - 1)^{-\alpha} dv}.$$

Multiplying both the numerator and the denominator by

$$\int_0^{-\frac{1}{b} \ln(1-b)} e^{-\beta u} (1 - e^{-bu})^{\alpha-1} du,$$

we denote by N the numerator and Q the denominator, then

$$N = (e^{-(-\frac{1}{b} \ln(1-b))})^\beta \int_0^{-\frac{1}{b} \ln(1-b)} e^{-\beta u} (1 - e^{-bu})^{\alpha-1} du,$$

and

$$\begin{aligned} Q = & (e^{-(-\frac{1}{b} \ln(1-b))})^\beta \int_0^{-\frac{1}{b} \ln(1-b)} e^{-\beta u} (1 - e^{-bu})^{\alpha-1} du \\ & + \left(\frac{b}{1-b}\right)^\alpha \int_0^{-\frac{1}{b} \ln(1-b)} \beta e^{-\beta v} (e^{bv} - 1)^{-\alpha} dv \int_0^{-\frac{1}{b} \ln(1-b)} e^{-\beta u} (1 - e^{-bu})^{\alpha-1} du. \end{aligned}$$

For the integral in the second term of the denominator, we split it into two parts

$$\begin{aligned} & \beta \int_0^{-\frac{1}{b} \ln(1-b)} e^{-\beta v} (e^{bv} - 1)^{-\alpha} dv \int_0^{-\frac{1}{b} \ln(1-b)} e^{-\beta u} (1 - e^{-bu})^{\alpha-1} du \\ = & \beta \int_0^{-\frac{1}{b} \ln(1-b)} e^{-\beta t} \int_0^t (e^{b(t-s)} - 1)^{-\alpha} (1 - e^{-bs})^{\alpha-1} ds dt \\ & + \beta \int_{-\frac{1}{b} \ln(1-b)}^{-2\frac{1}{b} \ln(1-b)} e^{-\beta t} \int_{t - (-\frac{1}{b} \ln(1-b))}^{-\frac{1}{b} \ln(1-b)} (e^{b(t-s)} - 1)^{-\alpha} (1 - e^{-bs})^{\alpha-1} ds dt, \end{aligned}$$

then we apply integral by parts to derive

$$\begin{aligned}
& \beta \int_0^{-\frac{1}{b} \ln(1-b)} e^{-\beta v} (e^{bv} - 1)^{-\alpha} dv \int_0^{-\frac{1}{b} \ln(1-b)} e^{-\beta u} (1 - e^{-bu})^{\alpha-1} du \\
&= \beta \int_0^{-\frac{1}{b} \ln(1-b)} e^{-\beta t} \int_0^t \frac{(1 - e^{-bs})^{\alpha-1}}{(e^{b(t-s)} - 1)^\alpha} ds dt \\
&+ e^{-\beta(-\frac{1}{b} \ln(1-b))} \int_0^{-\frac{1}{b} \ln(1-b)} \frac{(1 - e^{-bs})^{\alpha-1}}{(e^{b(-\frac{1}{b} \ln(1-b)-s)} - 1)^\alpha} ds \\
&+ \int_{-\frac{1}{b} \ln(1-b)}^{-2\frac{1}{b} \ln(1-b)} e^{-\beta t} \frac{\partial}{\partial t} \left(\int_{t-\frac{1}{b} \ln(1-b)}^{-\frac{1}{b} \ln(1-b)} (e^{b(t-s)} - 1)^{-\alpha} (1 - e^{-bs})^{\alpha-1} ds \right) dt \\
&= \frac{\pi \csc(\pi\alpha)}{b} - e^{-\beta(-\frac{1}{b} \ln(1-b))} \int_0^{-\frac{1}{b} \ln(1-b)} \frac{e^{-\beta s} (1 - e^{-bs})^{\alpha-1}}{(e^{b(-\frac{1}{b} \ln(1-b)-s)} - 1)^\alpha} ds \\
&- e^{-\beta(-\frac{1}{b} \ln(1-b))} \int_0^{-\frac{1}{b} \ln(1-b)} e^{-\beta u} \int_u^{-\frac{1}{b} \ln(1-b)} \frac{\alpha b e^{b(u+(-\frac{1}{b} \ln(1-b)-s))} (1 - e^{-bs})^{\alpha-1}}{(e^{b(u+(-\frac{1}{b} \ln(1-b)-s)} - 1)^{\alpha+1}} ds du.
\end{aligned}$$

Then, the denominator becomes

$$\begin{aligned}
\mathbb{Q} &= \frac{\pi \csc(\pi\alpha)}{b} (e^{b(-\frac{1}{b} \ln(1-b))} - 1)^\alpha - e^{-\beta(-\frac{1}{b} \ln(1-b))} \\
&\times \int_0^{-\frac{1}{b} \ln(1-b)} e^{-\beta u} \int_u^{-\frac{1}{b} \ln(1-b)} \frac{\alpha b e^{b(u+(-\frac{1}{b} \ln(1-b)-s))} (1 - e^{-bs})^{\alpha-1} (e^{b(-\frac{1}{b} \ln(1-b))} - 1)^\alpha}{(e^{b(u+(-\frac{1}{b} \ln(1-b)-s)} - 1)^{\alpha+1}} ds du,
\end{aligned}$$

where we have the following observation for the inner integral

$$\begin{aligned}
& \int_0^{-\frac{1}{b} \ln(1-b)} \int_u^{-\frac{1}{b} \ln(1-b)} \frac{\alpha b e^{b(u+(-\frac{1}{b} \ln(1-b)-s))} (1 - e^{-bs})^{\alpha-1} (e^{b(-\frac{1}{b} \ln(1-b))} - 1)^\alpha}{(e^{b(u+(-\frac{1}{b} \ln(1-b)-s)} - 1)^{\alpha+1}} ds du \\
&= (e^{b(-\frac{1}{b} \ln(1-b))} - 1)^\alpha \int_0^{-\frac{1}{b} \ln(1-b)} \frac{(1 - e^{-bs})^{\alpha-1}}{(e^{b(-\frac{1}{b} \ln(1-b)-s)} - 1)^\alpha} ds - \int_0^{-\frac{1}{b} \ln(1-b)} \frac{1}{(1 - e^{-bs})^{1-\alpha}} ds \\
&= (e^{b(-\frac{1}{b} \ln(1-b))} - 1)^\alpha \frac{\pi \csc(\pi\alpha)}{b} - \int_0^{-\frac{1}{b} \ln(1-b)} \frac{1}{(1 - e^{-bs})^{1-\alpha}} ds.
\end{aligned}$$

Hence the Laplace transform of σ can be expressed as the Laplace transform of a compound geometric distribution as follows

$$\begin{aligned}
& \left(p(e^{-(-\frac{1}{b} \ln(1-b))})^\beta \int_0^{-\frac{1}{b} \ln(1-b)} e^{-\beta u} \frac{(1 - e^{-bu})^{\alpha-1}}{M} du \right) / \\
& \left(1 - (1 - p)e^{-\beta(-\frac{1}{b} \ln(1-b))} \int_0^{-\frac{1}{b} \ln(1-b)} e^{-\beta u} \frac{1}{E} \right. \\
& \quad \left. \times \int_u^{-\frac{1}{b} \ln(1-b)} \frac{\alpha b e^{b(u+(-\frac{1}{b} \ln(1-b)-s))} (1 - e^{-bs})^{\alpha-1} (e^{b(-\frac{1}{b} \ln(1-b))} - 1)^\alpha}{(e^{b(u+(-\frac{1}{b} \ln(1-b)-s)} - 1)^{\alpha+1}} ds du \right)
\end{aligned}$$

where p , M and E are given as (21), (22) and (23). It is easy to check that

$$f_0(u) = \frac{(1 - e^{-bu})^{\alpha-1}}{M},$$

and

$$f(u) = \frac{1}{E} \int_u^{-\frac{1}{b} \ln(1-b)} \frac{\alpha b e^{b(u + (-\frac{1}{b} \ln(1-b)) - s)} (1 - e^{-bs})^{\alpha-1} (e^{b(-\frac{1}{b} \ln(1-b))} - 1)^\alpha}{(e^{b(u + (-\frac{1}{b} \ln(1-b)) - s)} - 1)^{\alpha+1}} ds,$$

are well-defined probability density functions over $u \in [0, -\frac{1}{b} \ln(1-b)]$. \square

Proof of Theorem 4.6.2. From Lemma 4.6.1, we know that σ follows a compound geometric distribution. In particular, we have

$$\sigma = \sigma_0 + \sum_{i=1}^G \sigma_i,$$

where

- G is a geometric distributed random variable with parameter p given in (21);
- $\sigma_0 = T_0 + (-\frac{1}{b} \ln(1-b))$, the probability density function of T_0 is f_0 ;
- $\sigma_i = T_i + (-\frac{1}{b} \ln(1-b))$, for $i = 1, \dots, G$, T_i are i.i.d. random variables with probability density function f .

To generate T_0 , we choose an envelope \bar{T}_0 with probability density function

$$f_{\bar{T}_0}(u) = \frac{\alpha}{(-\frac{1}{b} \ln(1-b))^\alpha u^{1-\alpha}}, \quad 0 < u < -\frac{1}{b} \ln(1-b),$$

then the associated A/R decision directly follows Step 2.

To generate T_i for $i \neq 0$, we develop a two-dimensional simulation scheme. Since the probability density function of T_i is f , and

$$\int_0^s \frac{\alpha b e^{b(u + (-\frac{1}{b} \ln(1-b)) - s)} (e^{b(-\frac{1}{b} \ln(1-b))} - 1)^\alpha}{(e^{b(u + (-\frac{1}{b} \ln(1-b)) - s)} - 1)^{\alpha+1}} du = \frac{(e^{b(-\frac{1}{b} \ln(1-b))} - 1)^\alpha}{(e^{b(-\frac{1}{b} \ln(1-b)) - s} - 1)^\alpha} - 1,$$

then the integrand in the expression of f can be expressed in terms of the joint

density of (T_i, S_i) ,

$$\begin{aligned}
& f_{T_i, S_i}(t, s) \\
&= \frac{1}{E} \frac{\alpha b e^{b(u + (-\frac{1}{b} \ln(1-b)) - s)} (e^{b(-\frac{1}{b} \ln(1-b))} - 1)^\alpha}{(e^{b(u + (-\frac{1}{b} \ln(1-b)) - s)} - 1)^{\alpha+1}} (1 - e^{-bs})^{\alpha-1} \\
&= \frac{\frac{\alpha b e^{b(u + (-\frac{1}{b} \ln(1-b)) - s)} (e^{b(-\frac{1}{b} \ln(1-b))} - 1)^\alpha}{(e^{b(u + (-\frac{1}{b} \ln(1-b)) - s)} - 1)^{\alpha+1}}}{\frac{(e^{b(-\frac{1}{b} \ln(1-b))} - 1)^\alpha}{(e^{b(-\frac{1}{b} \ln(1-b)) - s} - 1)^\alpha} - 1}} \frac{1}{E} \left(\frac{(e^{b(-\frac{1}{b} \ln(1-b))} - 1)^\alpha}{(e^{b(-\frac{1}{b} \ln(1-b)) - s} - 1)^\alpha} - 1 \right) (1 - e^{-bs})^{\alpha-1},
\end{aligned}$$

with $0 < u < s < -\frac{1}{b} \ln(1-b)$. We use A/R scheme to sample S_i by choosing an envelope \bar{S}_i with the following probability density function

$$f_{\bar{S}}(s) = \frac{\alpha}{(-\frac{1}{b} \ln(1-b))^\alpha} \left(-\frac{1}{b} \ln(1-b) - s\right)^{\alpha-1},$$

and

$$\begin{aligned}
\frac{f_S(s)}{f_{\bar{S}}(s)} &= \frac{(-\frac{1}{b} \ln(1-b))^\alpha}{\alpha E} \left(\frac{(e^{b(-\frac{1}{b} \ln(1-b))} - 1)^\alpha}{(e^{b(-\frac{1}{b} \ln(1-b)) - s} - 1)^\alpha} - 1 \right) (1 - e^{-bs})^{\alpha-1} \left(-\frac{1}{b} \ln(1-b) - s\right)^{1-\alpha} \\
&\leq \frac{(-\frac{1}{b} \ln(1-b))^\alpha}{\alpha E} C,
\end{aligned}$$

where C can be found via numerical optimisation. Given S , the cumulative density function of T_i is given as

$$F_{T|S}(t|s) = \frac{\frac{(e^{b(-\frac{1}{b} \ln(1-b))} - 1)^\alpha}{(e^{b(-\frac{1}{b} \ln(1-b)) - s} - 1)^\alpha} - \frac{(e^{b(-\frac{1}{b} \ln(1-b))} - 1)^\alpha}{(e^{b(t + (-\frac{1}{b} \ln(1-b)) - s)} - 1)^\alpha}}{\frac{(e^{b(-\frac{1}{b} \ln(1-b))} - 1)^\alpha}{(e^{b(-\frac{1}{b} \ln(1-b)) - s} - 1)^\alpha} - 1}},$$

which can be inverted explicitly by

$$F_{T|S}^{-1}(t|s) = s - \left(-\frac{1}{b} \ln(1-b)\right) + \frac{1}{b} \ln \left(\left(\frac{(e^{b(-\frac{1}{b} \ln(1-b))} - 1)^\alpha}{(e^{b(-\frac{1}{b} \ln(1-b))} - 1)^\alpha} - t \left(\frac{(e^{b(-\frac{1}{b} \ln(1-b))} - 1)^\alpha}{(e^{b(-\frac{1}{b} \ln(1-b)) - s} - 1)^\alpha} - 1 \right) \right)^{\frac{1}{\alpha}} + 1 \right).$$

Hence, T_i can be exactly simulated via Step 3. \square

Appendix D

Joint density of the random vector

$$(R_1, \dots, R_{n-1} \mid \Delta_1^{-\alpha} = w)$$

From Proposition 10 of Pitman and Yor (1997), we know that under the probability measure $\mathbb{P}_{\alpha,0}$,

$$R_k := \frac{\Delta_{k+1}}{\Delta_k} \stackrel{\text{law}}{=} \frac{(\sum_{i=1}^{k+1} \mathbf{e}_i)^{-1/\alpha}}{(\sum_{i=1}^k \mathbf{e}_i)^{-1/\alpha}} \quad \text{for } k = 1, 2, \dots,$$

where \mathbf{e}_i are independent standard exponential random variables. In particular, it is known that $\Delta_1^{-\alpha} \stackrel{\mathcal{D}}{=} \mathbf{e}_1$, see Lemma 24 of Pitman and Yor (1997).

On the other hand, define

$$R_k(\lambda) := \left(\frac{\sum_{i=1}^{k-1} \mathbf{e}_i + \lambda^\alpha}{\sum_{i=1}^k \mathbf{e}_i + \lambda^\alpha} \right)^{\frac{1}{\alpha}} \quad \text{for } k = 1, 2, \dots,$$

then Lemma 3.2 of James (2019) implies that $(R_1(\lambda), \dots, R_{n-1}(\lambda))$ has the joint density

$$f_{R_1, \dots, R_{n-1}}(r_1, \dots, r_{n-1}) = \alpha^{n-1} \lambda^{(n-1)\alpha} e^{\lambda^\alpha} e^{-\lambda^\alpha \prod_{j=1}^{n-1} r_j^{-\alpha}} \prod_{j=1}^{n-1} r_j^{-(n-j)\alpha-1}. \quad (\text{D.1})$$

We set $\lambda = \Delta_1^{-1}$, then $\lambda^\alpha \stackrel{\mathcal{D}}{=} \mathbf{e}_1$ and

$$R_k(\lambda) \stackrel{law}{=} \left(\frac{\sum_{i=1}^k \mathbf{e}_i}{\sum_{i=1}^{k+1} \mathbf{e}_i} \right)^{\frac{1}{\alpha}} = \frac{(\sum_{i=1}^{k+1} \mathbf{e}_i)^{-1/\alpha}}{(\sum_{i=1}^k \mathbf{e}_i)^{-1/\alpha}},$$

hence the random vector $(R_1(\lambda), \dots, R_{n-1}(\lambda) \mid \lambda = \Delta_1^{-1})$ has the identical distribution as (R_1, \dots, R_{n-1}) , and we obtain the joint density (5.4) by setting $\lambda = w^{\frac{1}{\alpha}}$ in (D.1).

Alternatively, the same result could be obtained by writing down the joint density of $\Delta_1, \dots, \Delta_n$ using the basic property of Poisson random measure, and change the variables with $R_k := \frac{\Delta_{k+1}}{\Delta_k}$.

Appendix E

Simulation of G^*

We give the algorithm for sampling from the density $h^*(u)$.

Theorem E.1. *Let G^* be a random variable with the probability density function*

$$h^*(u) = \frac{1}{\frac{\pi}{\sin(\alpha\pi)} - \frac{1}{\alpha}} \frac{u^{-\alpha} - u^\alpha}{u + 1} \quad \text{for } 0 < u < 1,$$

then G^* can be generated via the following steps.

1. Numerically maximising

$$C(u) = \frac{1}{\frac{\pi}{\sin(\alpha\pi)} - \frac{1}{\alpha}} \frac{u^{-\alpha} - u^\alpha}{u + 1} \frac{B(\theta, 2)}{u^{\theta-1}(1-u)},$$

where $\theta = 0.59 - 0.01\alpha - 0.60\alpha^2$ and $B(.,.)$ is the standard Beta function, record the optimal u^* and set $C = C(u^*, \theta)$.

2. Generate a Beta random variable G' by setting

$$G' \sim \text{Beta}(\theta, 2).$$

3. Set $V \sim U[0, 1]$, if

$$V \leq \frac{1}{C} \frac{1}{\frac{\pi}{\sin(\alpha\pi)} - \frac{1}{\alpha}} \frac{(G')^{-\alpha} - (G')^\alpha}{G' + 1} \frac{B(\theta, 2)}{(G')^{\theta-1}(1-G')},$$

accept this candidate and return $G^* = G'$, otherwise go back to Step 2.

Proof. This is a direct consequence of the accept rejection method, see Dassios et al. (2020) for details. □

Bibliography

- Al Labadi, L. and Zarepour, M. (2014). On simulations from the two-parameter Poisson-Dirichlet process and the normalized inverse-Gaussian process. *Sankhya A*, 76(1):158–176.
- Aldous, D. J. (1985). Exchangeability and related topics. In *École d'été de probabilités de Saint-Flour*, volume 1117 of *Lecture Notes in Math.* Springer, Berlin.
- Alexandrova-Kabadjova, B. and Solis, F. (2012). The mexican experience in how the settlement of large payments is performed in the presence of a high volume of small payments. *Diagnostics for the financial markets—computational studies of payment system.*
- Anderluh, J. H. M. and van der Weide, J. A. M. (2009). Double-sided Parisian option pricing. *Finance Stoch.*, 13(2):205–238.
- Arfken, G. B. and Weber, H. J. (2001). *Mathematical methods for physicists.* Harcourt/Academic Press, Burlington, MA, fifth edition.
- Barba Escribá, L. (1987). A stopped Brownian motion formula with two sloping line boundaries. *Ann. Probab.*, 15(4):1524–1526.
- Barlow, M., Pitman, J., and Yor, M. (1989). On Walsh's Brownian motions. In *Séminaire de Probabilités, XXIII*, volume 1372 of *Lecture Notes in Math.*, pages 275–293. Springer, Berlin.
- Bech, M. L., Faruqui, U., and Shirakami, T. (2020). Payments without borders. *BIS Quarterly Review, March.*
- Becher, C., Galbiati, M., and Tudela, M. (2008a). The timing and funding of CHAPS Sterling payments. *Economic Policy Review*, 14(2).
- Becher, C., Millard, S., and Soramaki, K. (2008b). The network topology of CHAPS Sterling. *Bank of England Working Paper.*

- Bellman, R. (1961). *A brief introduction to theta functions*. Athena Series: Selected Topics in Mathematics. Holt, Rinehart and Winston, New York.
- Billingsley, P. (1972). On the distribution of large prime divisors. *Period. Math. Hungar.*, 2:283–289.
- Bingham, N. H., Goldie, C. M., and Teugels, J. L. (1989). *Regular variation*, volume 27 of *Encyclopedia of Mathematics and its Applications*. Cambridge University Press, Cambridge.
- Blackwell, D. and MacQueen, J. B. (1973). Ferguson distributions via Pólya urn schemes. *Ann. Statist.*, 1:353–355.
- Borodin, A. N. and Salminen, P. (1996). *Handbook of Brownian motion—facts and formulae*. Probability and its Applications. Birkhäuser Verlag, Basel.
- Borodin, A. N. and Salminen, P. (2002). *Handbook of Brownian motion—facts and formulae*. Probability and its Applications. Birkhäuser Verlag, Basel, Second edition.
- Bowman, A. W. and Azzalini, A. (1997). *Applied smoothing techniques for data analysis: the kernel approach with S-Plus illustrations*, volume 18. OUP Oxford.
- Breiman, L. (1967). First exit times from a square root boundary. In *Proc. Fifth Berkeley Sympos. Math. Statist. and Probability (Berkeley, Calif., 1965/66)*, Vol. II: *Contributions to Probability Theory, Part 2*, pages 9–16. Univ. California Press, Berkeley, Calif.
- Çetin, U. (2012). Filtered Azéma martingales. *Electron. Commun. Probab.*, 17:no. 62, 13.
- Che, X. (2011). *Markov type models for large-valued interbank payment systems*. PhD thesis, The London School of Economics and Political Science (LSE).
- Che, X. and Dassios, A. (2013). Stochastic boundary crossing probabilities for the Brownian motion. *J. Appl. Probab.*, 50(2):419–429.
- Chesney, M., Jeanblanc-Picqué, M., and Yor, M. (1997). Brownian excursions and Parisian barrier options. *Adv. in Appl. Probab.*, 29(1):165–184.
- Chung, K. L. (1976). Excursions in Brownian motion. *Arkiv för Matematik*, 14(2):155–177.
- Cohen, A. M. (2007). *Numerical methods for Laplace transform inversion*, volume 5 of *Numerical Methods and Algorithms*. Springer, New York.

- Dassios, A. and Lim, J. W. (2017). An analytical solution for the two-sided Parisian stopping time, its asymptotics, and the pricing of Parisian options. *Math. Finance*, 27(2):604–620.
- Dassios, A. and Lim, J. W. (2019). A variation of the Azéma martingale and drawdown options. *Math. Finance*, 29(4):1116–1130.
- Dassios, A., Lim, J. W., and Qu, Y. (2019). Azéma martingales for Bessel and CIR processes and the pricing of Parisian zero-coupon bonds. *Math. Finance*.
- Dassios, A., Lim, J. W., and Qu, Y. (2020). Exact simulation of a truncated Lévy subordinator. *ACM Transactions on Modeling and Computer Simulation*, 30(3):Art. 17, 26.
- Dassios, A. and Wu, S. (2010). Perturbed Brownian motion and its application to Parisian option pricing. *Finance Stoch.*, 14(3):473–494.
- Dassios, A. and Zhang, J. (2020). Parisian time of reflected Brownian motion with drift on rays and its application in banking. *Risks*, 8(4).
- Dassios, A. and Zhang, J. (2021a). Exact simulation of two-parameter Poisson-Dirichlet random variables. *Electron. J. Probab.*, 26:Paper No. 5, 20.
- Dassios, A. and Zhang, J. (2021b). First hitting time of Brownian motion with drift on simple graph. *Methodology and Computing in Applied Probability*.
- Denbee, E. and Zimmerman, R. G.-P. (2012). Methods for evaluating liquidity provision in real-time gross settlement payment systems. *Diagnostics for the financial markets—computational studies of payment system*.
- Deng, D. and Li, Q. (2009). Communication in naturally mobile sensor networks. In *International Conference on Wireless Algorithms, Systems, and Applications*, pages 295–304. Springer.
- Devroye, L. (1986). *Non-Uniform Random Variate Generation*. Springer-Verlag.
- Doob, J. L. (1949). Heuristic approach to the Kolmogorov-Smirnov theorems. *Ann. Math. Statistics*, 20:393–403.
- Durrett, R. T., Iglehart, D. L., and Miller, D. R. (1977). Weak convergence to Brownian meander and Brownian excursion. *The Annals of Probability*, 5(1):117–129.
- Engen, S. (2013). *Stochastic abundance models: with emphasis on biological communities and species diversity*. Springer Science & Business Media.

- Evans, S. N. and Sowers, R. B. (2003). Pinching and twisting Markov processes. *Ann. Probab.*, 31(1):486–527.
- Ferguson, T. S. (1973). A Bayesian analysis of some nonparametric problems. *Ann. Statist.*, 1:209–230.
- Fitzsimmons, P. J. and Kuter, K. E. (2015). Harmonic functions of Brownian motions on metric graphs. *J. Math. Phys.*, 56(1):013504, 28.
- Freidlin, M. and Sheu, S.-J. (2000). Diffusion processes on graphs: stochastic differential equations, large deviation principle. *Probab. Theory Related Fields*, 116(2):181–220.
- Freidlin, M. I. and Wentzell, A. D. (1993). Diffusion processes on graphs and the averaging principle. *Ann. Probab.*, 21(4):2215–2245.
- Gettoor, R. K. and Sharpe, M. J. (1979). Excursions of Brownian motion and Bessel processes. *Zeitschrift für Wahrscheinlichkeitstheorie und Verwandte Gebiete*, 47(1):83–106.
- Glasserman, P. (2004). *Monte Carlo methods in financial engineering*, volume 53 of *Applications of Mathematics (New York)*. Springer-Verlag, New York. Stochastic Modelling and Applied Probability.
- Graversen, S. E. and Shiryaev, A. N. (2000). An extension of P. Lévy’s distributional properties to the case of a Brownian motion with drift. *Bernoulli*, 6(4):615–620.
- Guer, S. (2020). An adaptive monte carlo approach for pricing parisian options with general boundaries. *Journal of Computational Finance*, 23(5).
- Hajri, H. and Touhami, W. (2014). Itô’s formula for Walsh’s Brownian motion and applications. *Statist. Probab. Lett.*, 87:48–53.
- Hansen, J. C. (1994). Order statistics for decomposable combinatorial structures. *Random Structures Algorithms*, 5(4):517–533.
- Hoppe, F. M. (1987). The sampling theory of neutral alleles and an urn model in population genetics. *J. Math. Biol.*, 25(2):123–159.
- Ichiba, T., Karatzas, I., Prokaj, V., and Yan, M. (2018). Stochastic integral equations for Walsh semimartingales. *Ann. Inst. H. Poincaré Probab. Statist.*, 54(2):726–756.
- Ichiba, T. and Sarantsev, A. (2019). Stationary distributions and convergence for Walsh diffusions. *Bernoulli*, 25(4A):2439–2478.

- Imhof, J.-P. (1984). Density factorizations for Brownian motion, meander and the three-dimensional Bessel process, and applications. *Journal of Applied Probability*, 21(3):500–510.
- James, L. F. (2019). Stick-breaking pitman-yor processes given the species sampling size. *arXiv preprint arXiv:1908.07186*.
- Jeanblanc, M., Yor, M., and Chesney, M. (2009). *Mathematical methods for financial markets*. Springer Finance. Springer-Verlag London, Ltd., London.
- Karatzas, I. and Yan, M. (2019). Semimartingales on rays, Walsh diffusions, and related problems of control and stopping. *Stoch. Proc. Appl.*, 129(6):1921–1963.
- Kennedy, D. P. (1976a). The distribution of the maximum Brownian excursion. *Journal of Applied Probability*, 13(2):371–376.
- Kennedy, D. P. (1976b). Some martingales related to cumulative sum tests and single-server queues. *Stochastic Process. Appl.*, 4(3):261–269.
- Kingman, J. F. C. (1975). Random discrete distributions. *Journal of the Royal Statistical Society: Series B (Methodological)*, 37(1):1–15.
- Kingman, J. F. C. (1993). *Poisson processes*. Clarendon, Oxford.
- Kyprianou, A. E. (2006). *Introductory lectures on fluctuations of Lévy processes with applications*. Universitext. Springer-Verlag, Berlin.
- Labart, C. and Lelong, J. (2009). Pricing double barrier Parisian options using Laplace transforms. *Int. J. Theor. Appl. Finance*, 12(1):19–44.
- Lang, S. (2013). *Complex analysis*, volume 103. Springer Science & Business Media.
- Mandl, P. (1968). *Analytical treatment of one-dimensional Markov processes*. Die Grundlehren der mathematischen Wissenschaften, Band 151. Academia Publishing House of the Czechoslovak Academy of Sciences, Prague; Springer-Verlag New York Inc., New York.
- McCloskey, J. W. (1965). *A model for the distribution of individuals by species in an environment*. Michigan State University. Department of Statistics.
- McDonough, W. J. (1997). *Real-time gross settlement systems*. Committee on Payment and Settlement Systems, Bank for International Settlements.
- Nguyen-Ngoc, L. and Yor, M. (2005). Some martingales associated to reflected Lévy processes. In *Séminaire de Probabilités XXXVIII*, volume 1857 of *Lecture Notes in Math.*, pages 42–69. Springer, Berlin.

- Padoa-Schioppa, T. (2005). *New developments in large-value payment systems*. Committee on Payment and Settlement Systems, Bank for International Settlements.
- Papanicolaou, V. G., Papageorgiou, E. G., and Lepipas, D. C. (2012). Random motion on simple graphs. *Methodol. Comput. Appl. Probab.*, 14(2):285–297.
- Perman, M. (1993). Order statistics for jumps of normalised subordinators. *Stochastic Process. Appl.*, 46(2):267–281.
- Perman, M., Pitman, J., and Yor, M. (1992). Size-biased sampling of Poisson point processes and excursions. *Probab. Theory Related Fields*, 92(1):21–39.
- Peskir, G. (2002). On integral equations arising in the first-passage problem for Brownian motion. *J. Integral Equations Appl.*, 14(4):397–423.
- Peskir, G. (2006). On reflecting Brownian motion with drift. In *Proceedings of the 37th ISCIE International Symposium on Stochastic Systems Theory and its Applications*, pages 1–5.
- Picard, J. (2005). Stochastic calculus and martingales on trees. *Ann. Inst. H. Poincaré Probab. Statist.*, 41(4):631–683.
- Pitman, J. (1996). Random discrete distributions invariant under size-biased permutation. *Adv. in Appl. Probab.*, 28(2):525–539.
- Pitman, J. and Yor, M. (1992). Arcsine laws and interval partitions derived from a stable subordinator. *Proc. London Math. Soc. (3)*, 65(2):326–356.
- Pitman, J. and Yor, M. (1997). The two-parameter Poisson-Dirichlet distribution derived from a stable subordinator. *Ann. Probab.*, 25(2):855–900.
- Revuz, D. and Yor, M. (1999). *Continuous martingales and Brownian motion*, volume 293 of *Grundlehren der Mathematischen Wissenschaften [Fundamental Principles of Mathematical Sciences]*. Springer-Verlag, Berlin, third edition.
- Rochet, J.-C. and Tirole, J. (1996). Controlling risk in payment systems. *Journal of Money, Credit and Banking*, 28(4):832–862.
- Sacerdote, L., Telve, O., and Zucca, C. (2014). Joint densities of first hitting times of a diffusion process through two time-dependent boundaries. *Adv. in Appl. Probab.*, 46(1):186–202.
- Salminen, P. (1988). On the first hitting time and the last exit time for a Brownian motion to/from a moving boundary. *Adv. in Appl. Probab.*, 20(2):411–426.

- Scheike, T. H. (1992). A boundary-crossing result for Brownian motion. *J. Appl. Probab.*, 29(2):448–453.
- Schmidt, A. A. and Vershik, A. M. (1977). Limit measures that arise in the asymptotic theory of symmetric groups. I. *Teor. Veroyatnost. i Primenen.*, 22(1):72–88.
- Schröder, M. (2003). Brownian excursions and Parisian barrier options: a note. *J. Appl. Probab.*, 40(4):855–864.
- Shepp, L. A. and Lloyd, S. P. (1966). Ordered cycle lengths in a random permutation. *Trans. Amer. Math. Soc.*, 121:340–357.
- Soramäki, K., Bech, M. L., Arnold, J., Glass, R. J., and Beyeler, W. E. (2007). The topology of interbank payment flows. *Physica A: Statistical Mechanics and its Applications*, 379(1):317–333.
- Sosnovskiy, S. (2015). On financial applications of the two-parameter poisson-dirichlet distribution. *arXiv preprint arXiv:1501.01954*.
- Tsirelson, B. (1997). Triple points: from non-Brownian filtrations to harmonic measures. *Geom. Funct. Anal.*, 7(6):1096–1142.
- Vershik, A. M. (1986). Asymptotic distribution of decompositions of natural numbers into prime divisors. *Dokl. Akad. Nauk SSSR*, 289(2):269–272.
- Walsh, J. B. (1978). A diffusion with a discontinuous local time. In *Temps locaux*, number 52-53 in *Astérisque*, pages 37–45. Société mathématique de France.
- Wang, L. and Pötzelberger, K. (1997). Boundary crossing probability for Brownian motion and general boundaries. *J. Appl. Probab.*, 34(1):54–65.
- Watanabe, S. (1999). The existence of a multiple spider martingale in the natural filtration of a certain diffusion in the plane. In *Séminaire de Probabilités, XXXIII*. Springer, Berlin.
- Watterson, G. A. (1976). The stationary distribution of the infinitely-many neutral alleles diffusion model. *J. Appl. Probability*, 13(4):639–651.
- Yan, M. (2018). *Topics in Walsh Semimartingales and Diffusions: Construction, Stochastic Calculus, and Control*. PhD thesis, Columbia University.
- Yor, M. (1997). *Some aspects of Brownian motion. Part II*. Lectures in Mathematics ETH Zürich. Birkhäuser Verlag, Basel.
- Zhang, Y. (2014). *Brownian Excursions in Mathematical Finance*. PhD thesis, The London School of Economics and Political Science (LSE).